Visualisation and Characterisation of Apoflavodoxin Folding

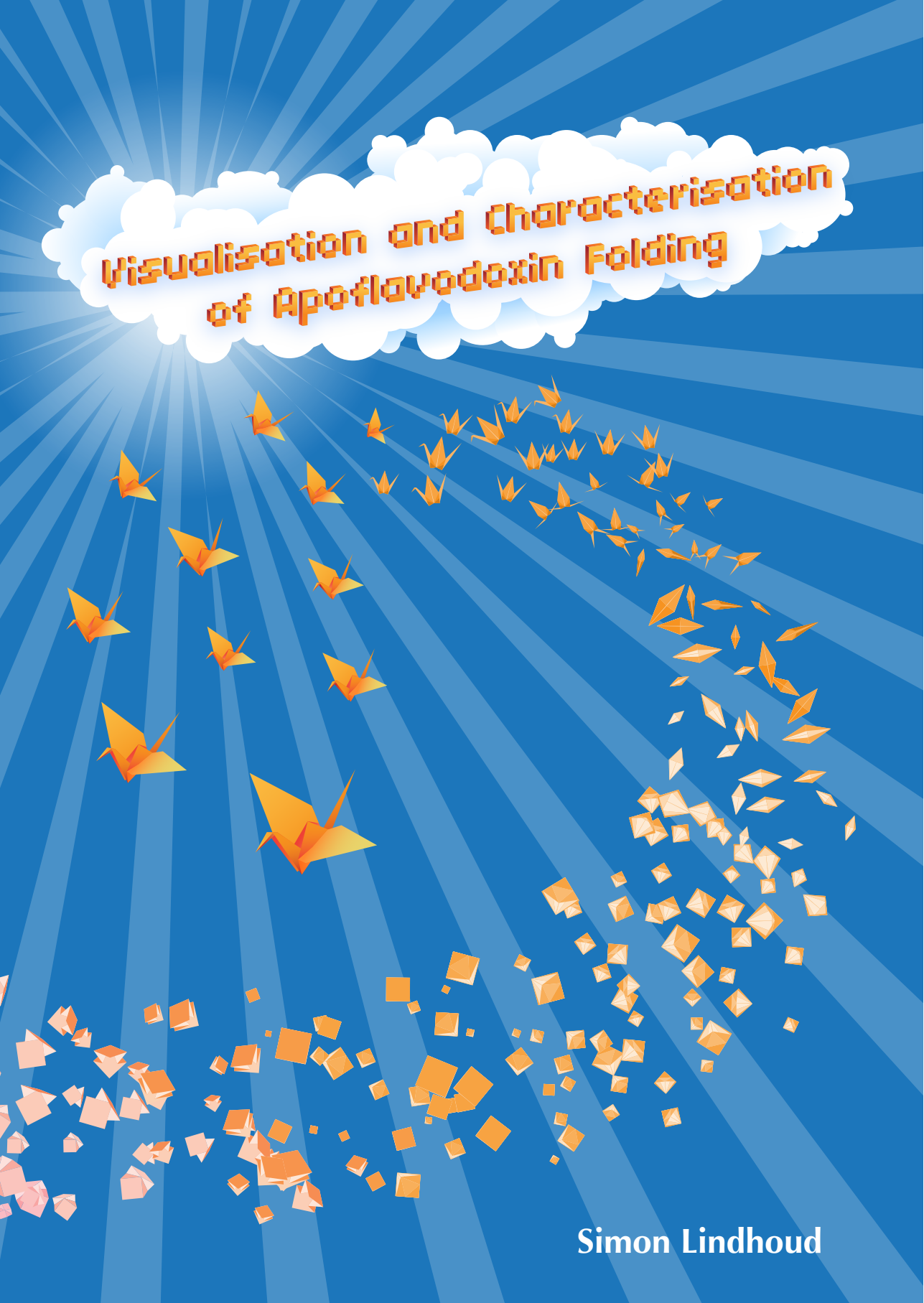

Simon Lindhoud

Visualisation and Characterisation of Apoflavodoxin Folding

Simon Lindhoud

Thesis committee

Thesis supervisor
Prof. dr. W.J.H. van Berkel
Personal chair at the Laboratory of Biochemistry
Wageningen University

Thesis co-supervisor
Dr. ir. C.P.M. van Mierlo
Assistant professor at the Laboratory of Biochemistry
Wageningen University

Other members
Prof. dr. H. van Amerongen, Wageningen University
Dr. M.M.A.E. Claessens, University of Twente, Enschede
Dr. M. Merkx, Eindhoven University of Technology
Prof. dr. A.M. van Oijen, University of Groningen

This research was conducted under the auspices of the Graduate School VLAG (Advanced studies in Food Technology, Agrobiotechnology, Nutrition and Health Sciences).

Visualisation and Characterisation of Apoflavodoxin Folding

Simon Lindhoud

Thesis
Submitted in fulfilment of the requirements for the degree of doctor
at Wageningen University
by the authority of the Rector Magnificus
Prof. dr. M.J. Kropff,
in the presence of the
Thesis Committee appointed by the Academic Board
to be defended in public
on Wednesday 12 September 2012
at 4 p.m. in the Aula.

Simon Lindhoud
Visualisation and Characterisation of Apoflavodoxin Folding
142 pages

PhD thesis, Wageningen University, Wageningen, NL (2012)
With references, with summaries in Dutch and English

ISBN 978-94-6173-305-4

Voor mijn ouders

Contents

Chapter 1

Introduction

Simon Lindhoud and Carlo P.M. van Mierlo

Folding of proteins to their functional conformation is paramount to life. This folding process is inherently complex, because proteins may fold along a myriad of different routes. Potentially, misfolded and aggregation prone intermediate states form during folding. These species have been linked to the onset of numerous devastating pathologies. Often, these folding intermediates are molten globule-like (see below).

Investigation of folding intermediates is hampered by the transient nature of their existence, their proneness to aggregation and their conformational heterogeneity. To elucidate properties of these folding species requires use of methods that detect them with high efficiency within an ensemble of interconverting protein conformers. The (single-molecule) fluorescence spectroscopy work presented in this thesis illuminates formation and conformational properties of the molten globule intermediate state that populates during folding of apoflavodoxin. Elucidation of how an unfolded protein forms a molten globule intermediate furthers our understanding about protein folding and offers insight into factors responsible for protein misfolding and aggregation.

Protein folding

Proteins are linear chains of amino acids with a specific length and order. This sequence of amino acids is referred to as the primary structure of a protein. In order to function, these polypeptides typically need to fold into a specific three-dimensional conformation, which is referred to as the tertiary structure. Within this conformation, three types of secondary structure elements are commonly found: α-helices, β-strands and loops (Figure 1.1). The functional, three-dimensional conformation of a protein is referred to as the native structure. Insight into protein function is aided by characterisation of protein structures at the atomic level. To this date, more than 80.000 protein structures have been elucidated since the elucidation of the first protein structure, i.e., the one of sperm whale myoglobin (Kendrew, Bodo et al. 1958).

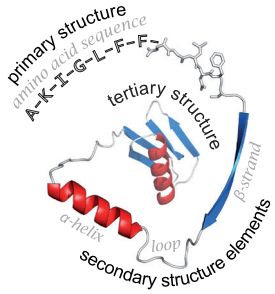

Figure 1.1 Primary, secondary and tertiary structure of proteins. The primary structure of a protein is the sequence of amino acids in the polypeptide. During protein folding, the polypeptide acquires secondary structure elements, such as α-helices, loops and β-strands. The tertiary structure is the result of stable long-distance interactions within the polypeptide.

The starting point for folding is an unfolded polypeptide. Under strongly denaturing conditions unfolded polypeptides adopt an astronomically large number of conformations (Tanford, Kawahara et al. 1966). In contrast to the unfolded state ensemble, the native state ensemble is a very small subset of protein conformations that is characterised by many stable interactions within the polypeptide. If protein folding would involve random sampling of all possible conformations until the native structure is reached, it would last almost infinitely long. However, most proteins are able to fold to their functional structure within seconds (Levinthal 1968). Seminal experiments by Anfinsen demonstrated that denatured proteins can reversibly fold to their native structure upon lifting of denaturing conditions (Anfinsen 1973). Anfinsen's thermodynamic hypothesis states that the three-dimensional structure of a native protein in its normal physiological milieu is the one that has the lowest free energy of all possible conformations, and hence the native state of a protein in a given environment is ultimately determined by its amino acid sequence (Anfinsen 1973). In light of this hypothesis, it is remarkable that proteins with similar or even identical sequences have been found to fold into completely different

three-dimensional structures (Davidson 2008; Tuinstra, Peterson et al. 2008; Alexander, He et al. 2009; Nabuurs, Westphal et al. 2009; Bryan and Orban 2010).

To describe protein folding, the concept of funnel shaped multidimensional folding energy landscapes arose from a combination of experimental data, theory and simulation (Figure 1.2) (Bryngelson, Onuchic et al. 1995; Wolynes, Onuchic et al. 1995; Dill and Chan 1997; Dinner, Sali et al. 2000; Vendruscolo, Paci et al. 2001; Fersht and Daggett 2002). These folding funnels depict the free energy of folding as a function of conformational entropy. The native state of a protein resides at the bottom of the funnel because this is the thermodynamically most favourable conformation under native conditions. In folding funnels, denatured protein molecules can be envisaged as skiers being distributed over a mountainside. Upon instantaneous lifting of denaturing conditions, they commence their descend towards their native state, along which they fold. Each denatured protein can undergo a different sequence of conformational rearrangements during folding towards the native state.

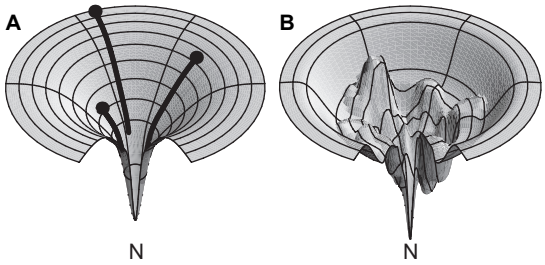

Figure 1.2 Schematic representations of funnel-shaped folding energy landscapes. Folding funnels show the free energy of folding as a function of conformational entropy. The native conformation (i.e., the conformation with the lowest free energy) is labelled N. (A) Idealised funnel landscape. As the chain forms increasing numbers of intra-chain contacts, and lowers its internal free energy, its conformational freedom is also reduced. All unfolded conformations have direct and kinetically identical folding paths towards the native state. (B) A rugged energy landscape with kinetic traps, energy barriers and some narrow throughway paths to the native state. Folding can be multi-state. Figures are adapted from (Dill and Chan 1997).

Idealised folding funnels are smooth, and have direct and kinetically identical folding routes from any unfolded conformation to the native state (Figure 1.2A). Although folding energy landscapes have evolved to be as smooth as possible in order to favour unbridled folding, local energetic minima cause folding energy landscapes to be rugged. These minima cause kinetic traps and barriers and are associated with formation of intermediate states (Figure 1.2B). Intermediate folding states are distinguished in terms of being on- or off-pathway to the native state. On-pathway intermediates form *en route* to the native state, whereas off-pathway folding intermediates form stable contacts that need to be disrupted before the native state can be formed. Folding intermediates form transiently along folding pathways of most proteins (Brockwell and Radford 2007). Often, early kinetic

folding intermediates resemble molten globules (Ohgushi and Wada 1983; Ptitsyn, Pain et al. 1990; Christensen and Pain 1991; Arai and Kuwajima 2000). Molten globules are ensembles of relatively compact interconverting protein conformers that contain substantial secondary structure, but lack the tertiary packing characteristics of a native protein molecule. These folding species have loosely packed cores and exposed hydrophobic residues, which render them prone to aggregation.

Protein folding in vivo

In vivo, protein molecules fold in the presence of 300 – 400 g l^{-1} of biological macromolecules (Zimmerman and Trach 1991). This crowded environment considerably enhances protein aggregation, particularly in the case of molten globules (van den Berg, Ellis et al. 1999; Engel, Westphal et al. 2008). To counter these effects, mechanisms exist that 'chaperone' folding of protein molecules (see e.g. (Hartl and Hayer-Hartl 2002)). Despite the presence of molecular chaperones *in vivo*, protein misfolding and aggregation still can occur. Deposition of insoluble protein aggregates is associated to for example Alzheimer's and Parkinson's disease, spongiform encephalopathies and type II diabetes (Dobson 2003; Chiti and Dobson 2006).

It is currently well established that many proteins do not fold to a well-defined structure under the conditions that exist in living cells. Such proteins are referred to as natively unfolded and intrinsically disordered (Uversky 2002). This class of proteins attracts considerable attention, because of their abstruse nature, and involvement in many biological processes and diseases (Uversky, Oldfield et al. 2008). Intrinsically disordered proteins may exist as collapsed molten globule-like conformations or as extended coils, and can become ordered upon interaction with other macromolecules, ligands, or by post-translational modifications (Uversky, Oldfield et al. 2008).

Apoflavodoxin folding

Folding of small single-domain proteins of less than 100 amino acid residues has been studied extensively and is generally well described by two-state equilibrium behaviour, in which only unfolded and native protein needs to be taken into account (Jackson 1998). Folding of larger proteins is complex and involves population of partially folded intermediate states, like molten globules. Such a folding species is prominent during folding of the 179-residue apoflavodoxin of this study.

Flavodoxins are small monomeric flavoproteins (15-20 kDa) that non-covalently, but tightly bind a flavin mononucleotide (FMN) cofactor. Binding of this cofactor allows flavodoxins to function as electron carriers in redox reaction pathways (Mayhew and Tollin 1992). Flavodoxin II (henceforth referred to as flavodoxin) from *Azotobacter vinelandii* is involved in the nitrogen fixation pathway of this bacterium (Yoch, Benemann et al. 1969; Klugkist, Voorberg et al. 1986). Native flavodoxin is

characterised by a central parallel β-sheet that is surrounded by α-helices. This structure is classified as the flavodoxin-like fold, which is an α-β parallel topology (Figure 1.3). Flavodoxins share this topology with many functionally and sequentially unrelated proteins, such as catalases, chemotactic proteins, cutinases, and esterases (Bollen and van Mierlo 2005).

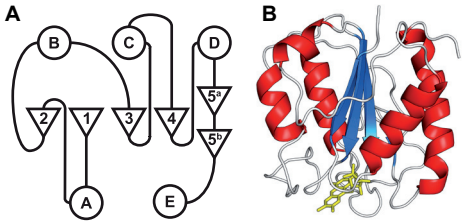

Figure 1.3 Flavodoxin-like topology and crystal structure of *A. vinelandii* flavodoxin II.
(A) The flavodoxin-like topology is characterised by a central parallel β-sheet that is flanked by α-helices on either side. (B) Cartoon rendering of the crystal structure of flavodoxin (pdb ID: 1YOB) (Alagaratnam, van Pouderoyen et al. 2005). α-Helices are shown in red, β-strands are shown in blue, the non-covalently bound FMN cofactor is shown in yellow. Cartoon rendering is generated with PyMOL (Schrödinger, LLC, Palo Alto, Ca, USA)

Binding of FMN is the last step in flavodoxin folding, because folding of native apoflavodoxin (i.e., flavodoxin without FMN) is independent of the cofactor (Bollen, Nabuurs et al. 2005). The three-dimensional structures of flavodoxin and apoflavodoxin are identical, apart from dynamic disorder in apoflavodoxin's FMN binding site (Steensma, Nijman et al. 1998; Steensma and van Mierlo 1998). Kinetic folding of apoflavodoxin involves formation of both on- and off-pathway intermediates and is described by Scheme 1.1 (Bollen, Sanchéz et al. 2004):

$$I_{off} \rightleftharpoons \textit{Unfolded apoflavodoxin} \rightleftharpoons I_{on} \rightleftharpoons \textit{Native apoflavodoxin} \quad \text{[Scheme 1.1]}$$

On-pathway intermediate I_{on} is an obligatory, high energy folding intermediate that rapidly forms native apoflavodoxin. Therefore this folding intermediate does not populate during denaturant-dependent equilibrium folding of apoflavodoxin. In contrast, off-pathway intermediate I_{off} is a relatively stable folding species. Approximately 90 % of unfolded molecules temporarily adopt this molten globule conformation upon lifting of denaturing conditions, before they fold to the native state. This intermediate state populates considerably during apoflavodoxin's denaturant-dependent folding equilibrium, which is described by Scheme 1.2:

$$I_{off} \rightleftharpoons \textit{Unfolded apoflavodoxin} \rightleftharpoons \textit{Native apoflavodoxin} \quad \text{[Scheme 1.2]}$$

Fitting of a three-state model for protein folding to equilibrium folding data as measured by tryptophan fluorescence and Circular Dichroism (CD) reveals that the folding state that corresponds to I_{off} populates considerably between 1 and 3.4 M GuHCl (Figure 1.4) (van Mierlo, van Dongen et al. 1998; Bollen, Sanchéz et al. 2004). Formation of such an off-pathway folding intermediate appears to be

a characteristic feature of proteins with α-β parallel topologies (Bollen and van Mierlo 2005), because it also has been observed for apoflavodoxin from *Anabaena* (Fernandez-Recio, Genzor et al. 2001), cutinase (Otzen, Giehm et al. 2007), chemotactic protein CheY (Kathuria, Day et al. 2008), and UMP/CMP kinase (Lorenz and Reinstein 2008).

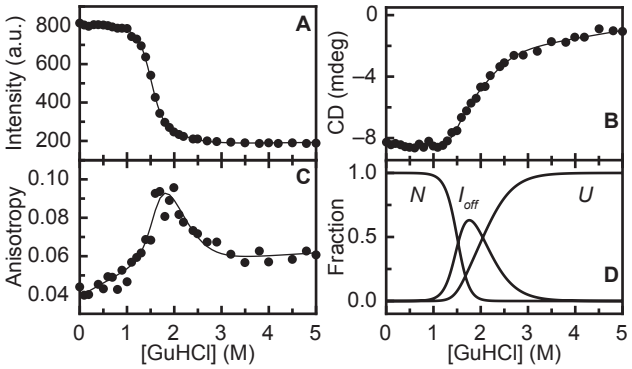

Figure 1.4 Denaturant-dependent equilibrium folding shows involvement of an intermediate during apoflavodoxin folding (Bollen, Sanchéz et al. 2004). (A) Fluorescence emission intensity of tryptophan detected at 340 nm upon excitation at 280 nm. (B) CD signal at 222 nm. (C) Fluorescence anisotropy data detected with a 335 nm cut-off filter, excitation is at 300 nm. Solid lines in panels A to C are the result of a global fit of a three-state model for equilibrium (un)folding. (D) Normalised fractions of native (N), off-pathway intermediate (I_{off}), and unfolded (U) apoflavodoxin as a function of denaturant concentration. Protein concentration is 5.6 μM in 100 mM potassium pyrophosphate, pH 6.0, and data are recorded at 25 °C.

Whereas folding of native apoflavodoxin is highly cooperative, the off-pathway intermediate forms non-cooperatively (van Mierlo, van den Oever et al. 2000; Nabuurs, Westphal et al. 2009). Apoflavodoxin's off-pathway intermediate has molten globule-like characteristics, and aggregates severely at elevated protein concentrations and under conditions that mimic the crowded intracellular environment (Engel, Westphal et al. 2008). Conformational dynamics of this molten globule on the micro to millisecond timescale render it undetectable to NMR spectroscopy (van Mierlo, van den Oever et al. 2000; Nabuurs, Westphal et al. 2009).

Characterisation of the unfolded state of apoflavodoxin using NMR spectroscopy reveals that four ordered regions form upon decreasing denaturant concentration (Figure 1.5). Three of these regions within the unfolded protein form α-helical structure, whereas one of these regions is neither α-helix nor β-sheet. These α-helices transiently interact upon formation of the molten globule. One of the α-helices that form in unfolded apoflavodoxin is part of the central parallel β-sheet of native apoflavodoxin (Nabuurs, Westphal et al. 2008; Nabuurs, Westphal et al. 2009). Using NMR spectroscopy to study the denaturant dependence of unfolded apoflavodoxin at the residue level reveals that structure formation in essentially all parts of unfolded apoflavodoxin precedes formation of the molten globule. Only a single region within the N-terminal part of the protein

maintains properties of unfolded apoflavodoxin at denaturant concentrations as low as 1.58 M GuHCl (Nabuurs, Westphal et al. 2009; Nabuurs and van Mierlo 2010).

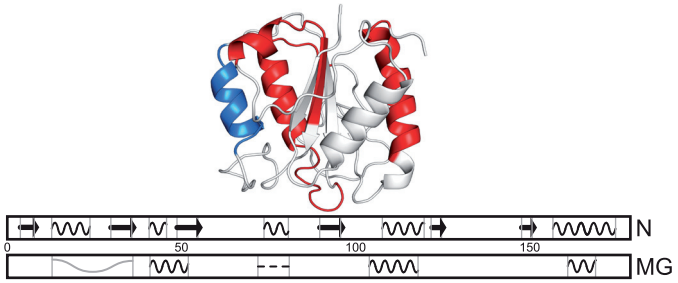

Figure 1.5. The topologies of native and molten globule apoflavodoxin differ. Top: cartoon drawing of native apoflavodoxin, which shows in red regions that transiently form α-helices in unfolded apoflavodoxin at 3.4 M GuHCl, and in blue the region of apoflavodoxin that has restricted flexibility at 3.4 M GuHCl, but that forms neither α helical nor β-strand (Nabuurs, Westphal et al. 2008). Transient interaction between these structured elements leads to formation of the core of the molten globule (Nabuurs, Westphal et al. 2009). Bottom: topologies of native (N) and molten globule (MG) apoflavodoxin. Waves indicate α-helices and arrows highlight β-strands. The dashed line represents the region that forms neither α-helical nor β-strand structure, and the grey wiggle highlights the region of the molten globule that has random coil properties down to 1.58 M GuHCl (Nabuurs, Westphal et al. 2009).

Destabilisation of apoflavodoxin's native state by introduction of a single oxygen atom into a hydrophobic pocket within the protein (i.e. the Phe44Tyr mutation) results in considerable population of this molten globule intermediate state under near-native conditions. Characterisation of this folding intermediate shows that it is predominantly α-helical and lacks β-sheet structure and reveals that this molten globule is almost completely structured in absence of denaturant (Nabuurs, Westphal et al. 2009; Nabuurs and van Mierlo 2010).

Thus far, insight into apoflavodoxin's molten globule has been mainly obtained by methods that either indirectly detect this folding species or infer its properties by employing fitting of a three-state model for protein folding. Direct characterisation of molten globules is hampered by the often transient nature of their existence, their usually relatively low population at equilibrium, and their tendency to aggregate at high protein concentrations (Jaenicke and Seckler 1997). Illuminating the formation and conformational properties of apoflavodoxin's molten globule requires use of methods that efficiently and directly detect this folding species, and are able to elucidate the heterogeneity of the protein folding process. Single-molecule fluorescence spectroscopy and Förster Resonance Energy Transfer are well suited for this purpose.

Fluorescence

Fluorescence spectroscopy is arguably the most versatile tool in studying protein folding (Royer 2006; Bartlett and Radford 2009). On the one hand, fluorescence spectroscopy is a sensitive technique, which enables the use of low (i.e., sub-micromolar) protein concentrations. Often, at these low concentrations, protein solubility and aggregation issues are negligible. On the other hand fluorescent molecules typically sense changes in their local environment. This property makes fluorescence particularly useful for monitoring folding-induced changes.

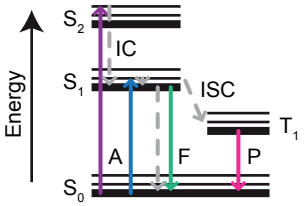

Figure 1.6 Jablonski diagram. Electronic states (S_n) are depicted as thick lines, and thin lines indicate vibrational energy levels. Upward arrows correspond to absorption of a photon (A). Dashed arrows indicate non-radiative processes, which are internal conversion (IC) and intersystem crossing (ISC) to the first triplet state (T_1). Downward solid arrows show fluorescence emission of a photon from S_1 (F) and phosphorescence emission of a photon from T_1 (P) (adapted from (Lakowicz 2006)).

Fluorescence is the emission of a photon that occurs as an electron relaxes from an excited singlet state to its ground state. This process is schematically depicted using a Jablonski diagram (Figure 1.6). Excitation of an electron from ground state S_0 to an excited singlet state (i.e., S_1 or S_2, or a corresponding vibrational level) is established by absorption of a photon with sufficiently high energy (i.e., at an appropriate wavelength). The excited electron then rapidly relaxes to the lowest vibrational level of S_1. Relaxation from S_1 to S_0 can occur by non-radiative processes (e.g., internal conversion and quenching), or by radiative relaxation (i.e., emission of a fluorescence photon). Alternatively, intersystem crossing to the first triplet state T_1 can occur, which eventually results in emission of a phosphorescence photon (Lakowicz 2006).

Several non-radiative relaxation processes compete with radiative relaxation processes (i.e., fluorescence) during the excited state lifetime of a molecule (i.e., the time that the excited electron spends in S_1) (Figure 1.6). The excited state lifetime of a fluorophore is described by:

$$\tau = \frac{1}{k_r + k_{nr}} \qquad [1.1]$$

in which k_r and k_{nr} are the rate constants (s^{-1}) for radiative and non-radiative deexcitation processes, respectively.

Fluorescence quantum yield is the ratio of the radiative relaxation rate to the sum of all de-excitation rates, according to equation 1.2:

$$Q = \frac{k_r}{k_r + k_{nr}} \qquad [1.2]$$

Fluorescence lifetime and fluorescence quantum yield of a fluorophore are intimately linked. Thus, alterations of k_r or k_{nr} lead to changes in both fluorescence lifetime and fluorescence quantum yield, and therefore also affect fluorescence intensity (i.e., the number of photons observed during a particular time span).

Rotational diffusion of an excited fluorophore during its excited state lifetime brings about a difference in polarisation of emitted light as compared to excitation light. This phenomenon is exploited in measurement of fluorescence anisotropy, and gives insight into for example the dimensions of the molecule involved and viscosity of its environment (Lakowicz 2006). Rotational diffusion of solvent molecules is typically orders of magnitude faster than rotational diffusion of a fluorophore. Solvent molecules in proximity of a fluorophore sense the change in dipole moment of the fluorophore upon excitation. Rapid reorientation of solvent molecules around the excited-state dipole attenuates the energy difference between S_1 and S_0. Hence, fluorescence emission spectra are shifted towards higher wavelengths compared to the corresponding excitation spectra. This sensitivity of fluorescence emission spectra can be used to track folding-induced changes in local environment of a fluorophore. For instance, fluorescence emission of tryptophan residues that reside within the hydrophobic environment of a folded protein typically occurs at lower wavelengths than fluorescence emission of tryptophan residues that are exposed to aqueous solutions (Lakowicz 2006).

Processes that cause a decrease in fluorescence intensity and fluorescence lifetime of a fluorophore are generally referred to as quenching of fluorescence. If quenching is the result of interaction between a fluorophore and quencher that pertains during the excited state lifetime of the fluorophore, it is referred to as static quenching. This quenching involves formation of a non-fluorescent ground state complex, which instantaneously returns to the ground state upon excitation. Static quenching causes diminishing of fluorescence intensity, but does not affect fluorescence lifetimes (Lakowicz 2006). In contrast, transient collision of an excited fluorophore with quencher molecules during the excited state lifetime of a fluorophore establishes an additional non-radiative decay path from the excited state. This 'dynamic' quenching causes a proportional decrease in fluorescence lifetime and fluorescence intensity, because lifetimes and quantum yields are related.

Förster Resonance Energy Transfer

Förster Resonance Energy Transfer (FRET) is the distance dependent transfer of electronic excitation energy from a donor molecule in the excited state to an acceptor molecule in the ground state through dipole-dipole interactions. FRET establishes an additional non-radiative decay path for an excited fluorophore (Figure 1.7). The rate of energy transfer (k_t) is related to the distance between donor and acceptor through equation 1.3:

$$k_t = \tau_D^{-1}\left(R_0 / r\right)^6 \qquad [1.3]$$

in which r is the actual distance between donor and acceptor, τ_D is the fluorescence lifetime of donor in absence of acceptor and R_0 is the Förster distance (Förster 1948) (see below). The efficiency of energy transfer can be determined experimentally from the relative decrease in donor fluorescence intensity and/or fluorescence lifetime due to presence of an acceptor, by using equation 1.4:

$$E = 1 - \frac{I_{DA}}{I_D} = 1 - \frac{\tau_{DA}}{\tau_D} \qquad [1.4]$$

in which I is the fluorescence intensity, τ is the fluorescence lifetime and subscripts *DA* and *D* indicate donor signal in presence and absence of acceptor, respectively.

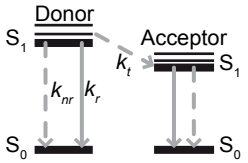

Figure 1.7 Jablonski diagram for donor and acceptor in close proximity. The excited donor can relax to its ground state by emission of a photon with associated rate constant k_r (solid arrow), non-radiative decay with associated rate constant k_{nr} (dashed arrow), or by Förster Resonance Energy Transfer with associated rate constant k_t, followed by excitation of the acceptor, which then may emit a photon, depending on fluorescence quantum yield of acceptor.

The efficiency of energy transfer (E) depends on the inverse sixth power of the distance between donor and acceptor, as described by equation 1.5:

$$E = \frac{1}{1 + \left(r / R_0\right)^6} \qquad [1.5]$$

Energy transfer efficiencies change strongly as function of D-to-A distance (r) in the range of $0.5 \times R_0 < r < 2 \times R_0$ (Figure 1.8). This steep dependency of FRET efficiency on r enables monitoring of distances between donor and acceptor that typically fall in between 1 and 10 nm. Thus, FRET can be used as a 'spectroscopic ruler' (Förster 1948; Stryer and Haugland 1967; Steinberg 1971).

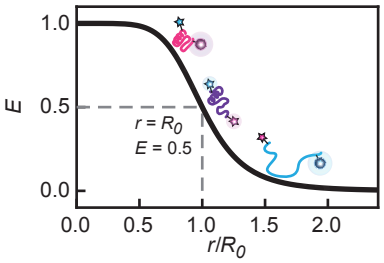

Figure 1.8 Dependence of the efficiency of energy transfer (*E*) on the distance (*r*) between donor and acceptor. The horizontal axis shows the distance relative to the Förster distance (R_0). Different inter-dye separations, and thus FRET efficiencies, characterise native molecules (magenta), folding intermediate (purple) and unfolded protein (blue). Fluorescence emission intensities of donor (blue star) and acceptor (magenta star) vary accordingly.

R_0 is the distance corresponding an energy transfer efficiency of 50 %, and is defined by equation 1.6:

$$R_0 = 0.211\left(Q_D n^{-4} \kappa^2 J(\lambda)\right)^{1/6} \qquad [1.6]$$

in which R_0 is the Förster distance in Å, Q_D is the donor fluorescence quantum yield, n is the refractive index of the medium intervening donor and acceptor (Knox and van Amerongen 2002), κ^2 represents the relative orientation between donor and acceptor transition dipoles, and $J(\lambda)$ (M^{-1} cm^{-1} nm^4) expresses the overlap between donor emission spectrum and acceptor absorption spectrum (equation 1.7).

$$J(\lambda) = \int_0^\infty F_D(\lambda)\varepsilon_A(\lambda)\lambda^4 \, d\lambda \qquad [1.7]$$

in which $F_D(\lambda)$ is the normalised emission spectrum of donor and $\varepsilon_A(\lambda)$ is the molar extinction coefficient (M^{-1} cm^{-1}) of acceptor as function of wavelength λ. Figure 1.9 shows an example of overlap between fluorescence emission spectrum of a donor and the absorption spectrum of an acceptor.

Equation 1.4 shows that the acceptor used in FRET studies does not need to be fluorescent. However, when the acceptor is fluorescent it will emit photons upon excitation of the donor. This sensitised acceptor emission is frequently used as readout for FRET because it is proportional to the efficiency of energy transfer.

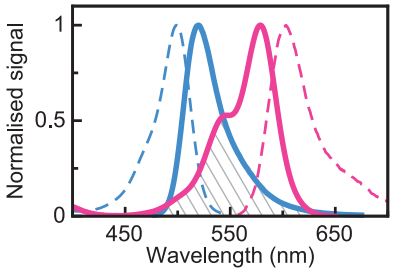

Figure 1.9 Spectral overlap between fluorescence emission of a donor and absorption of an acceptor. Spectral data of the Alexa Fluor 488 (donor) and Alexa Fluor 568 (acceptor) FRET pair are shown (Invitrogen). Donor absorption spectrum is shown as dashed blue line, donor fluorescence emission spectrum as solid blue line, acceptor absorption spectrum as solid magenta line, and acceptor emission spectrum as dashed magenta line. All spectra are normalised to their respective maximum. The hatched area indicates spectral overlap between donor fluorescence emission and acceptor absorption.

Dipole orientation factor κ^2 relates the orientation of donor emission transition dipole relative to acceptor absorption transition dipole according to equations 1.8 and 1.9:

$$\kappa^2 = \left(\cos\theta_T - 3\cos\theta_D\cos\theta_A\right)^2 \quad [1.8]$$

$$\kappa^2 = \left(\sin\theta_D\sin\theta_A\cos\varphi - 2\cos\theta_D\cos\theta_A\right)^2 \quad [1.9]$$

in which θ_T is the angle between donor emission transition dipole and acceptor absorption transition dipole, θ_D and θ_A are the angles between these dipoles and the vector joining donor and acceptor, and φ is the angle between projections of these dipoles on planes perpendicular to the vector joining them (Lakowicz 2006) (Figure 1.10). κ^2 Can range from 0 to 4, in case of randomised orientation of donor and acceptor transition dipoles during the excited state lifetime of the donor κ^2= 2/3 (Lakowicz 2006).

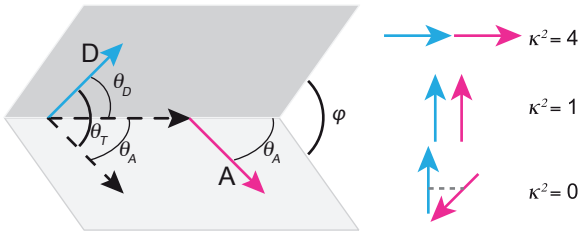

Figure 1.10 Orientations of donor (D) emission and acceptor (A) absorption transition dipoles. Donor and acceptor dipoles are depicted as blue and magenta arrows, respectively. θ_T is the angle between donor emission transition dipole and acceptor absorption transition dipole, θ_D and θ_A are the angles between these dipoles and the vector joining the donor and the acceptor, and φ is the angle between projections of these dipoles on planes perpendicular to the vector joining them. Effect of dipole orientation on the value of κ^2 is shown on the right.

Labelling of proteins with fluorescence dyes facilitates use of FRET to study protein folding

FRET is particularly useful for studying protein conformation and conformational dynamics, because of the steep dependency of energy transfer efficiency on distance between donor and acceptor in the nanometre regime (see e.g., (Steinberg 1971; Amir and Haas 1987; Amir and Haas 1988; Haran, Haas et al. 1992; Sinev, Sineva et al. 1996)) for protein folding (see e.g., (Mcwherter, Haas et al. 1986; Nishimura, Riley et al. 2000; Lakshmikanth, Sridevi et al. 2001; Ratner, Amir et al. 2005; Orevi, Ishay et al. 2009)). Compared to using of intrinsic fluorophores like tryptophan, labelling of proteins with fluorescent donor and acceptor dyes considerably facilitates the use of FRET to study protein folding. Ideally, donor and acceptor dyes have high molar extinction coefficients and high fluorescence quantum yields. In addition, donor fluorescence emission spectrum and acceptor absorption spectrum should overlap significantly and be well separated to enable separate excitation and detection of donor and acceptor (Figure 1.9).

Attachment of donor and acceptor to the protein of interest is preferably site-specific, because properties of fluorescent molecules are often affected by changes in their local environment. Several methods for site-specific modification of proteins exist (Pennington 1994; Schuler and Pannell 2002; Brustad, Lemke et al. 2008; Popp, Antos et al. 2009; Sunbul and Yin 2009). A commonly used approach is to covalently attach fluorescent dye-labels to cysteine residues (Haran, Haas et al. 1992; Pennington 1994; Sinev, Sineva et al. 1996; Sinev, Landsmann et al. 2000). The unique reactive properties of the sulphhydryl group of this amino acid enable its selective modification. Furthermore, natural abundance of cysteine residues is relatively low. Consequently, site-directed mutagenesis approaches can be used to introduce cysteine residues into specific sites of the protein of interest or remove them from sites where they are not required. Selective labelling of two cysteine residues within one protein can be achieved when reaction conditions are found in which the reactivity or accessibility of these residues towards the reactive group of a particular label differs significantly (Ratner, Kahana et al. 2002; Jacob, Amir et al. 2005; Kuiper, Pluta et al. 2009; Puljung and Zagotta 2011). After labelling of a specific cysteine residue, singly dye-labelled protein can be purified by affinity chromatography approaches, such as ion exchange and hydrophobic interaction chromatography. Subsequent labelling of the second cysteine is established after modification of labelling conditions, e.g., by denaturant-induced unfolding of singly labelled protein.

Single-molecule FRET

'Classical' fluorescence and FRET approaches to study denaturant-dependent protein folding equilibria and kinetics provide ensemble-averaged data: i.e., the corresponding fluorescence signal is the result of averaging of fluorescent properties over the whole population of folding molecules

(Figure 1.11A-C). This averaging obscures underlying complexities and conformational dynamics. Direct assessment of heterogeneity that exists within an ensemble of folding molecules is achieved by using single-molecule fluorescence spectroscopy (Deniz, Dahan et al. 1999; Ha, Ting et al. 1999; Ha, Ting et al. 1999; Deniz, Laurence et al. 2000; Schuler, Lipman et al. 2002).

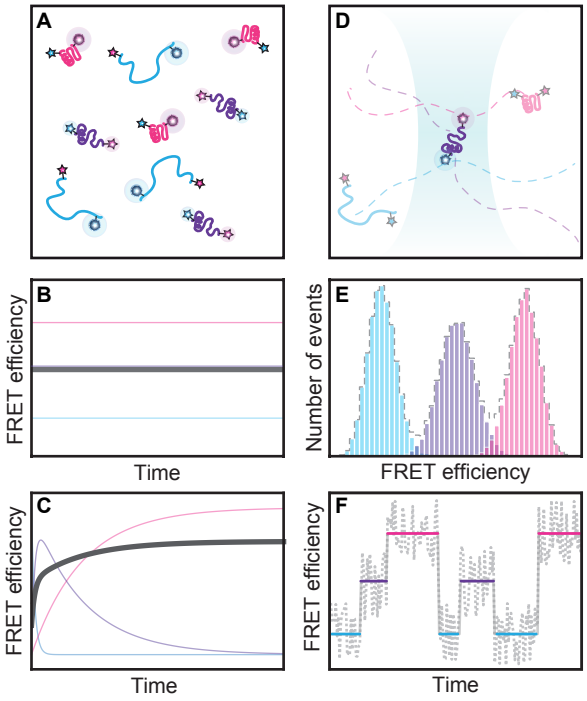

Figure 1.11 Ensemble averaging versus single-molecule detection. Folded protein (magenta), folding intermediate (purple), and unfolded protein (blue) are characterised by high, intermediate and low FRET efficiencies, respectively (see Figure 1.8). In the following, corresponding signals are coloured accordingly. (A) Simultaneous excitation of many molecules. (B) Under equilibrium conditions, each folding species is characterised by a specific FRET efficiency, whereas an ensemble-averaged signal is recorded (solid grey line). (C) Rapid lifting of denaturing conditions at $t = 0$ induces folding, of which the kinetics can be monitored in time. In this example, the ensemble averaged FRET efficiency as function of time (solid grey line) reveals a bi-exponential trend, from which populations of folding species (coloured lines) can be inferred. (D) Single-molecule detection employs focussing of a laser into a solution to obtain a femtolitre sized excitation spot. Only molecules that diffuse (dashed paths) into the laser spot are observed. Conformational heterogeneity can be resolved by registering FRET efficiencies of many molecules (proteins and laser spot are not drawn to scale). (E) smFRET Histograms show the number of events corresponding to a particular FRET efficiency, and reveal populations of three thermodynamic states. (F) Inter-conversion between folding states can be detected in FRET trajectories during prolonged observation of single immobilised molecules.

Single-molecule (sm) FRET employs focussing of laser light into a solution of doubly dye-labelled protein, whereby an excitation spot of micrometre dimensions is obtained (Figure 1.11D). Only in this laser spot, donor fluorophore of doubly dye-labelled protein is efficiently excited. Photons emitted by molecules that are present in the laser spot are collected in detection channels that correspond to wavelengths of donor and acceptor, respectively. Subsequently, the apparent FRET efficiency (E_{app}) is calculated using equation 1.10:

$$E_{app} = \frac{n_A}{n_A + n_D} \qquad [1.10]$$

in which n_A and n_D are the number of acceptor and donor photons detected, respectively. In contrast to traditional methods that employ fluorescent signals of donor both in presence and absence of acceptor to calculate the corresponding FRET efficiency (equation 1.4), calculation of E_{app} uses fluorescence emission from both donor and acceptor of doubly dye-labelled molecules. With identical detection efficiencies and fluorescence quantum yields of donor and acceptor, E_{app}equals E.

The most straightforward smFRET approach to study protein folding uses freely diffusing doubly dye-labelled molecules. Protein concentration in such an smFRET experiment is in the picomolar range, which ensures that the probability of two molecules being present in the excitation volume is negligible. Frequently, an individual molecule diffuses into the laser focus, which gives rise to a burst of fluorescence photons from which the FRET efficiency can be calculated. By obtaining fluorescence bursts from thousands of molecules, smFRET efficiency histograms can be constructed (Figure 1.11E). The number of distributions in an smFRET histogram corresponds to the minimum of thermodynamic states that populate at a specific concentration of denaturant. Thus, smFRET histograms give model free insight into conformational heterogeneity that exists within the ensemble of folding molecules (Schuler, Lipman et al. 2002). smFRET histograms generally reveal two distributions in the transition region of folding. One of these distributions is found at high FRET efficiency and corresponds to native protein; the other one is found at lower FRET efficiency and arises from unfolded protein. Upon folding, the amplitude of the distribution corresponding to the unfolded state decreases, and concomitantly the amplitude of the distribution corresponding to the native state increases, as observed for e.g., cold-shock protein (Schuler, Lipman et al. 2002), chymotrypsin inhibitor 2 (Deniz, Laurence et al. 2000; Laurence, Kong et al. 2005), acyl-CoA-binding protein (Laurence, Kong et al. 2005), ribonuclease H (Kuzmenkina, Heyes et al. 2005; Kuzmenkina, Heyes et al. 2006), protein A (Huang, Sato et al. 2007), protein L (Sherman and Haran 2006) and immunity protein Im9 (Tezuka-Kawakami, Gell et al. 2006).

smFRET approaches that employ immobilised molecules, effectively keep labelled molecules in the focussed laser and thereby prolong the observation time of these molecules. This enables monitoring of transitions between folded, folding intermediate and unfolded molecules (Figure 1.11F). Protein can be immobilised through coupling to a functionalised surface (Kuzmenkina, Heyes et al. 2006). Alternatively, a protein molecule can be encapsulated in a surface tethered lipid vesicle, where it is able to freely diffuse within the confined space of the vesicle (Boukobza, Sonnenfeld et al. 2001). Photon trajectories obtained from these immobilised molecules give detailed insight into protein folding kinetics, and transient population of folding intermediate states (Talaga, Lau et al. 2000; Rhoades, Gussakovsky et al. 2003; Rhoades, Cohen et al. 2004; Kuzmenkina, Heyes et al. 2005; Chung, Louis et al. 2009; Pirchi, Ziv et al. 2011).

Outline of this thesis

This thesis describes the visualisation and characterisation of apoflavodoxin folding by (single-molecule) fluorescence spectroscopy and FRET. To enable monitoring of denaturant-dependent conformational changes during apoflavodoxin folding by this methodology, requires labelling of the protein with appropriate fluorescent donor and acceptor dyes.

Cysteine residues are commonly used targets for dye labelling of proteins. These residues are generally sensitive to irreversible oxidation under conditions of oxidative stress, which is linked to disease and aging (Ames, Shigenaga et al. 1993; Chao, Ma et al. 1997; Stadtman and Berlett 1998). However, cysteine oxidation has also been identified as a common and functional post-translational modification for *in vivo* regulation of protein function (Perez, Bokov et al. 2009). **Chapter 2** describes the effects of hydrogen peroxide-induced oxidative stress on flavodoxin and apoflavodoxin. The single cysteine of flavodoxin (i.e., Cys69) resides near the flavin cofactor in a loop that is functionally important (Peelen, Wijmenga et al. 1996). Replacement of Cys69 with Ala shows that this cysteine does not affect the redox properties of protein-bound FMN (Steensma, Heering et al. 1996). However, Cys69 turns out to be oxidation sensitive. Oxidative stress causes dimerisation of apoflavodoxin and leads to consecutive formation of sulphenic, sulphinic and sulphonic acid states of Cys69. In contrast, in case of flavodoxin, oxidation beyond the sulphenic acid state is not detected. Under the conditions used, flavodoxin does not form dimers and its Cys69 is considerably less susceptible to covalent modification than in apoflavodoxin. Besides its primary role as redox-active moiety, FMN considerably improves flavodoxin's stability against unfolding and protects the protein against irreversible oxidation and other covalent thiol modifications.

Chapter 3 describes labelling of Cys69 with the commonly used FRET donor fluorophore Alexa Fluor 488 (A488). Ideally, fluorescence parameters of fluorescent labels used in FRET studies solely report on changes in distance between donor and acceptor. However, often, changes in local

environments of these dyes affect their fluorescence properties, which profoundly complicate interpretation of FRET. Coupling of A488 to apoflavodoxin results in a slight destabilisation of native apoflavodoxin, but the three-state folding characteristics of this protein, which involves a molten globule-like intermediate, are preserved. Folding induced changes in A488 fluorescence are characterised. Fluorescence emission intensity of A488 changes significantly upon folding of apoflavodoxin. Use of time-resolved and steady state fluorescence spectroscopy approaches provides insight into the mechanisms that underlie folding induced changes of A488 fluorescence properties.

Covalent labelling of proteins with fluorescent donor and acceptor labels enables the use of FRET to probe conformational changes during folding. To enable double dye labelling of apoflavodoxin, an additional cysteine residue is introduced into the protein, either on position 1, 131 or 178 (**Chapter 4**). Exploiting the attenuated reactivity of Cys69 in cofactor bound protein enables selective labelling of the introduced cysteine residue with acceptor label Alexa Fluor 568 (A568) and labelling of Cys69 with donor A488. Thus, a1-d69-, d69-a131-, and d69-a178-apoflavodoxin are generated. Subsequently, fluorescence spectroscopy and FRET are used to monitor folding-induced conformational changes within different parts of apoflavodoxin. Folding of each of the doubly dye-labelled apoflavodoxin variants involves formation of a stable folding intermediate, like is the case for non-labelled apoflavodoxin. Use of FRET as a qualitative spectroscopic ruler reveals that the N-terminal 69 residues of apoflavodoxin's molten globule fold last and that striking conformational differences exist between molten globule and native protein. Shorter inter-label distances are sampled within the 111-residue C-terminal segment of the ensemble of molten globule-like conformers than in native apoflavodoxin. Thus, ensemble FRET sheds light on the off-pathway nature of the molten globule during folding of an α-β parallel protein.

The major change in FRET-efficiency upon apoflavodoxin folding is due to the transition from unfolded to molten globule protein. To gain direct, model-free insight into conformational heterogeneity that exists within the transition region of denaturant-dependent apoflavodoxin folding, single-molecule fluorescence spectroscopy and FRET (smFRET) are used (**Chapter 5**). smFRET histograms of doubly dye-labelled protein variants that report on formation of the ordered core of apoflavodoxin's molten globule (i.e., d69-a131 and d69-a178) are recorded at several concentrations denaturant. Remarkably, at all denaturant concentrations used, a single smFRET efficiency distribution is observed in each histogram. Despite this unimodality, all three apoflavodoxin folding species are tracked, because (i) the plot of the average smFRET efficiency versus concentration denaturant reports a biphasic folding curve, and (ii) unfolding of native apoflavodoxin coincides with broadening of the corresponding smFRET histogram. Starting with unfolded apoflavodoxin,

smFRET exposes that upon lowering of denaturant concentration formation of the molten globule folding intermediate is strongly favoured. Upon folding of the molten globule, the unimodal smFRET efficiency distribution gradually shifts to larger FRET value due to progressive extension of its ordered core. This non-cooperative compaction happens during folding of every single molten globule molecule. Consequently, during kinetic folding of unfolded apoflavodoxin molecules, they swiftly form this molten globule upon lifting denaturing conditions.

References

Alagaratnam, S., G. van Pouderoyen, et al. (2005). "A crystallographic study of Cys69Ala flavodoxin II from *Azotobacter vinelandii*: structural determinants of redox potential." Protein Sci. 14(9): 2284-2295.

Alexander, P. A., Y. A. He, et al. (2009). "A minimal sequence code for switching protein structure and function." Proc. Natl. Acad. Sci. U.S.A. 106(50): 21149-21154.

Ames, B. N., M. K. Shigenaga, et al. (1993). "Oxidants, Antioxidants, and the Degenerative Diseases of Aging." Proc. Natl. Acad. Sci. U.S.A. 90(17): 7915-7922.

Amir, D. and E. Haas (1987). "Estimation of Intramolecular Distance Distributions in Bovine Pancreatic Trypsin-Inhibitor by Site-Specific Labeling and Nonradiative Excitation Energy-Transfer Measurements." Biochemistry 26(8): 2162-2175.

Amir, D. and E. Haas (1988). "Reduced Bovine Pancreatic Trypsin-Inhibitor Has a Compact Structure." Biochemistry 27(25): 8889-8893.

Anfinsen, C. B. (1973). "Principles that govern the folding of protein chains." Science 181(4096): 223-230.

Arai, M. and K. Kuwajima (2000). "Role of the molten globule state in protein folding." Adv. Protein. Chem. 53: 209-282.

Bartlett, A. I. and S. E. Radford (2009). "An expanding arsenal of experimental methods yields an explosion of insights into protein folding mechanisms." Nat. Struct. Mol. Biol. 16(6): 582-588.

Bollen, Y. J., I. E. Sanchéz, et al. (2004). "Formation of on- and off-pathway intermediates in the folding kinetics of *Azotobacter vinelandii* apoflavodoxin." Biochemistry 43(32): 10475-10489.

Bollen, Y. J. and C. P. van Mierlo (2005). "Protein topology affects the appearance of intermediates during the folding of proteins with a flavodoxin-like fold." Biophys. Chem. 114(2-3): 181-189.

Bollen, Y. J. M., S. M. Nabuurs, et al. (2005). "Last in, first out." J. Biol. Chem. 280(9): 7836-7844.

Boukobza, E., A. Sonnenfeld, et al. (2001). "Immobilization in surface-tethered lipid vesicles as a new tool for single biomolecule spectroscopy." J. Phys. Chem. B 105(48): 12165-12170.

Brockwell, D. J. and S. E. Radford (2007). "Intermediates: ubiquitous species on folding energy landscapes?" Curr. Opin. Struct. Biol. 17(1): 30-37.

Brustad, E. M., E. A. Lemke, et al. (2008). "A general and efficient method for the site-specific dual-labeling of proteins for single molecule fluorescence resonance energy transfer." J. Am. Chem. Soc. 130(52): 17664-17665.

Bryan, P. N. and J. Orban (2010). "Proteins that switch folds." Curr. Opin. Struct. Biol. 20(4): 482-488.

Bryngelson, J. D., J. N. Onuchic, et al. (1995). "Funnels, pathways, and the energy landscape of protein folding: a synthesis." Proteins Struct. Funct. Bioinf. 21(3): 167-195.

Chao, C. C., Y. S. Ma, et al. (1997). "Modification of protein surface hydrophobicity and methionine oxidation by oxidative systems." Proc. Natl. Acad. Sci. U.S.A. 94(7): 2969-2974.

Chiti, F. and C. M. Dobson (2006). "Protein misfolding, functional amyloid, and human disease." Annu. Rev. Biochem. 75: 333-366.

Christensen, H. and R. H. Pain (1991). "Molten Globule Intermediates and Protein Folding." Eur. Biophys. J. 19(5): 221-229.

Chung, H. S., J. M. Louis, et al. (2009). "Experimental determination of upper bound for transition path times in protein folding from single-molecule photon-by-photon trajectories." Proc. Natl. Acad. Sci. U.S.A. 106(29): 11837-11844.

Davidson, A. R. (2008). "A folding space odyssey." Proc. Natl. Acad. Sci. U.S.A. 105(8): 2759-2760.

Deniz, A. A., M. Dahan, et al. (1999). "Single-pair fluorescence resonance energy transfer on freely diffusing molecules: Observation of Forster distance dependence and subpopulations." Proc. Natl. Acad. Sci. U.S.A. 96(7): 3670-3675.

Deniz, A. A., T. A. Laurence, et al. (2000). "Single-molecule protein folding: Diffusion fluorescence resonance energy transfer studies of the denaturation of chymotrypsin inhibitor 2." Proc. Natl. Acad. Sci. U.S.A. 97(10): 5179-5184.

Dill, K. A. and H. S. Chan (1997). "From Levinthal to pathways to funnels." Nat. Struct. Biol. 4(1): 10-19.

Dinner, A. R., A. Sali, et al. (2000). "Understanding protein folding via free-energy surfaces from theory and experiment." Trends Biochem. Sci. 25(7): 331-339.

Dobson, C. M. (2003). "Protein folding and misfolding." Nature 426(6968): 884-890.

Engel, R., A. H. Westphal, et al. (2008). "Macromolecular crowding compacts unfolded apoflavodoxin and causes severe aggregation of the off-pathway intermediate during apoflavodoxin folding." J. Biol. Chem. 283(41): 27383-27394.

Fernandez-Recio, J., C. G. Genzor, et al. (2001). "Apoflavodoxin folding mechanism: An alpha/beta protein with an essentially off-pathway Intermediate." Biochemistry 40(50): 15234-15245.

Fersht, A. R. and V. Daggett (2002). "Protein folding and unfolding at atomic resolution." Cell 108(4): 573-582.

Förster, T. (1948). "Zwischenmolekulare Energiewanderung Und Fluoreszenz." Ann. Phys. 2(1-2): 55-75.

Ha, T. J., A. Y. Ting, et al. (1999). "Single-molecule fluorescence spectroscopy of enzyme conformational dynamics and cleavage mechanism." Proc. Natl. Acad. Sci. U.S.A. 96(3): 893-898.

Ha, T. J., A. Y. Ting, et al. (1999). "Temporal fluctuations of fluorescence resonance energy transfer between two dyes conjugated to a single protein." Chem. Phys. 247(1): 107-118.

Haran, G., E. Haas, et al. (1992). "Domain Motions in Phosphoglycerate Kinase - Determination of Interdomain Distance Distributions by Site-Specific Labeling and Time-Resolved Fluorescence Energy-Transfer." Proc. Natl. Acad. Sci. U.S.A. 89(24): 11764-11768.

Hartl, F. U. and M. Hayer-Hartl (2002). "Protein folding - Molecular chaperones in the cytosol: from nascent chain to folded protein." Science 295(5561): 1852-1858.

Huang, F., S. Sato, et al. (2007). "Distinguishing between cooperative and unimodal downhill protein folding." Proc. Natl. Acad. Sci. U.S.A. 104(1): 123-127.

Jackson, S. E. (1998). "How do small single-domain proteins fold?" Fold Des. 3(4): R81-R91.

Jacob, M. H., D. Amir, et al. (2005). "Predicting reactivities of protein surface cysteines as part of a strategy for selective multiple labeling." Biochemistry 44(42): 13664-13672.

Jaenicke, R. and R. Seckler (1997). "Protein misassembly *in vitro*." Adv. Protein Chem. 50: 1-59.

Kathuria, S. V., I. J. Day, et al. (2008). "Kinetic traps in the folding of βα-repeat proteins: CheY initially misfolds before accessing the native conformation." J. Mol. Biol. 382(2): 467-484.

Kendrew, J. C., G. Bodo, et al. (1958). "3-Dimensional Model of the Myoglobin Molecule Obtained by X-Ray Analysis." Nature 181(4610): 662-666.

Klugkist, J., J. Voorberg, et al. (1986). "Characterization of 3 Different Flavodoxins from Azotobacter-Vinelandii." Eur. J. Biochem. 155(1): 33-40.

Knox, R. S. and H. van Amerongen (2002). "Refractive index dependence of the Förster resonance excitation transfer rate." J. Phys. Chem. B 106(20): 5289-5293.

Kuiper, J. M., R. Pluta, et al. (2009). "A method for site-specific labeling of multiple protein thiols." Protein Sci. 18(5): 1033-1041.

Kuzmenkina, E. V., C. D. Heyes, et al. (2005). "Single-molecule Forster resonance energy transfer study of protein dynamics under denaturing conditions." Proc. Natl. Acad. Sci. U.S.A. 102(43): 15471-15476.

Kuzmenkina, E. V., C. D. Heyes, et al. (2006). "Single-molecule FRET study of denaturant induced unfolding of RNase H." J. Mol. Biol. 357(1): 313-324.

Lakowicz, J. R. (2006). Principles of fluorescence spectroscopy. New York, Springer.

Lakshmikanth, G. S., K. Sridevi, et al. (2001). "Structure is lost incrementally during the unfolding of barstar." Nat. Struct. Biol. 8(9): 799-804.

Laurence, T. A., X. X. Kong, et al. (2005). "Probing structural heterogeneities and fluctuations of nucleic acids and denatured proteins." Proc. Natl. Acad. Sci. U.S.A. 102(48): 17348-17353.

Levinthal, C. (1968). "Are There Pathways for Protein Folding." J. Chim. Phys. 65(1): 44-&.

Lorenz, T. and J. Reinstein (2008). "The influence of proline isomerization and off-pathway intermediates on the folding mechanism of eukaryotic UMP/CMP kinase." J. Mol. Biol. 381(2): 443-455.

Mayhew, S. G. and G. Tollin (1992). Chemistry and Biochemistry of Flavoenzymes.

Mcwherter, C. A., E. Haas, et al. (1986). "Conformational Unfolding in the N-Terminal Region of Ribonuclease-a Detected by Nonradiative Energy-Transfer." Biochemistry 25(8): 1951-1963.

Nabuurs, S. M. and C. P. van Mierlo (2010). "Interrupted hydrogen/deuterium exchange reveals the stable core of the remarkably helical molten globule of α-β parallel protein flavodoxin." J. Biol. Chem. 285(6): 4165-4172.

Nabuurs, S. M., A. H. Westphal, et al. (2009). "Topological switching between an α-β parallel protein and a remarkably helical molten globule." J. Am. Chem. Soc. 131: 8290-8295.

Nabuurs, S. M., A. H. Westphal, et al. (2008). "Extensive formation of off-pathway species during folding of an α-β parallel protein is due to docking of (non)native structure elements in unfolded molecules." J. Am. Chem. Soc. 130(50): 16914-16920.

Nabuurs, S. M., A. H. Westphal, et al. (2009). "Non-cooperative formation of the off-pathway molten globule during folding of the α-β parallel protein apoflavodoxin." J. Am. Chem. Soc. 131: 2739-2746.

Nishimura, C., R. Riley, et al. (2000). "Fluorescence energy transfer indicates similar transient and equilibrium intermediates in staphylococcal nuclease folding." J. Mol. Biol. 299(4): 1133-1146.

Ohgushi, M. and A. Wada (1983). "'Molten-globule state': a compact form of globular proteins with mobile side-chains." FEBS Lett. 164(1): 21-24.

Orevi, T., E. B. Ishay, et al. (2009). "Early Closure of a Long Loop in the Refolding of Adenylate Kinase: A Possible Key Role of Non-Local Interactions in the Initial Folding Steps." J. Mol. Biol. 385(4): 1230-1242.

Otzen, D. E., L. Giehm, et al. (2007). "Aggregation as the basis for complex behaviour of cutinase in different denaturants." Biochim. Biophys. Acta 1774(2): 323-333.

Peelen, S., S. S. Wijmenga, et al. (1996). "Possible role of a short extra loop of the long-chain flavodoxin from *Azotobacter chroococcum* in electron transfer to nitrogenase: Complete H-1, N-15 and C-13 backbone assignments and secondary solution structure of the flavodoxin." J. Biomol. NMR 7(4): 315-330.

Pennington, M. W. (1994). "Site-specific chemical modification procedures." Methods Mol. Biol. 35: 171-185.

Perez, V. I., A. Bokov, et al. (2009). "Is the oxidative stress theory of aging dead?" Biochim. Biophys. Acta, Gen. Subj. 1790(10): 1005-1014.

Pirchi, M., G. Ziv, et al. (2011). "Single-molecule fluorescence spectroscopy maps the folding landscape of a large protein." Nat. Comm. 2.

Popp, M. W., J. M. Antos, et al. (2009). "Site-specific protein labeling via sortase-mediated transpeptidation." Curr. Protoc. Protein Sci. Chapter 15: Unit 15 13.

Ptitsyn, O. B., R. H. Pain, et al. (1990). "Evidence for a molten globule state as a general intermediate in protein folding." FEBS Lett. 262(1): 20-24.

Puljung, M. C. and W. N. Zagotta (2011). "Labeling of Specific Cysteines in Proteins Using Reversible Metal Protection." Biophys. J. 100(10): 2513-2521.

Ratner, V., D. Amir, et al. (2005). "Fast collapse but slow formation of secondary structure elements in the refolding transition of *E. coli* adenylate kinase." J. Mol. Biol. 352(3): 683-699.

Ratner, V., E. Kahana, et al. (2002). "A general strategy for site-specific double labeling of globular proteins for kinetic FRET studies." Bioconjugate Chem. 13(5): 1163-1170.

Rhoades, E., M. Cohen, et al. (2004). "Two-state folding observed in individual protein molecules." J. Am. Chem. Soc. 126(45): 14686-14687.

Rhoades, E., E. Gussakovsky, et al. (2003). "Watching proteins fold one molecule at a time." Proc. Natl. Acad. Sci. U.S.A. 100(6): 3197-3202.

Royer, C. A. (2006). "Probing protein folding and conformational transitions with fluorescence." Chem. Rev. 106(5): 1769-1784.

Schuler, B., E. A. Lipman, et al. (2002). "Probing the free-energy surface for protein folding with single-molecule fluorescence spectroscopy." Nature 419(6908): 743-747.

Schuler, B. and L. K. Pannell (2002). "Specific labeling of polypeptides at amino-terminal cysteine residues using Cy5-benzyl thioester." Bioconjugate Chem. 13(5): 1039-1043.

Sherman, E. and G. Haran (2006). "Coil-globule transition in the denatured state of a small protein." Proc. Natl. Acad. Sci. U.S.A. 103(31): 11539-11543.

Sinev, M., P. Landsmann, et al. (2000). "Design consideration and probes for fluorescence resonance energy transfer studies." Bioconjugate Chem. 11(3): 352-362.

Sinev, M. A., E. V. Sineva, et al. (1996). "Domain closure in adenylate kinase." Biochemistry 35(20): 6425-6437.

Stadtman, E. R. and B. S. Berlett (1998). "Reactive oxygen-mediated protein oxidation in aging and disease." Drug. Metab. Rev. 30(2): 225-243.

Steensma, E., H. A. Heering, et al. (1996). "Redox properties of wild-type, Cys69Ala, and Cys69Ser *Azotobacter vinelandii* flavodoxin II as measured by cyclic voltammetry and EPR spectroscopy." Eur. J. Biochem. 235(1-2): 167-172.

Steensma, E., M. J. Nijman, et al. (1998). "Apparent local stability of the secondary structure of *Azotobacter vinelandii* holoflavodoxin II as probed by hydrogen exchange: implications for redox potential regulation and flavodoxin folding." Protein Sci. 7(2): 306-317.

Steensma, E. and C. P. van Mierlo (1998). "Structural characterisation of apoflavodoxin shows that the location of the stable nucleus differs among proteins with a flavodoxin-like topology." J. Mol. Biol. 282(3): 653-666.

Steinberg, I. Z. (1971). "Long-Range Nonradiative Transfer of Electronic Excitation Energy in Proteins and Polypeptides." Annu. Rev. Biochem. 40: 83-&.

Stryer, L. and R. P. Haugland (1967). "Energy transfer: a spectroscopic ruler." Proc. Natl. Acad. Sci. U.S.A. 58(2): 719-726.

Sunbul, M. and J. Yin (2009). "Site specific protein labeling by enzymatic posttranslational modification." Org. Biomol. Chem. 7(17): 3361-3371.

Talaga, D. S., W. L. Lau, et al. (2000). "Dynamics and folding of single two-stranded coiled-coil peptides studied by fluorescent energy transfer confocal microscopy." Proc. Natl. Acad. Sci. U.S.A. 97(24): 13021-13026.

Tanford, C., K. Kawahara, et al. (1966). "Proteins in 6m Guanidine Hydrochloride - Demonstration of Random Coil Behavior." J. Biol. Chem. 241(8): 1921-&.

Tezuka-Kawakami, T., C. Gell, et al. (2006). "Urea-induced unfolding of the immunity protein Im9 monitored by spFRET." Biophys. J. 91(5): L42-L44.

Tuinstra, R. L., F. C. Peterson, et al. (2008). "Interconversion between two unrelated protein folds in the lymphotactin native state." Proc. Natl. Acad. Sci. U.S.A. 105(13): 5057-5062.

Uversky, V. N. (2002). "Natively unfolded proteins: A point where biology waits for physics." Protein Sci. 11(4): 739-756.

Uversky, V. N., C. J. Oldfield, et al. (2008). "Intrinsically disordered proteins in human diseases: Introducing the D(2) concept." Annu. Rev. Biophys. 37: 215-246.

van den Berg, B., R. J. Ellis, et al. (1999). "Effects of macromolecular crowding on protein folding and aggregation." EMBO J. 18(24): 6927-6933.

van Mierlo, C. P. M., J. M. P. van den Oever, et al. (2000). "Apoflavodoxin (un)folding followed at the residue level by NMR." Protein Sci. 9(1): 145-157.

van Mierlo, C. P. M., W. M. A. M. van Dongen, et al. (1998). "The equilibrium unfolding of *Azotobacter vinelandii* apoflavodoxin II occurs via a relatively stable folding intermediate." Protein Sci. 7(11): 2331-2344.

Vendruscolo, M., E. Paci, et al. (2001). "Three key residues form a critical contact network in a protein folding transition state." Nature 409(6820): 641-645.

Wolynes, P. G., J. N. Onuchic, et al. (1995). "Navigating the Folding Routes." Science 267(5204): 1619-1620.

Yoch, D. C., J. R. Benemann, et al. (1969). "Electron Transport System in Nitrogen Fixation by *Azotobacter* .2. Isolation and Function of a New Type of Ferredoxin." Proc. Natl. Acad. Sci. U.S.A. 64(4): 1404-&.

Zimmerman, S. B. and S. O. Trach (1991). "Estimation of Macromolecule Concentrations and Excluded Volume Effects for the Cytoplasm of *Escherichia-Coli*." J. Mol. Biol. 222(3): 599-620.

Chapter 2

Cofactor binding protects flavodoxin against oxidative stress

Simon Lindhoud[1], Willy A.M. van den Berg[1], Robert H.H. van den Heuvel[2], Albert J.R. Heck[3], Carlo P.M. van Mierlo, and Willem J.H. van Berkel

Abstract

In organisms, various protective mechanisms against oxidative damaging of proteins exist. Here, we show that cofactor binding is among these mechanisms, because flavin mononucleotide (FMN) protects *Azotobacter vinelandii* flavodoxin against hydrogen peroxide-induced oxidation. We identify an oxidation sensitive cysteine residue in a functionally important loop close to the cofactor, i.e., Cys69. Oxidative stress causes dimerisation of apoflavodoxin (i.e., flavodoxin without cofactor), and leads to consecutive formation of sulphinate and sulphonate states of Cys69. Use of 7-chloro-4-nitrobenzo-2-oxa-1,3-diazole (NBD-Cl) reveals that Cys69 modification to a sulphenic acid is a transient intermediate during oxidation. Dithiothreitol converts sulphenic acid and disulphide into thiols, whereas the sulphinate and sulphonate forms of Cys69 are irreversible with respect to this reagent. A variable fraction of Cys69 in freshly isolated flavodoxin is in the sulphenic acid state, but neither oxidation to sulphinic and sulphonic acid nor formation of intermolecular disulphides is observed under oxidising conditions. Furthermore, flavodoxin does not react appreciably with NBD-Cl. Besides its primary role as redox-active moiety, binding of flavin leads to considerably improved stability against protein unfolding and to strong protection against irreversible oxidation and other covalent thiol modifications. Thus, cofactors can protect proteins against oxidation and modification.

1. These authors contributed equally to this work
2. Merck, Sharpe & Dohme, Oss, the Netherlands
3. Biomolecular Mass Spectrometry and Proteomics, Bijvoet Center of Biomolecular Research and Utrecht Institute for Pharmaceutical Sciences, Utrecht University
4. A paper based on this chapter is published as: Lindhoud, S., van den Berg, WAM., et al. *PLoS ONE*, 2012

Introduction

Proteins are sensitive to oxidative damage and the resulting protein modifications often have considerable biological effects. For example, protein oxidation has been suggested as a causative or contributory factor in many diseases (Ames, Shigenaga et al. 1993). Furthermore, oxidised proteins have been found to increase in aged organisms, suggesting that protein oxidation contributes to aging (Chao, Ma et al. 1997; Stadtman and Berlett 1998). Of particular interest is oxidation of methionine and cysteine residues, because this conversion happens for a wide variety of proteins and often affects their biological activity (Brandes, Schmitt et al. 2009; Wang, Yang et al. 2011).

Oxidation of methionine to its sulphoxide state can be stimulated by biological oxidants such as H_2O_2, but also by environmental oxidants like ozone (Banerjee and Mudd 1992). Methionine oxidation can be (partially) reversed by the action of methionine sulphoxide reductases (Davis, Newcomb et al. 2002). Such repair of oxidative damage suggests a potential for *in vivo* regulation of protein function by reversible methionine oxidation (Moskovitz, Bar-Noy et al. 2001; Cabreiro, Picot et al. 2008; Perez, Bokov et al. 2009; De Luca, Sanna et al. 2010).

The most oxidation sensitive and reactive amino-acid residue is cysteine. The presence of reactive cysteine residues is indicative of functionality, and affects many biochemical processes (Weerapana, Wang et al. 2010). Oxidation of protein thiols involves consecutive formation of sulphenic, sulphinic and sulphonic acids (Little and O'Brien 1969), as shown in Scheme 2.1. Sulphenic acids are intermediates during formation of disulphide bonds (Allison 1976), but have also been recognised as naturally occurring states of cysteinyl residues critical to catalytic and regulatory processes (Claiborne, Miller et al. 1993; Claiborne, Yeh et al. 1999). Recent evidence suggests that protein sulphenic acids are widespread posttranslational oxidative modifications in healthy mammalian tissues, and that their presence increases in response to elevated concentrations of H_2O_2 (Saurin, Neubert et al. 2004; Chang, Huang et al. 2010; Chiappetta, Ndiaye et al. 2010; Jeong, Jung et al. 2011; Leonard and Carroll 2011).

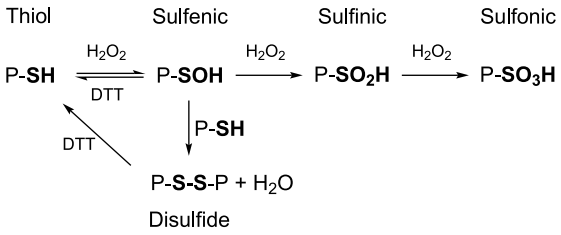

Scheme 2.1 Oxidation states of protein cysteines, and their reversibility by DTT.

When protective mechanisms fail, protein thiols may be further oxidised to the sulphinic acid state or the irreversible sulphonic acid state, (van Berkel and Müller 1987; Hamann, Zhang et al. 2002). Consequently, protein sulphinylation and sulphonylation have been linked to cell aging and cell death (Hochgrafe, Mostertz et al. 2005). Aging has been investigated for several purified proteins. For example, in case of *p*-hydroxybenzoate hydroxylase from *Pseudomonas fluorescens*, oxidative aging produces sulphonic acid derivatives of Cys116 (van Berkel and Müller 1987). Substitution of this cysteine by a serine precludes oxidation and prevents protein aggregation (Eschrich, van Berkel et al. 1990). In case of *Trigonopsis variabilis* D-amino acid oxidase, stress-induced oxidation results in decreased protein stability due to the irreversible formation of the sulphinic acid state of Cys108 (Slavica, Dib et al. 2005). However, in case of peroxidoredoxin, the sulphinic acid state of the active site cysteine can be rapidly transformed to the catalytically active thiol state (Woo, Chae et al. 2003). This reduction probably requires specific enzymes. In contrast, matrix metalloproteinase-7 is activated by oxidation of Cys70 into sulphinic acid (Fu, Kassim et al. 2001).

In this study, we report the sensitivity towards oxidative damage of a 179-residue flavodoxin from *A. vinelandii*. The protein functions as an FMN-dependent one-electron transporter to nitrogenase in the nitrogen fixation pathway of this bacterium (Benemann, Yoch et al. 1969). Flavodoxin adopts the α-β parallel topology (Alagaratnam, van Pouderoyen et al. 2005), also referred to as the doubly-wound or flavodoxin-like topology, which is one of the most common folds observed. Flavodoxins are the structurally most investigated flavoproteins and have emerged as prototypes for the investigation of protein folding (Bollen, Sanchéz et al. 2004; Bollen and van Mierlo 2005; Bollen, Kamphuis et al. 2006; Engel, Westphal et al. 2008; Nabuurs, Westphal et al. 2008; Nabuurs, Westphal et al. 2009). Furthermore, flavodoxins are found in many prokaryotes, but also as protein domains in eukaryotes (e.g., in nitric oxide synthase) (Punta, Coggill et al. 2012).

A. vinelandii flavodoxin contains two residues that are potentially sensitive to oxidation: a methionine at position 30 and a cysteine at position 69. Whereas the side chain of the methionine is hidden in the protein interior, the cysteine is located in a loop at the surface and in immediate vicinity of the FMN cofactor (Figure 2.1), as is the case for many other flavodoxins. NMR studies on the nearly identical flavodoxin from *Azotobacter chroococcum* show that this loop is involved in intermolecular interactions with the nitrogenase enzyme system (Peelen, Wijmenga et al. 1996). Indeed, biological activity is lost upon covalent dimerisation of *A. vinelandii* flavodoxin molecules through formation of an intermolecular disulphide bridge. (Yoch 1975; Tanaka, Haniu et al. 1977; Steensma, Heering et al. 1996). Currently, the exact physiological role of Cys69 is unclear. It is suggested to function as an additional redox active centre to FMN, or to be involved in an activation/deactivation mechanism of the protein (Wolfova, Smatanova et al. 2009).

Upon removal of the non-covalently bound flavin from flavodoxin, apoflavodoxin is generated. NMR data show that apoflavodoxin strongly resembles flavodoxin, except for dynamic disorder in the flavin-binding region (Steensma and van Mierlo 1998). Due to this flexibility, disulphide-linked dimerisation of apoflavodoxin happens more rapidly than is the case for flavodoxin (Yoch 1975). Here, we use H_2O_2 to induce oxidative stress on flavodoxin as well as apoflavodoxin. We address the effects of oxidative stress through analysis of the various protein modifications formed, and highlight the importance of the cofactor in protecting flavoproteins against irreversible oxidation and potentially other covalent thiol modifications.

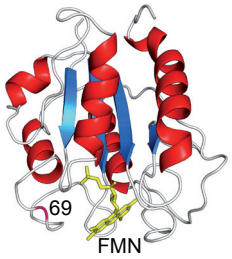

Figure 2.1 Cartoon drawing of the X-ray structure of flavodoxin from *A. vinelandii*. α-Helices are shown in red, β-strands in blue and loops in white. The FMN cofactor is coloured yellow and the backbone of residue 69 is coloured magenta. Note that this residue is in immediate vicinity of FMN. The X-ray structure is of the C69A variant of the protein (pdb ID 1YOB) (Alagaratnam, van Pouderoyen et al. 2005), in which the single cysteine at position 69 is replaced by alanine. This protein variant is largely similar to flavodoxin regarding both redox potential of holoprotein and stability of apoprotein (Steensma, Heering et al. 1996; van Mierlo, van Dongen et al. 1998).

Materials and Methods

Chemicals

FMN and 1,4-dithiothreitol (DTT) were from Sigma-Aldrich. Ammonium acetate and 5,5'-dithiobis-(2-nitrobenzoic acid) (DTNB) were from Merck, and H_2O_2 (30 % w/v) was from Fisher. NBD-Cl from Acros Organics was dissolved in dimethyl sulphoxide.

Protein purification and preparation of apoprotein

Wild-type flavodoxin II from *A. vinelandii* strain ATCC 478 was expressed in *E. coli* TG2 (pAV34) and purified as described (van Mierlo, van Dongen et al. 1998), with omission of DTT. The purified protein migrated as one homogeneous band in SDS-polyacrylamide gel electrophoresis. Holoprotein gave rise to an A276/A450 absorbance ratio of 5.4. C69A flavodoxin was prepared as described (van Mierlo, van Dongen et al. 1998). To produce apoflavodoxin, FMN was removed from flavodoxin by trichloroacetic acid (TCA) precipitation (van Mierlo, van Dongen et al. 1998). Before dissolving in 300 mM Tris-HCl pH 8.5, protein pellet was washed twice with 3 % (w/v) TCA containing 1 mM DTT (Bollen, Sanchéz et al. 2004). To avoid disulphide bond formation between apoprotein monomers,

apoflavodoxin was stored in the presence of 10 mM DTT. Prior to experiments, by using Biogel-P6DG gel filtration (BioRad), flavodoxin as well as apoflavodoxin were brought into 50 mM ammonium acetate, 0.1 mM EDTA, pH 6.8. All experiments with holo- and apoprotein were performed using this buffer.

Protein modification

Reactions of flavodoxin (41 µM) and apoflavodoxin (31 µM) with DTNB were carried out at 20 °C according to the method of Ellman (Ellman 1959) with the modifications of Habeeb (Habeeb 1972). DTNB concentration was 200 µM. Time-dependent release of 2-nitro-5-thio-benzoate anion (TNB) was measured at 412 nm (ε_{412}(TNB) = 13.6 mM^{-1} cm^{-1}). Apoflavodoxin (20 µM) was also treated for 1 hour at 20 °C with 200 µM NBD-Cl (stock contained 100 mM NBD-Cl in dimethyl sulphoxide). In another experiment, apoflavodoxin was first oxidised at room temperature with 10 mM H_2O_2 for periods of 10 and 90 minutes, respectively, and subsequently incubated with NBD-Cl, as described. In addition, DTT-pre-treated flavodoxin (28 µM) was incubated for 100 minutes at 20 °C with 190 µM NBD-Cl.

Fast protein liquid chromatography

Size-exclusion chromatography was performed using a Superdex 75 HR 10/30 column. Anion exchange chromatography was done using a MonoQ HR5/5 column. All FPLC separations were performed at room temperature using an ÄKTA Explorer (GE healthcare).

Spectral analysis

Absorption spectra were recorded at 25 °C on a Hewlett Packard 8453 diode array spectrophotometer. Flavodoxin's molar absorption coefficient of 10.8 mM^{-1} cm^{-1} at 450 nm was determined by recording absorption spectra of protein in presence and absence of 0.1 % (w/v) SDS, using a molar absorption coefficient for free FMN of 12.2 mM^{-1} cm^{-1} at 445 nm.

Nano-electrospray mass spectrometry

Native MS spectra of protein were obtained by using an LC-T nano-electrospray ionisation orthogonal time-of-flight mass spectrometer (Micromass, Manchester, UK), operating in positive ion mode. Spraying conditions were: needle voltage 1250-1450 V, cone voltage 50-125 V and source temperature 80 °C. To prepare nano-electrospray needles, borosilicate glass capillaries (Kwik-FilTM, World Precision Instruments Inc., Sarasota, FL) and a P-97 puller (Sutter Instrument Co., Novato, CA) were used. The resulting needles were subsequently coated with a thin gold layer (~500 Å) by using an Edwards Scancoat six Pirani 501 sputter coater (Edwards High Vacuum International, Crawley, UK).

Liquid chromatography-mass spectrometry (LC-MS)

For liquid chromatography use was made of a LC-10AD Shimadzu two pump system coupled to a SPD-10A UV-VIS Shimadzu detector, which was set to 210 nm. Protein samples were brought onto a Vydac 218TP54 C18-reversed phase analytical column (250 x 4.6 mm internal diameter, 5 µm particle size) and a Vydac 218TP5115 C18-reversed phase microbore column (150 x 1 mm internal diameter, 5 µm particle size), which was protected by an Optimize technologies OPTI-GUARD C18-reversed phase 1 mm guard column. Flow rate of the mobile phase through the analytical Vydac column was 0.6 mL/minute. Flow rate through the microbore column was 0.05 mL/minute. The mobile phase was a mixture of solvent A (milli-Q water containing 0.05 % (v/v) trifluoroacetic acid (TFA)) and solvent B (95 % (v/v) acetonitrile, containing 0.05 (v/v) TFA). This mixture initially contained 40 % solvent B for a period of 5 minutes. Subsequently, in a time span of 10 minutes, the concentration of solvent B was increased to 60 % and kept isocratically for 5 minutes. After this time period, solvent mixture was brought back in 5 minutes to initial composition (i.e., 40 % B). The LC-T mass spectrometer of the LC-MS set-up operated in positive ion mode with 3 kV capillary voltage, 50 V cone voltage, 120 °C source temperature and 250 L/hour desolvation gas flow.

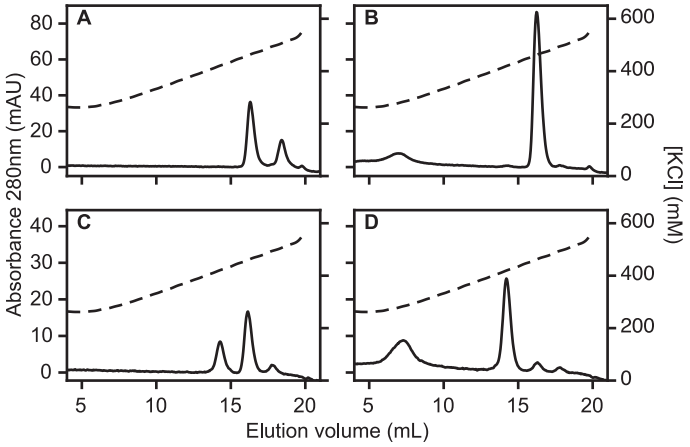

Figure 2.2 MonoQ anion exchange chromatography elution profiles of flavodoxin and apoflavodoxin. (A) Flavodoxin (40 µM). (B) Flavodoxin (40 µM), kept in the presence of 10 mM DTT for a period of 10 minutes. (C) Apoflavodoxin (50 µM). (D) Apoflavodoxin (50 µM), kept in the presence of 10 mM DTT for a period of 10 minutes. Gradient composition: buffer A is 25 mM Tris-HCl pH 8.0, and buffer B is 25 mM Tris-HCl pH 8.0, containing 1 M KCl. Flow rate is 1.0 mL/minute. Dashed lines show conductivities of elution buffers. The molecule eluting at 7 mL is DTT. Temperature is 25 °C.

Results

Cys69 of (apo)flavodoxin is sensitive to oxidation

MonoQ anion exchange chromatography of freshly purified flavodoxin shows the presence of two protein species, eluting at 470 and 510 mM KCl, respectively (Figure 2.2A). Depending on protein preparation protein preparation, the first eluting species amounts to about 50 – 70 % of total protein. Incubation of flavodoxin with 10 mM DTT for a period of 10 minutes causes complete conversion of the second into the first eluting species (Figure 2.2B). This observation shows that Cys69 is reversibly modified in the second eluting species. Preparations of Cys69Ala (C69A) flavodoxin elute as a single species during anion exchange chromatography.

During size-exclusion chromatography, flavodoxin elutes almost exclusively as monomer. Thus, the second flavodoxin species detected by anion exchange chromatography is not disulphide linked protein dimer, but instead involves another thiol modification. We propose that the species eluting at 510 mM KCl at pH 8 (Figure 2.2A), is protein with Cys69 in the sulphenic acid state (Scheme 2.1), because it is converted into protein that elutes at 470 mM KCl after incubation with DTT (Figure 2.2B). This DTT-induced conversion is not expected to happen when flavodoxin's thiol would be oxidised to the sulphinic or sulphonic acid state (van Berkel and Müller 1987; Hamann, Zhang et al. 2002; Leferink, van Duijn et al. 2009). In addition, because the pK_a of sulphenic acid is about 5.9 (Claiborne, Yeh et al. 1999), at pH 8 one expects retarded elution on an anion exchange column of the sulphenic acid state of flavodoxin compared to non-oxidised protein, just as we observe (Figure 2.2A).

In case of apoflavodoxin, MonoQ anion exchange chromatography reveals two major protein species, eluting at 420 and 460 mM KCl, respectively (Figure 2.2C). The fraction of the second species increases proportional to the time during which apoprotein stock is left in absence of DTT. Subsequent incubation of apoflavodoxin with 10 mM DTT causes almost complete conversion of this second species into the first eluting one (Figure 2.2D). Thus, Cys69 is reversibly modified in the second eluting species. Size-exclusion chromatography shows that freshly prepared apoflavodoxin is predominantly monomeric but slowly dimerises during storage (data not shown). Apoflavodoxin dimers elute at 460 mM KCl in MonoQ anion exchange chromatography. These dimers are disulphide-linked, because upon incubation with excess DTT, they convert into monomeric species.

Reactivity with DTNB and NBD-Cl

Incubation of apoflavodoxin (stored in presence of DTT prior to experiments, to avoid protein dimerisation) as well as of flavodoxin with DTNB leads to formation of nearly stoichiometric amounts of TNB. In case of flavodoxin, protein modification proceeds rather slowly and takes about 30 minutes to complete, whereas apoflavodoxin is modified within 2 minutes (for experimental circumstances see Materials and Methods). The observed difference in reactivity shows that Cys69 is better accessible to Ellman's reagent in apoprotein than it is in holoprotein, consistent with the observation that the flavin-binding region of apoflavodoxin (and thus of the loop in which Cys69 resides) is flexible, whereas this region is rigid in flavodoxin (Steensma and van Mierlo 1998). To explain stoichiometric formation of TNB in case of flavodoxin, holoprotein with Cys69 in the sulphenic acid state must react with DTNB. Indeed, reactivity of sulphenic acids with TNB has been reported (Poole and Ellis 2002).

Flavodoxin does not react appreciably with NBD-Cl, whereas the reaction of this reagent with freshly prepared, DTT-pre-treated, apoflavodoxin takes 60 minutes to complete. The absorption maximum at 420 nm of the apoflavodoxin adduct formed (Figure 2.3) is characteristic for thioether linked NBD (Scheme 2.2) (Ellis and Poole 1997). Hence, Cys69 of apoflavodoxin stock is in the thiol state. No sulphoxide adduct is detected, because (i) apoflavodoxin preparation

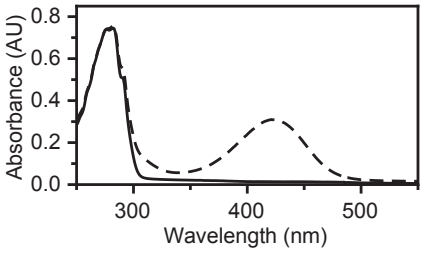

Figure 2.3 Spectroscopic characteristics of apoflavodoxin modified with NBD. Apoprotein (20 μM) before (solid line) and after (dashed line) incubation with 200 μM NBD-Cl for 1 hour. Modified protein absorbs maximally at 420 nm, which is characteristic for the presence of a thiol-NBD conjugate (Ellis and Poole 1997)

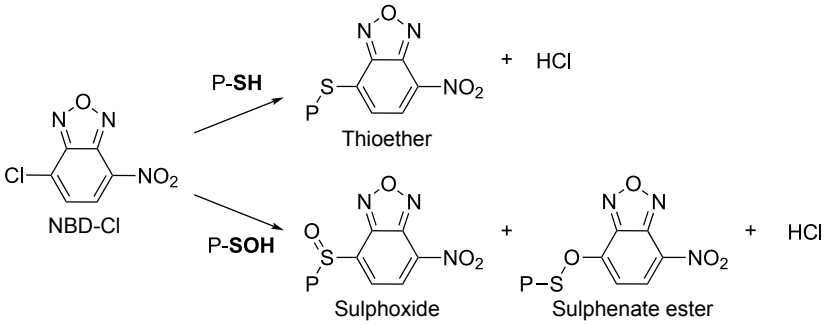

Scheme 2.2 Reactions of NBD-Cl with protein cysteine and sulphenic acid states.

involves TCA precipitation of holoprotein and at the resulting low pH sulphenic acid is unstable (Claiborne, Miller et al. 1993), and (ii) apoflavodoxin is stored in presence of 10 mM DTT prior to NBD-Cl treatment, causing sulphenic acid to transform into thiol.

Native MS and LC-MS analysis

By using native mass spectrometry (Heck 2008) we detect flavodoxin, which has an MS spectrum that shows a narrow charge state distribution (i.e., +7 to +9) (Figure 2.4). The corresponding molecular mass equals (19995 ± 3) Da, which closely agrees with the expected mass of the holoprotein with cysteine in the thiol state (Table 2.1). Freshly prepared, DTT-pre-treated, native apoflavodoxin exhibits a similar narrow distribution of charge states (i.e., +7 to +9), and the corresponding molecular mass is (19538 ± 3) Da (Table 3.1). The mass difference between holo- and apoprotein establishes that flavodoxin indeed contains a single, non-covalently bound, FMN cofactor.

Table 2.1 Native mass spectrometry of (apo)flavodoxin.

Species	Label in Figure 2.4	Expected mass (Da)	Measured mass (Da)	Δ(mass) (Da)
Apoflavodoxin	M	19531.8	19538 ± 3	6.2
Flavodoxin	M_H	19987.1	19995 ± 3	7.9

Monomeric protein species are labelled M, Molecular mass of FMN is 455.3 Da. Expected mass and measured mass are average masses.

During LC-MS analysis, we first inject flavodoxin into the LC part of the set-up and subsequently electrospray it into a mass spectrometer. In the reverse-phase chromatography step, which involves use of acetonitrile and TFA, flavodoxin loses FMN and subsequently apoprotein unfolds. As a consequence of this unfolding, the corresponding LC-MS spectrum displays a broad distribution of charged protein molecules (i.e., +7 to +17) (Figure 2.4), clearly distinct from the native MS data. Again due to unfolding, the LC-MS spectrum of apoflavodoxin is identical to the one of holoprotein. Unfolded apo- and holoprotein both are observed with a molecular mass of (19533 ± 1.5) Da, which agrees very well with their predicted masses (i.e., 19531.8 Da; Table 2.2), assuming that cysteine is in the thiol state and that the co-factor has been released from the holoprotein. In case of holo- as well as apoprotein we observe no sulphenic acid, because acetonitrile-TFA usage during the reversed phase chromatography step of LC-MS and resulting low pH causes instability of sulphenic acid (Claiborne, Miller et al. 1993).

The above observations show that flavodoxin and apoflavodoxin are sensitive to thiol oxidation, prompting further investigation of this phenomenon.

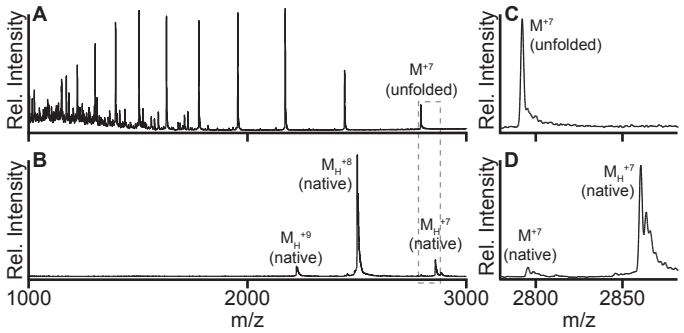

Figure 2.4 LC-MS and native MS spectra of flavodoxin. (A) LC-MS spectrum of flavodoxin. (B) Nano-electrospray mass spectrum of flavodoxin. M_H^{+n} represents flavodoxin monomer with n positive charges, and M^{+n} is apoflavodoxin monomer with n positive charges. (C and D) Spectra of the area indicated by the dashed grey contour in (A) and (B), respectively. Flavodoxin (5 µM) is in 50 mM ammonium acetate, 0.1 mM EDTA, pH 6.8.

Table 2.2 LC-MS analysis of (apo)flavodoxin.

Species	Label in Figure 2.6	Expected mass (Da)	Measured mass (Da)	Δ(mass) (Da)
Apoflavodoxin	M	19531.8	19533 ± 1.5	+ 1.2
Apoflavodoxin + 1 O	MO	19547.8	Not observed	-
Apoflavodoxin + 2 O	MO2	19563.8	19565 ± 2	+ 1.2
Apoflavodoxin + 3 O	MO3	19579.8	19582 ± 2	+ 2.2
Apoflavodoxin + NBD	M-NBD	19695.9	19697 ± 2	+ 1.1
Apoflavodoxin + 1 O + NBD	MO-NBD	19711.9	19713 ± 2	+ 1.1
Apoflavodoxin dimer	D	39063.6	39066 ± 5	+ 2.4

Monomeric protein species are labelled M. Molecular masses of NBD-Cl and NBD are 199.6 and 164.1 Da, respectively. Expected mass and measured mass are average masses.

Hydrogen peroxide-mediated oxidation of apoflavodoxin

To prevent intermolecular disulphide bond formation in apoflavodoxin, protein is stored in presence of 10 mM DTT. Just before incubation with H_2O_2, this reducing agent is removed to avoid interference with H_2O_2. Size-exclusion chromatography shows that freshly prepared apoflavodoxin is predominantly monomeric (Figure 2.5A). Upon incubation of apoflavodoxin with 10 mM H_2O_2 the relative amount of protein dimers strongly increases (Figure 2.5B). In contrast, upon incubation of C69A apoflavodoxin with H_2O_2 no protein dimerisation takes place (Figure 2.5C-D).

We used LC-MS to follow H_2O_2-induced oxidation of apoflavodoxin at room temperature. Figure 2.6A shows the LC-MS spectrum of apoprotein prior to its incubation with H_2O_2. Clearly, only monomeric, non-oxidised, apoflavodoxin is detected. After incubating apoflavodoxin with 10 mM H_2O_2 for 30 minutes, the corresponding LC-MS spectrum shows appearance of signal of protein dimer (measured mass (39066 ± 5) Da) (Figure 2.6B). The population of dimer rises upon increasing incubation time. Again, this dimer is disulphide-linked, because upon incubation with 10 mM DTT it converts into monomeric species. Besides a tiny population of protein in sulphinic acid state (labelled MO2 in Figure 2.4B), no other oxidation products of monomeric apoflavodoxin are detected, even when incubation with H_2O_2 lasts up to 2 hours. Thus, under the conditions applied, Met30 of apoflavodoxin is not susceptible to peroxide-mediated sulphoxidation.

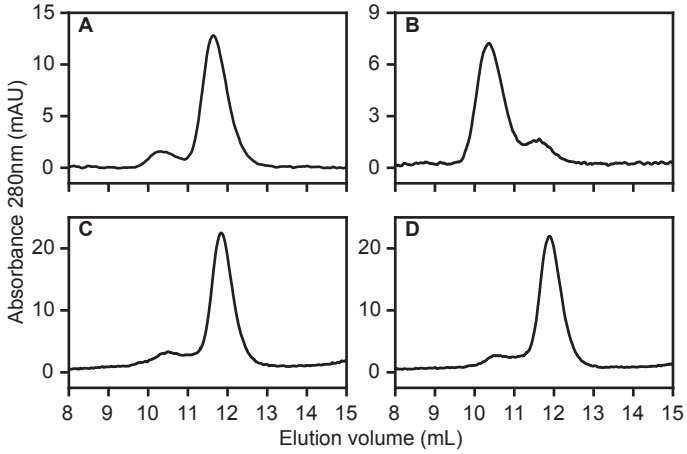

Figure 2.5 Superdex 75 size-exclusion chromatography elution profiles of apoflavodoxin. (A) Apoflavodoxin (38 μM). (B) Apoflavodoxin (38 μM) after 22 h incubation with 10 mM H_2O_2 at 4 °C. (C) C69A apoflavodoxin (79 μM). (D) C69A apoflavodoxin (79 μM) after 24 h incubation with 10 mM H_2O_2 at 4 °C. Flow rate is 0.5 mL/minute and temperature is 25 °C.

Incubation of apoflavodoxin with 100 mM H_2O_2 for a period of 30 minutes leads to detection of four protein species by LC-MS (Figure 2.6C). These species are: non-oxidised protein monomer (M), protein dimer, and protein monomer in sulphinic or sulphonic acid state (labelled MO2 and MO3, respectively). Upon incubation with DTT, only the apoflavodoxin dimer disappears from the LC-MS spectrum, showing that oxidation of Cys69 to its sulphinic or sulphonic acid state is irreversible. No ion intensity at the expected mass of the sulphenic acid state of apoflavodoxin is observed (Figure 2.6C). Again, usage of acetonitrile and TFA during the reversed phase chromatography step destabilises sulphenic acid, preventing its detection by LC-MS. Upon increasing the H_2O_2-incubation period, dimer intensity in LC-MS spectra no further raises. The latter phenomenon is in line with Scheme 2.1, which shows the proposed mechanism for apoflavodoxin oxidation. The most likely first

event during H_2O_2 treatment is formation of sulphenic acid (Claiborne, Yeh et al. 1999). Subsequently, this intermediate either reacts rapidly with Cys69 of another apoflavodoxin monomer to form protein dimer or oxidises further under influence of H_2O_2 to sulphinic and sulphonic acid states of apoflavodoxin. Upon increasing the time of incubation with 100 mM H_2O_2 beyond 30 minutes, competition between both processes depletes sulphenic acid intermediate and hence no increase in relative population of apoflavodoxin dimer is observed.

Trapping of sulphenic acid state during apoflavodoxin oxidation

To support actual formation of a sulphenic acid intermediate during oxidation of apoflavodoxin, H_2O_2-mediated oxidation of apoprotein was studied in presence of NBD-Cl. This procedure enables spectroscopic and mass discrimination between NBD adducts of thiols and sulphenic acids (Ellis and Poole 1997; Denu and Tanner 1998; Poole and Ellis 2002). Now, a 30 minutes incubation at

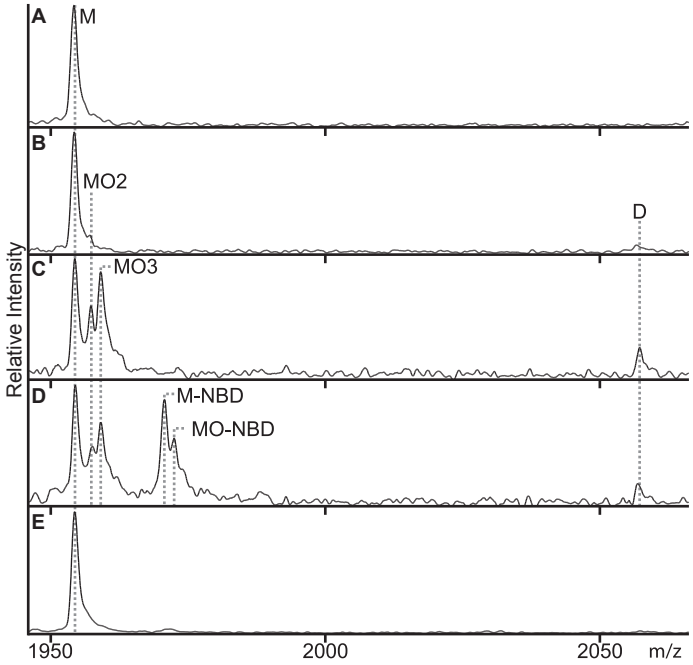

Figure 2.6 Monitoring of (apo)flavodoxin under H_2O_2-induced oxidative stress by LC-MS. For clarity, the zoomed in LC-MS regions that display the +10 charge state of monomer and the +19 charge state of dimer are shown (i.e., m/z range of 1940 to 2070); however, analysis is done on the whole m/z range. (A) Apoflavodoxin. (B) Apoflavodoxin incubated for 30 minute with 10 mM H_2O_2. (C) Apoflavodoxin incubated for 30 minute with 100 mM H_2O_2. (D) Apoflavodoxin incubated for 30 minute with 200 µM NBD-Cl and 100 mM H_2O_2. (E) Flavodoxin incubated for 30 minute with 190 µM NBD-Cl and 100 mM H_2O_2. Protein concentration is 5 µM and incubations were done at room temperature. M represents apoflavodoxin monomer with non-oxidised thiol; MO, MO2 and MO3 are the sulphenic, sulphinic and sulphonic acid states of apoflavodoxin, respectively. M-NBD is monomer protein with the thiol adduct of NBD-Cl, MO-NBD is monomer protein with the sulphenic acid adduct of NBD-Cl, and D represents disulphide-linked apoflavodoxin dimer.

room temperature gives rise to formation of only a minor population of protein dimers (Figure 2.6D) that does not increase upon prolonged incubation. Besides dimer, LC-MS detects five additional monomeric apoflavodoxin species, including protein with non-oxidised thiol (M) and protein in sulphinic (MO2) or sulphonic (MO3) acid state. In addition, protein with the thiol adduct of NBD-Cl (labelled M-NBD) and with the sulphenic acid adduct of NBD-Cl (labelled MO-NBD) are identified (Scheme 2.2). This observation shows that the sulphenic acid intermediate can be trapped by NBD-Cl and indeed forms during H_2O_2-induced oxidation of apoflavodoxin.

Hydrogen peroxide-mediated oxidation of flavodoxin

In contrast to apoflavodoxin, incubation of flavodoxin for a 30 minute period with 100 mM H_2O_2 and 190 µM NBD-Cl does not cause formation of protein dimer, nor of protein species MO2, MO3, M-NBD and MO-NBD, as LC-MS reveals (Figure 2.6E). Clearly, flavodoxin is much better protected against formation of these products than apoflavodoxin is. In addition, like in apoflavodoxin, Met30 of flavodoxin is not susceptible to peroxide-mediated sulphoxidation.

Does H_2O_2-mediated oxidation of flavodoxin cause production of holoprotein with Cys69 in the sulphenic acid state? Whereas the LC-MS methodology prevents detection of protein with sulphenic acid, due to usage of acetonitrile-TFA during reversed phase chromatography, MonoQ anion exchange chromatography can detect such species, as discussed (Figure 2.2A-B). Using the latter methodology, we indeed observe that upon incubation of flavodoxin with 10 mM H_2O_2 for a period of 30 minutes at room temperature, approximately 85 % of protein is in the sulphenic acid state (i.e., elutes at 510 mM KCl, data not shown). However, in holoprotein, neither subsequent further oxidation to sulphinic and sulphonic acid nor formation of intermolecular disulphides is observed (Figure 2.6).

Discussion

Cofactor binding protects flavodoxin against oxidative stress

Many proteins require binding of a non-covalently bound cofactor to be functional. However, the role such in protein oxidation and stability is scarcely addressed (Hefti, Vervoort et al. 2003). Binding of cofactors stabilises proteins against global unfolding (Creighton 1993). Due to bound FMN, the stability against global unfolding of flavodoxin is much higher than that of apoflavodoxin. As a result, global unfolding of flavodoxin is a rare event, occurring approximately once every 3 hours (Bollen and van Mierlo 2005). The stability of flavodoxin is so high that FMN needs to be released first before global unfolding of the protein can occur (Bollen and van Mierlo 2005). Hydrogen/deuterium exchange studies revealed that FMN binding protects the majority of flavodoxin's residues against local protein unfolding (Steensma and van Mierlo 1998; van Mierlo, van Dongen et al. 1998;

van Mierlo and Steensma 2000). In contrast to apoflavodoxin, the backbone amide protons of several residues in the flavin-binding region of flavodoxin exchange extremely slowly with deuterons of deuterium oxide (Steensma and van Mierlo 1998; van Mierlo, van Dongen et al. 1998). This slow exchange reflects the rigidity of the flavin-binding region in flavodoxin, which is caused by the many interactions that exist between FMN and apoprotein. These observations highlight that flavin binding protects flavoproteins against unfolding.

The study presented here highlights another role of flavin binding: i.e., the importance of the FMN cofactor in protecting flavodoxin against irreversible oxidative damage. The data show that apoflavodoxin is much more susceptible to H_2O_2-induced oxidative stress than holoprotein. This is likely caused by increased acessibility of Cys69. Furthermore, dissociation of FMN potentially affects the pK_a of this residue. Both apo- and holoprotein first reversibly oxidise to their sulphenic acid states (Scheme 2.1). Subsequently, in case of apoflavodoxin, sulphenic acid is irreversibly oxidised to sulphinic and sulphonic acid states. In addition, part of the sulphenic acid population reacts with unmodified apoflavodoxin monomers, thereby generating disulphide-linked protein dimers. In contrast, in case of flavodoxin, oxidation beyond the sulphenic acid state is not detected. Flavodoxin does not dimerise and is also considerably less susceptible to covalent modification by TNB and NBD-Cl than apoflavodoxin. Apparently, upon sulphenylation, the side chain of Cys69 becomes even further stabilised and protected against subsequent modification.

In conclusion, besides its primary role as redox-active moiety, binding of FMN leads to considerably improved stability of flavodoxin against unfolding and to strong protection against oxidative stress.

Acknowledgments

We thank Nora Tahallah and Kees Versluis for help with mass spectrometry experiments.

References

Alagaratnam, S., G. van Pouderoyen, et al. (2005). "A crystallographic study of Cys69Ala flavodoxin II from *Azotobacter vinelandii*: structural determinants of redox potential." Protein Sci. 14(9): 2284-2295.

Allison, W. S. (1976). "Formation and reactions of sulfenic acids in proteins." Acc. Chem. Res. 9: 293-299.

Ames, B. N., M. K. Shigenaga, et al. (1993). "Oxidants, antioxidants, and the degenerative diseases of aging." Proc. Natl. Acad. Sci. U. S. A. 90(17): 7915-7922.

Banerjee, S. K. and J. B. Mudd (1992). "Reaction of Ozone with Glycophorin in Solution and in Lipid Vesicles." Arch. Biochem. Biophys. 295(1): 84-89.

Benemann, J. R., D. C. Yoch, et al. (1969). "The electron transport system in nitrogen fixation by *Azotobacter*. I. Azotoflavin as an electron carrier." Proc. Natl. Acad. Sci. U. S. A. 64(3): 1079-1086.

Bollen, Y. J., M. B. Kamphuis, et al. (2006). "The folding energy landscape of apoflavodoxin is rugged: Hydrogen exchange reveals nonproductive misfolded intermediates." Proc. Natl. Acad. Sci. U. S. A. 103(11): 4095-4100.

Bollen, Y. J., I. E. Sanchéz, et al. (2004). "Formation of on- and off-pathway intermediates in the folding kinetics of *Azotobacter vinelandii* apoflavodoxin." Biochemistry 43(32): 10475-10489.

Bollen, Y. J. and C. P. van Mierlo (2005). "Protein topology affects the appearance of intermediates during the folding of proteins with a flavodoxin-like fold." Biophys. Chem. 114(2-3): 181-189.

Brandes, N., S. Schmitt, et al. (2009). "Thiol-based redox switches in eukaryotic proteins." Antioxidants & redox signaling 11(5): 997-1014.

Cabreiro, F., C. R. Picot, et al. (2008). "Overexpression of mitochondrial methionine sulfoxide reductase B2 protects leukemia cells from oxidative stress-induced cell death and protein damage." J. Biol. Chem. 283(24): 16673-16681.

Chang, Y. C., C. N. Huang, et al. (2010). "Mapping protein cysteine sulfonic acid modifications with specific enrichment and mass spectrometry: an integrated approach to explore the cysteine oxidation." Proteomics 10(16): 2961-2971.

Chao, C. C., Y. S. Ma, et al. (1997). "Modification of protein surface hydrophobicity and methionine oxidation by oxidative systems." Proc. Natl. Acad. Sci. U. S. A. 94(7): 2969-2974.

Chiappetta, G., S. Ndiaye, et al. (2010). "Proteome screens for Cys residues oxidation: the redoxome." Methods Enzymol. 473: 199-216.

Claiborne, A., H. Miller, et al. (1993). "Protein-sulfenic acid stabilization and function in enzyme catalysis and gene regulation." Faseb J. 7(15): 1483-1490.

Claiborne, A., J. I. Yeh, et al. (1999). "Protein-sulfenic acids: diverse roles for an unlikely player in enzyme catalysis and redox regulation." Biochemistry 38(47): 15407-15416.

Creighton, T. E. (1993). Proteins, stuctures and molecular properties. New York, W. H. Freeman and Company.

Davis, D. A., F. M. Newcomb, et al. (2002). "Reversible oxidation of HIV-2 protease." Methods Enzymol. 348: 249-259.

De Luca, A., F. Sanna, et al. (2010). "Methionine sulfoxide reductase A down-regulation in human breast cancer cells results in a more aggressive phenotype." Proc. Natl. Acad. Sci. U. S. A. 107(43): 18628-18633.

Denu, J. M. and K. G. Tanner (1998). "Specific and reversible inactivation of protein tyrosine phosphatases by hydrogen peroxide: evidence for a sulfenic acid intermediate and implications for redox regulation." Biochemistry 37(16): 5633-5642.

Ellis, H. R. and L. B. Poole (1997). "Novel application of 7-chloro-4-nitrobenzo-2-oxa-1,3-diazole to identify cysteine sulfenic acid in the AhpC component of alkyl hydroperoxide reductase." Biochemistry 36(48): 15013-15018.

Ellman, G. L. (1959). "Tissue sulfhydryl groups." Arch. Biochem. Biophys. 82(1): 70-77.

Engel, R., A. H. Westphal, et al. (2008). "Macromolecular crowding compacts unfolded apoflavodoxin and causes severe aggregation of the off-pathway intermediate during apoflavodoxin folding." J. Biol. Chem. 283(41): 27383-27394.

Eschrich, K., W. J. van Berkel, et al. (1990). "Engineering of microheterogeneity-resistant *p*-hydroxybenzoate hydroxylase from *Pseudomonas fluorescens*." FEBS Lett. 277(1-2): 197-199.

Fu, X., S. Y. Kassim, et al. (2001). "Hypochlorous acid oxygenates the cysteine switch domain of pro-matrilysin (MMP-7). A mechanism for matrix metalloproteinase activation and atherosclerotic plaque rupture by myeloperoxidase." J. Biol. Chem. 276(44): 41279-41287.

Habeeb, A. F. S. A. (1972). "Reaction of protein sulfhydryl groups with Ellman's reagent." Methods Enzymol. 25: 457-464.

Hamann, M., T. Zhang, et al. (2002). "Quantitation of protein sulfinic and sulfonic acid, irreversibly oxidized protein cysteine sites in cellular proteins." Methods Enzymol. 348: 146-156.

Heck, A. J. R. (2008). "Native mass spectrometry: a bridge between interactomics and structural biology." Nat. Methods 5(11): 927-933.

Hefti, M. H., J. Vervoort, et al. (2003). "Deflavination and reconstitution of flavoproteins." Eur. J. Biochem. 270(21): 4227-4242.

Hochgrafe, F., J. Mostertz, et al. (2005). "Fluorescence thiol modification assay: oxidatively modified proteins in *Bacillus subtilis*." Mol. Microbiol. 58(2): 409-425.

Jeong, J., Y. Jung, et al. (2011). "Novel oxidative modifications in redox-active cysteine residues." Mol. Cell. Proteomics 10(3): M110.0005131-00051313.

Leferink, N. G., E. van Duijn, et al. (2009). "Galactonolactone dehydrogenase requires a redox-sensitive thiol for optimal production of vitamin C." Plant Physiol. 150(2): 596-605.

Leonard, S. E. and K. S. Carroll (2011). "Chemical 'omics' approaches for understanding protein cysteine oxidation in biology." Curr. Opin. Chem. Biol. 15(1): 88-102.

Little, C. and P. J. O'Brien (1969). "Mechanism of peroxide-inactivation of the sulphydryl enzyme glyceraldehyde-3-phosphate dehydrogenase." Eur. J. Biochem. 10(3): 533-538.

Moskovitz, J., S. Bar-Noy, et al. (2001). "Methionine sulfoxide reductase (MsrA) is a regulator of antioxidant defense and lifespan in mammals." Proc. Natl. Acad. Sci. U. S. A. 98(23): 12920-12925.

Nabuurs, S. M., A. H. Westphal, et al. (2009). "Topological switching between an α-β parallel protein and a remarkably helical molten globule." J. Am. Chem. Soc. 131: 8290-8295.

Nabuurs, S. M., A. H. Westphal, et al. (2008). "Extensive formation of off-pathway species during folding of an alpha-beta parallel protein is due to docking of (non)native structure elements in unfolded molecules." J. Am. Chem. Soc. 130(50): 16914-16920.

Peelen, S., S. Wijmenga, et al. (1996). "Possible role of a short extra loop of the long-chain flavodoxin from *Azotobacter chroococcum* in electron transfer to nitrogenase: complete 1H, 15N and 13C backbone assignments and secondary solution structure of the flavodoxin." J. Biomol. NMR 7(4): 315-330.

Perez, V. I., A. Bokov, et al. (2009). "Is the oxidative stress theory of aging dead?" Biochim. Biophys. Acta 1790(10): 1005-1014.

Poole, L. B. and H. R. Ellis (2002). "Identification of cysteine sulfenic acid in AhpC of alkyl hydroperoxide reductase." Methods Enzymol. 348: 122-136.

Punta, M., P. C. Coggill, et al. (2012). "The Pfam protein families database." Nucleic Acids Res. 40(D1): D290-D301.

Saurin, A. T., H. Neubert, et al. (2004). "Widespread sulfenic acid formation in tissues in response to hydrogen peroxide." Proc. Natl. Acad. Sci. U. S. A. 101(52): 17982-17987.

Slavica, A., I. Dib, et al. (2005). "Single-site oxidation, cysteine 108 to cysteine sulfinic acid, in D-amino acid oxidase from *Trigonopsis variabilis* and its structural and functional consequences." Appl. Environ. Microbiol. 71(12): 8061-8068.

Stadtman, E. R. and B. S. Berlett (1998). "Reactive oxygen-mediated protein oxidation in aging and disease." Drug Metab. Rev. 30(2): 225-243.

Steensma, E., H. A. Heering, et al. (1996). "Redox properties of wild-type, Cys69Ala, and Cys69Ser *Azotobacter vinelandii* flavodoxin II as measured by cyclic voltammetry and EPR spectroscopy." Eur. J. Biochem. 235(1-2): 167-172.

Steensma, E. and C. P. van Mierlo (1998). "Structural characterisation of apoflavodoxin shows that the location of the stable nucleus differs among proteins with a flavodoxin-like topology." J. Mol. Biol. 282(3): 653-666.

Tanaka, M., M. Haniu, et al. (1977). "Complete amino acid sequence of azotoflavin, a flavodoxin from *Azotobacter vinelandii*." Biochemistry 16(16): 3525-3537.

van Berkel, W. J. and F. Müller (1987). "The elucidation of the microheterogeneity of highly purified *p*-hydroxybenzoate hydroxylase from *Pseudomonas fluorescens* by various biochemical techniques." Eur. J. Biochem. 167(1): 35-46.

van Mierlo, C. P. and E. Steensma (2000). "Protein folding and stability investigated by fluorescence, circular dichroism (CD), and nuclear magnetic resonance (NMR) spectroscopy: the flavodoxin story." J. Biotechnol. 79(3): 281-298.

van Mierlo, C. P., W. M. van Dongen, et al. (1998). "The equilibrium unfolding of *Azotobacter vinelandii* apoflavodoxin II occurs via a relatively stable folding intermediate." Protein Sci. 7(11): 2331-2344.

Wang, Y., J. Yang, et al. (2011). "Redox Sensing by Proteins: Oxidative Modifications on Cysteines and the Consequent Events." Antioxidants & redox signaling 16: 649-657.

Weerapana, E., C. Wang, et al. (2010). "Quantitative reactivity profiling predicts functional cysteines in proteomes." Nature 468(7325): 790-795.

Wolfova, J., I. K. Smatanova, et al. (2009). "Structural organization of WrbA in apo- and holoprotein crystals." Biochim. Biophys. Acta 1794(9): 1288-1298.

Woo, H. A., H. Z. Chae, et al. (2003). "Reversing the inactivation of peroxiredoxins caused by cysteine sulfinic acid formation." Science 300(5619): 653-656.

Yoch, D. C. (1975). "Dimerization of *Azotobacter vinelandii* flavodoxin (azotoflavin)." Arch. Biochem. Biophys. 170(1): 326-333.

Chapter 3

Fluorescence of Alexa Fluor dye tracks protein folding

Simon Lindhoud, Adrie H. Westphal, Antonie J.W.G. Visser, Jan Willem Borst, and Carlo P.M. van Mierlo

Abstract

Fluorescence spectroscopy is an important tool for the characterisation of protein folding. Often, a protein is labelled with appropriate fluorescent donor and acceptor probes and folding-induced changes in Förster Resonance Energy Transfer (FRET) are monitored. However, conformational changes of the protein potentially affect fluorescence properties of both probes, thereby profoundly complicating interpretation of FRET data. In this study, we assess the effects protein folding has on fluorescence properties of Alexa Fluor 488 (A488), which is commonly used as FRET donor. Here, A488 is covalently attached to Cys69 of apoflavodoxin from *Azotobacter vinelandii*. Although coupling of A488 slightly destabilises apoflavodoxin, the three-state folding of this protein, which involves a molten globule intermediate, is unaffected. Upon folding of apoflavodoxin, fluorescence emission intensity of A488 changes significantly. To illuminate the molecular sources of this alteration, we applied steady state and time-resolved fluorescence techniques. The results obtained show that tryptophans cause folding-induced changes in quenching of Alexa dye. Compared to unfolded protein, static quenching of A488 fluorescence is increased in the molten globule. Upon populating the native state both static and dynamic quenching of A488 decrease considerably. We show that fluorescence quenching of Alexa Fluor dyes is a sensitive reporter of conformational changes during protein folding.

(Submitted)

Introduction

The manner by which proteins attain their functional conformation has been a major puzzle in Biochemistry since the seminal experiments of Anfinsen (Anfinsen 1973). Combinations of theory, simulation and experiment have led to the concept of funnel-shaped folding energy landscapes (Bryngelson, Onuchic et al. 1995; Dill and Chan 1997; Dinner, Sali et al. 2000). In this concept, unfolded protein molecules descend along a funnel describing the free energy of folding, until the folding molecules reach the state that has the lowest free energy, which is the native state. Presence of kinetic traps and barriers in a folding energy landscape can lead to population of partially folded or misfolded states in the ensemble of folding molecules. The corresponding folding intermediates may form *en route* to the native state (i.e., they are on-pathway), or may require significant unfolding before the native state can be reached (i.e., they are off-pathway). Often these intermediates are molten globules. Molten globules are ensembles of interconverting conformers with significant amounts of secondary structure, but lack the tertiary packing characteristics of native proteins (Ptitsyn 1995; Arai and Kuwajima 2000). Formation of these aggregation-prone molten globules is linked to the development of various devastating pathologies (Vendruscolo, Paci et al. 2001; Dobson 2003).

Various approaches exist to experimentally tackle protein folding (Ohgushi and Wada 1983). Frequently, fluorescence spectroscopy is chosen, because this technique is versatile and very sensitive. Several fluorescence read-outs can be used to track protein folding (Eftink 1994). For instance, fluorescence intensity of tryptophan residues reports on folding-induced changes in the polarity of the microenvironment of these residues. Emission spectra can shift to shorter or longer wavelengths upon folding, and fluorescence anisotropy is folding-state dependent (Visser, Westphal et al. 2008; Laptenok, Visser et al. 2011). Upon appropriate labelling of proteins with bright fluorescent dyes, such as Alexa fluorophores (Panchuk-Voloshina, Haugland et al. 1999), even folding of single-molecules can be detected (Deniz, Dahan et al. 1999; Deniz, Laurence et al. 2000; Schuler, Lipman et al. 2002; Rhoades, Cohen et al. 2004).

Through recording of changes in FRET, folding-induced conformational alterations can be monitored (Haas, Katchalski-Katzir et al. 1978; Amir and Haas 1987). FRET is the distance dependent transfer of electronic excitation energy from an excited donor fluorophore to an acceptor chromophore through non-radiative dipole-dipole coupling (Förster 1948; Stryer and Haugland 1967). The efficiency of FRET depends on the inverse 6th power of the distance (r) between donor and acceptor:

$$E = \frac{1}{1 + \left(r / R_0 \right)^6} \qquad [3.1]$$

in which R_0 is the Förster distance, i.e., the distance at which E = 50 %. The Förster distance is calculated according to (Lakowicz 2006):

$$R_0 = 0.211\left(Q_D n^{-4} \kappa^2 J(\lambda)\right)^{1/6} \quad [3.2]$$

in which Q_D is the fluorescence quantum yield of donor, n is the refractive index of the medium through which the energy is transferred (Knox and van Amerongen 2002), κ^2 is the relative orientation of the donor emission dipole with respect to the acceptor absorption dipole, and J is the spectral overlap integral between donor fluorescence emission spectrum and acceptor absorption spectrum. Fluorescence quantum yield Q_D equals:

$$Q = \frac{k_r}{k_r + k_{nr}} \quad [3.3]$$

Measuring fluorescence emission intensities of donor label, in presence and absence of acceptor, enables determination of the FRET efficiency (Lakowicz 2006). Alternatively, this efficiency can be determined from the fluorescence lifetime of donor in presence and absence of acceptor (Lakowicz 2006). The fluorescence lifetime (τ) of a fluorophore depends on radiative and non-radiative de-excitation processes, with rate constants k_r and k_{nr}, respectively:

$$\tau = \frac{1}{k_r + k_{nr}} \quad [3.4]$$

Introduction of an acceptor fluorophore in the vicinity (i.e., up to ~ 10 nm) of a donor fluorophore establishes an additional relaxation path for the excited donor, resulting in a decreased fluorescence lifetime of the donor. Regarding FRET studies, ideally, only changes in inter-dye distance lead to altered fluorescence properties of donor and acceptor. However, apart from FRET, changes in protein conformation potentially also affect fluorescence intensities and lifetimes of the probes involved.

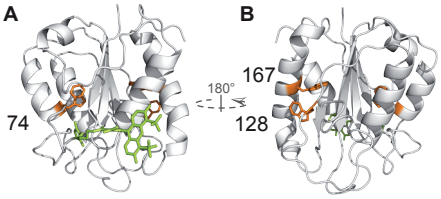

Figure 3.1 Cartoon model of donor-only labelled apoflavodoxin (i.e., flavodoxin without FMN). A488 is shown in bright green and is attached to Cys69. Flavodoxin's tryptophan residues (i.e., Trp74, Trp128 and Trp167) are shown in orange. The model in B is rotated by 180 degrees along the z-axis, compared to the model shown in A. Cartoon models are generated with PyMOL (Schrödinger, LLC, Palo Alto, Ca, USA) using the crystal structure of *A. vinelandii* flavodoxin (pdb ID 1YOB (Alagaratnam, van Pouderoyen et al. 2005)) and the molecular structure of A488, as provided by Invitrogen. Apoflavodoxin strongly resembles flavodoxin, except for dynamic disorder in the flavin-binding region.

Often, Alexa Fluor 488 (A488) is used as donor fluorophore in FRET-detected protein folding (see e.g., (Schuler, Lipman et al. 2002; Rhoades, Gussakovsky et al. 2003; Engel, Westphal et al. 2008)), since it is photostable, readily excited at 488 nm, and has a high fluorescence quantum yield. In this study, we assess the effects protein folding has on fluorescence properties of A488 that is covalently attached to Cys69 of apoflavodoxin from *A. vinelandii*. This protein is referred to as A488-apoflavodoxin (Figure 3.1). Apoflavodoxin kinetic folding is described by (Bollen, Sanchéz et al. 2004; Bollen, Kamphuis et al. 2006):

$$I_{off} \rightleftharpoons \textit{Unfolded apoflavodoxin} \rightleftharpoons I_{on} \rightleftharpoons \textit{Native apoflavodoxin} \quad \text{[Scheme 3.1]}$$

On-pathway species I_{on} is a high energy intermediate, and the corresponding folding state does not populate at equilibrium. The intermediate that is observed during denaturant-dependent equilibrium folding of apoflavodoxin is off-pathway species I_{off}, which is relatively stable. Hence, equilibrium folding of apoflavodoxin is described by:

$$I_{off} \rightleftharpoons \textit{Unfolded apoflavodoxin} \rightleftharpoons \textit{Native apoflavodoxin} \quad \text{[Scheme 3.2]}$$

Non-covalent binding of FMN to native apoflavodoxin leads to formation of flavodoxin (Bollen, Nabuurs et al. 2005), which functions in *A. vinelandii* as one-electron transporter with a strongly negative redox potential (Steensma, Heering et al. 1996). NMR spectroscopy revealed that the off-pathway character of I_{off} arises from formation of native and non-native helices in unfolded apoflavodoxin and their subsequent non-native docking (Nabuurs, Westphal et al. 2008; Nabuurs, de Kort et al. 2009; Nabuurs, Westphal et al. 2009). I_{off} is a molten globule, and aggregates severely under conditions that mimic macromolecular crowding inside cells (Engel, Westphal et al. 2008).

Here, we show that fluorescence of A488 increases significantly upon folding of A488-apoflavodoxin. This observation potentially affects FRET data of folding-induced conformational changes and their interpretation. To illuminate the molecular sources of the changes in fluorescence quenching, we use steady state and time-resolved fluorescence spectroscopy.

Materials and Methods

Engineering, expression and purification of flavodoxin

Wild-type flavodoxin (i.e., flavodoxin containing Cys69 as single cysteine residue) was expressed in *Escherichia coli* TG2 cells, grown in Terrific Broth medium, and was purified according to well-established procedures (van Mierlo, van Dongen et al. 1998). To avoid oxidation of cysteine, dithiothreitol (DTT) was present during protein purification. The buffer used in all experiments with purified protein was 100 mM potassium pyrophosphate, pH 6.0, unless otherwise mentioned.

Labelling of Cys69 with A488

To optimise accessibility of Cys69 for labelling, flavodoxin was unfolded in 6 M guanidine hydrochloride (GuHCl; Fluka), 100 mM potassium pyrophosphate, pH 7.0. Subsequent addition of 10-fold molar excess of Alexa Fluor 488 C_5 maleimide (i.e., A488 (Invitrogen)), for a period exceeding 60 minutes, led to labelling of Cys69. The resulting A488 labelled apoflavodoxin molecules (A488-apoflavodoxin) were separated from unreacted label, FMN and GuHCl, using gel filtration with a Superdex75 10/30 HR column (Pharmacia). To determine the concentration of dye-labelled protein stock, absorption spectra were acquired on an HP-8453 diode array spectrophotometer. Dye-labelled protein stock was divided into 50 µL aliquots, frozen in liquid nitrogen, and stored at -80 °C.

Denaturant-dependent equilibrium folding

Steady-state fluorescence and Circular Dichroism (CD) were used to follow denaturant-dependent equilibrium folding of A488-apoflavodoxin. Each data point was acquired at 25 °C using 2 µM protein in the appropriate GuHCl concentration. Steady-state fluorescence measurements were done on a Cary Eclipse fluorescence spectrophotometer (Varian). Several combinations of excitation and emission wavelengths were used. Tryptophan fluorescence was measured at 330, 340, 350 and 360 nm, upon excitation at 280 nm. A488 was excited at 475 nm and 493 nm, and fluorescence emission was measured at 515 nm. Fluorescence signals were recorded for 7.125 seconds and averaged. Excitation and emission slits were set to a width of 5 nm. CD signals were acquired by use of a J715 spectropolarimeter (Jasco). Denaturant-dependent protein folding was followed in a 1 mm quartz cuvette by measuring ellipticities at 222, 225 and 255 nm, and the corresponding signal was averaged over 3 minutes/wavelength with a 1 s data interval. The averaged ellipticity at 255 nm was subtracted from the averaged ellipticities measured at 222 and 225 nm.

We also acquired time-resolved fluorescence of a denaturant-dependent equilibrium folding series of 62.5 nM dye-labelled apoflavodoxin. Use was made of the time-correlated single photon counting set-up described elsewhere (Borst, Hink et al. 2005). Pulse duration was 0.2 ps, pulse energies were at the pJ level and the repetition rate of pulses was 3.8×106 Hz. Decay curves were constructed by collecting photons in 4096 channels of a multi-channel analyser using a channel time spacing of 5.0 ps. A488 fluorescence lifetimes were measured using excitation at 450 nm, the fluorescence emission was filtered through a 512.2 ± 13.4 nm interference filter with a 3 mm GG 475 cut-off filter (all filters are from Schott, Mainz, Germany). Background fluorescence was measured using the same conditions. The dynamic instrumental response function was determined using a freshly made solution of erythrosine B in water as reference compound (OD_{450nm} is 0.1; τ is 89 ps

at 20 °C (Borst, Hink et al. 2005)). Fluorescence decay curves were analysed using the TRFA data processor (SSTCenter, Minsk, Belarus).

To avoid protein adsorbing to surfaces, Tween-20 was added to all solutions to a final concentration of 0.0035 % (w/v). This addition does not affect apoflavodoxin stability, since no change in thermal midpoint of apoflavodoxin unfolding is observed. Prior to measurements, samples stood for 16 to 24 hours in the dark at 25 °C, and were at equilibrium. Refractometry was used to determine the GuHCl concentration in each individual sample (Nozaki 1972).

Thermodynamic analysis of equilibrium folding data

A three-state model (equations 3.5 to 3.9), was globally fitted to equilibrium folding data of A488-apoflavodoxin, monitored by fluorescence emission of tryptophan and of A488, and by far-UV CD, using ProFit (QuantumSoft, Zürich, Switzerland):

$$I \rightleftharpoons U \rightleftharpoons N \qquad [3.5]$$

$$K_{UI} = [I]/[U],\ K_{IN} = [N]/[I] \qquad [3.6]$$

$$K_{ij}([D]) = K_{ij}^{0}\exp(m_{ij}[D]) \qquad [3.7]$$

$$\begin{aligned} f_U &= 1/(1 + K_{UI} + K_{UI}K_{IN}) \\ f_I &= K_{UI}/(1 + K_{UI} + K_{UI}K_{IN}) \\ f_N &= K_{UI}K_{IN}/(1 + K_{UI} + K_{UI}K_{IN}) \end{aligned} \qquad [3.8]$$

$$Y^{obs} = (a_U + b_U[D])f_U + (a_I + b_I[D])f_I + (a_N + b_N[D])f_N \qquad [3.9]$$

in which *U*, *I* and *N* represent unfolded protein, off-pathway folding intermediate and native apoflavodoxin, respectively, K_{ij} is the equilibrium constant of the *i-j* equilibrium, mij is the constant that describes the denaturant concentration-dependence of K_{ij}, superscript *0* designates the parameter at zero denaturant concentration, [*D*] is the denaturant concentration, f_i is the fractional population of state *i* at a particular denaturant concentration, Y_{obs} is the observed spectroscopic signal, a_i is the spectroscopic property of state *i* at zero denaturant concentration, and b_i is the constant describing the denaturant concentration-dependence of the spectroscopic signal of state i.

The denaturant-dependence of the spectroscopic parameters of the off-pathway folding intermediate (b_I) in equation 3.9 cannot be accurately determined because the corresponding folding state populates only in a small range of GuHCl concentrations. Therefore b_I is set to zero in the global fit procedure (Bollen, Sanchéz et al. 2004). Each individual data point was weighted by the square of the corresponding standard error during the global fit procedure.

Results and Discussion

Alexa Fluor 488 fluorescence is a reporter of apoflavodoxin folding

To optimise accessibility of Cys69, we unfold flavodoxin in 6 M guanidine hydrochloride. Subsequent addition of A488 leads to labelling of this amino acid residue. Upon removal of denaturant, unfolded A488-apoflavodoxin autonomously folds to native dye-labelled apoprotein, because apoflavodoxin unfolding is reversible (van Mierlo, van Dongen et al. 1998). Subsequent addition of FMN leads to full reconstitution of dye-labelled holoprotein (data not shown). Hence, coupling of A488 to Cys69, which resides in the flavin-binding region of the protein, does not impede the ability of apoflavodoxin to bind the FMN cofactor.

We determined denaturant-dependent folding curves of 2 μM A488-apoflavodoxin by acquiring (i) fluorescence emission of A488 at 515 nm (upon excitation at 475 (Figure 3.2A) and 493 nm, respectively), (ii) tryptophan fluorescence at 330 (Figure 3.2B), 340, 350 and 360 nm (upon excitation at 280 nm), and (iii) CD at 222 (Figure 3.2C) and 225 nm. Fluorescence emission of A488 tracks folding of A488-apoflavodoxin (Figure 3.2A), because quenching of this fluorescence changes significantly upon going from unfolded A488-apoflavodoxin in 6 M GuHCl to native dye-labelled protein at 0 M denaturant. The folding curve obtained by CD (Figure 3.2C) has a transition midpoint that lies at higher concentration of denaturant than the midpoints of the folding curves obtained by fluorescence (Figures 3.2A-B). This observation implies involvement of a stable intermediate during folding of A488-apoflavodoxin, just as happens for apoflavodoxin folding.

Table 3.1 Thermodynamic parameters extracted from a global fit of a three-state model to folding data of apoflavodoxin (FLD) (Bollen, Sanchéz et al. 2004) and of A488-apoflavodoxin (A488-FLD)(see Figure 3.2 and Results section).

	FLD	A488-FLD		FLD	A488-FLD
ΔG_{UI} (kcal mol^{-1})	3.74 ± 0.49	2.67 ± 0.62	m_{UI} (kcal mol^{-1} M^{-1})	-1.83 ± 0.19	-1.45 ± 0.25
ΔG_{IN} (kcal mol^{-1})	6.70 ± 0.17	4.27 ± 0.13	m_{IN} (kcal mol^{-1} M^{-1})	-4.40 ± 0.11	-3.21 ± 0.12
ΔG_{UN} (kcal mol^{-1})	10.45 ± 0.52	6.94 ± 0.63	m_{UN} (kcal mol^{-1} M^{-1})	-6.23 ± 0.23	-4.66 ± 0.28

ΔG_{ij} is the difference in free energy between species i *and* j *at 0 M denaturant, and* m_{ij} *is the dependence of* ΔG_{ij} *on denaturant concentration. Errors shown are standard errors.*

The three-state model for thermodynamic analysis of apoflavodoxin folding (equations 3.5-3.9) fits the above-mentioned folding data (Figure 3.2). The corresponding thermodynamic parameters (Table 3.1) show that coupling of A488 to Cys69 predominantly destabilises native apoflavodoxin. Analogous to modifying cysteine by this attachment, the stability of native apoflavodoxin decreases upon mutating amino acid residues (van Mierlo, van Dongen et al. 1998;

Nabuurs, de Kort et al. 2009; Nabuurs, Westphal et al. 2009; Laptenok, Visser et al. 2011). Yet, just as observed here for A488-apoflavodoxin, folding occurs according to a three-state model, because this is a typical feature of proteins with a flavodoxin-like fold (Bollen and van Mierlo 2005).

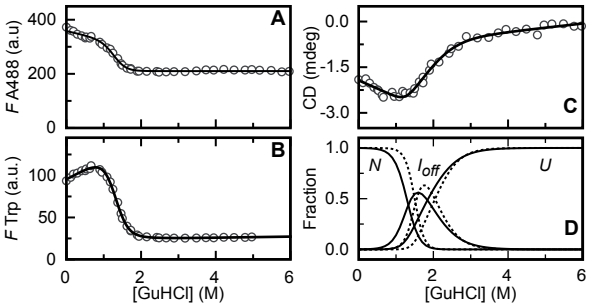

Figure 3.2 An intermediate populates during denaturant-dependent equilibrium folding of A488-apoflavodoxin. (A) Fluorescence emission intensity of A488 at 515 nm upon excitation at 475 nm. (B) Fluorescence emission intensity of tryptophan at 330 nm upon excitation at 280 nm. (C) CD at 222 nm. Solid lines in panels a to c are the result of a global fit of a three-state model of equilibrium folding to all data acquired (see Materials and Methods and Results sections). (D) Denaturant-dependence of the populations of native (*N*), off-pathway intermediate (I_{off}) and unfolded (*U*) A488-apoflavodoxin (solid lines) and of apoflavodoxin (dotted lines), respectively. Protein concentration is 2 μM in 100 mM potassium pyrophosphate, pH 6.0, and data are recorded at 25 °C.

The folding intermediate of A488-apoflavodoxin is a molten globule

Tryptophan fluorescence acquired at 330 nm of folding intermediate and of unfolded A488-apoflavodoxin, both in absence of denaturant, are calculated to be 30 % and 24 % of the tryptophan fluorescence intensity that characterises native A488-labelled protein, respectively. Hence, the intermediate lacks the tertiary side-chain packing characteristics of native A488-apoflavodoxin. Thus, tryptophans of the folding intermediate likely experience a less hydrophobic environment than in native protein. Under native conditions, ellipticity at 222 nm of the intermediate is calculated to be -2.6 ± 0.3 mdeg, whereas the corresponding ellipticity of native protein is -1.9 ± 0.1 mdeg. The intermediate thus has substantial α-helical content. Just as for apoflavodoxin, the intermediate observed during folding of A488-apoflavodoxin is a molten globule.

Identification of the sources that cause folding-induced changes in quenching of A488 fluorescence

Fluorescence of A488 alters significantly upon folding of A488-apoflavodoxin (Figure 3.2A). This phenomenon is due to changes in dynamic and/or static quenching of A488 fluorescence. Static quenching is the result of a non-fluorescent ground-state complex between a fluorophore and quencher that pertains during the excited state lifetime of the fluorophore. When this complex absorbs light it immediately returns to the ground state without emission of a photon. Fluorescence

quantum yield Q_D of fluorophores that do not form a complex with quencher is unperturbed. In contrast, dynamic quenching results from transient collisional encounters between a fluorophore and quencher during the lifetime of the excited state, and is a time-dependent process (Lakowicz 2006). Thus, dynamic quenching introduces an additional non-radiative decay path from the excited state of A488, and as a result, Q_D as well as R_0 decrease. Hence, to be able to quantitatively analyse inter-dye distances in FRET studies of protein folding requires identification of the mechanisms that cause quenching of donor dye, as this study reports for A488. In FRET studies of protein folding one should therefore determine for each folding species whether static and/or dynamic quenching affects fluorescence intensity of donor, and, if necessary, adjust R_0. In the following, we describe how to experimentally identify the sources that cause folding-induced changes in quenching of A488 fluorescence emission of A488-apoflavodoxin.

Dynamic quenching causes a proportional decrease of fluorescence lifetime and intensity of the fluorophore involved. The Stern-Volmer equation describes collisional quenching of fluorescence:

$$\frac{\tau_0}{\tau} = \frac{F_0}{F} = 1 + K_D[Q] \qquad [3.10]$$

in which τ_0 and τ are fluorescence lifetimes and F_0 and F are the fluorescence intensities in the absence and presence of quencher, respectively, K_D is the Stern-Volmer quenching constant ($K_D = k_q\tau_0$, in which k_q is the bimolecular quenching constant (Lakowicz 2006)), and [Q] is the concentration of quencher.

In contrast, when static quenching is the source of diminished fluorescence intensity, no decrease in fluorescence lifetime is detected, because only fluorescent molecules are observed (Lakowicz 2006). Therefore, in case of static quenching:

$$\frac{\tau_0}{\tau} < \frac{F_0}{F} \qquad [3.11]$$

Thus, by comparing the ratio of fluorescence intensities in the absence and the presence of quencher, versus the ratio of their corresponding fluorescence lifetimes, the sources for quenching of a fluorophore can be identified (Sillen and Engelborghs 1998).

With respect to elucidating the contributions of static and dynamic quenching in folding-induced changes of A488 fluorescence, we measured A488 fluorescence intensity decay $I(t)$ of dye-labelled apoflavodoxin at various denaturant concentrations. By using a sum of discrete exponentials with lifetimes τ_i and amplitudes α_i, a global fit to the data is made according to Equation 3.12.

$$I(t) = \sum_{i=1}^{3} \alpha_i \exp(t / \tau_i) \otimes g(t) \qquad [3.12]$$

with $g(t)$ the instrumental response function used for deconvolution of the measured signal. Figure 3.3 shows examples of A488 fluorescence intensity decay curves obtained for A488-apoflavodoxin. Across the whole denaturant range used, three fluorescence lifetimes (i.e., τ_1 = 0.349, τ_2 = 4.150, and τ_3 = 3.161 ns) describe the decay of A488 fluorescence of dye-labelled apoflavodoxin (global χ^2 = 1.077). The corresponding amplitudes track the folding of A488-apoflavodoxin (Figure 3.3C). Because A488 fluorescence decay is tri-exponential, we need to use the average fluorescence lifetime (Sillen and Engelborghs 1998):

$$\langle \tau \rangle = \sum_{i=1}^{3} \alpha_i \tau_i \Big/ \sum_{i=1}^{3} \alpha_i \qquad [3.13]$$

as substitute for fluorescence life times in equation 3.10. Figure 3.3D shows that $\langle\tau\rangle$ tracks folding of A488-apoflavodoxin.

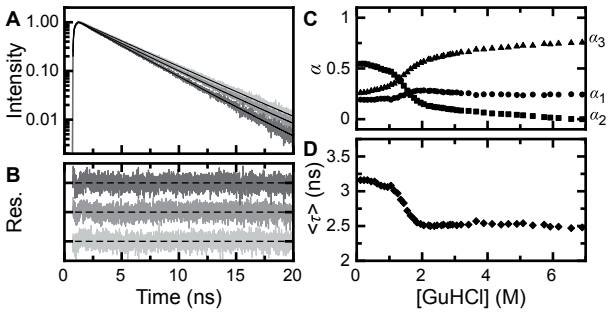

Figure 3.3 Examples of fluorescence intensity decay curves of A488-apoflavodoxin and denaturant-dependencies of normalised amplitudes and average lifetime of the tri-exponential fluorescence decay curves of A488 of dye-labelled apoflavodoxin. (A) Normalised fluorescence decay of A488 of dye-labelled apoflavodoxin at 0.1, 1.5 and 6.9 M denaturant (light grey to dark grey, respectively). Solid lines show the results of a tri-exponential fit of equation 3.12 to the data. (B) Weighted residuals of the fits. (C) Denaturant-dependence of normalised amplitudes α_1 (dots), α_2 (squares) and α_3 (triangles). Corresponding fluorescence lifetimes are: τ_1 = 0.349 ns, τ_2 = 4.150 ns, and τ_3 = 3.161 ns. (D) Denaturant-dependence of average lifetime $\langle\tau\rangle$. To calculate $\langle\tau\rangle$, equation 3.13 is used.

We define F_0 and $\langle\tau_0\rangle$ as fluorescence intensity and average fluorescence lifetime of native A488-apoflavodoxin at the lowest denaturant concentration used, respectively. Figure 3.2A shows that the native baseline of the A488 fluorescence-detected folding curve of apoflavodoxin, which encompasses the GuHCl range of 0 to about 0.7 M, has a rather steep negative slope. As a result, for native protein F_0/F changes markedly upon increasing denaturant concentration (Figure 3.4A). In contrast, the average fluorescence lifetime decreases only slightly in the native baseline (Figure 3.3D).

To elucidate the origin of the change of F_0/F in the native baseline we note that the absorption maximum of A488 shifts from 495 to 499 nm upon going from 0 to 6 M GuHCl (Figure 3.4B). This 4 nm shift causes a ~ 10 % decrease in molar extinction coefficient of A488, and thus in efficiency of excitation of A488 at 475 nm, which is the wavelength used to acquire the data of Figure 3.2A. In addition, the fluorescence emission maximum shifts slightly to longer wavelength upon increasing GuHCl concentration.

To avoid both phenomena that cause the change of A488 fluorescence in the native baseline of Figure 3.2A and the corresponding increase of F_0/F, we determine F_0/F by exciting A488 at its fluorescence excitation maximum and record fluorescence at the fluorescence emission maximum of A488 (Sillen and Engelborghs 1998). Figure 3.4C shows the results of this experiment and Figure 3.4D reports the corresponding denaturant dependence of F_0/F. Using the fluorescence lifetime data of Figure 3.3D, we establish the denaturant dependence of $\langle\tau_0\rangle/\langle\tau\rangle$, which is shown in Figure 3.4D. By comparing the denaturant dependencies of F_0/F and $\langle\tau_0\rangle/\langle\tau\rangle$, the changes in static and dynamic quenching of A488 fluorescence during folding of dye-labelled apoflavodoxin can now be identified.

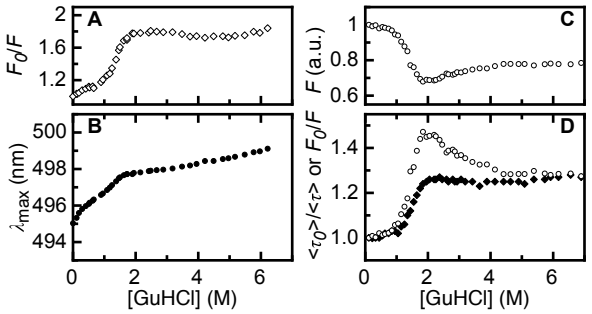

Figure 3.4 Tracking of changes in static and dynamic quenching of A488 fluorescence upon folding of A488-apoflavodoxin. (A) Denaturant-dependence of F_0/F of A488-apoflavodoxin, using the data of Figure 3.2A. (B) The absorption maximum λ_{max} of A488-apoflavodoxin shifts from 495 to 499 nm upon going from 0 to 6 M GuHCl. (C) Denaturant dependence of A488 fluorescence F. A488 is excited at its denaturant-dependent fluorescence excitation maximum and A488 fluorescence is recorded at its denaturant-dependent fluorescence emission maximum. (D) Denaturant dependence of F_0/F (open dots) and $\langle\tau_0\rangle/\langle\tau\rangle$ (filled diamonds), calculated from the data in panel (C) and Figure 3.3D, respectively.

Dynamic and static quenching of A488 fluorescence tracks protein folding

Recently, fluorescence emission of Alexa dyes was measured as function of the concentration of the 20 naturally occurring L-amino acids (Chen, Ahsan et al. 2010). Tryptophan, tyrosine, methionine, and histidine residues were identified as quenchers of A488. Fluorescence quenching of Alexa 488 originates from photoinduced electron transfer (Chen, Ahsan et al. 2010; Choi, Kim et al. 2011) and typically occurs when the distance between fluorophore and quencher is within a few Ångstroms.

In case of static quenching, quencher and fluorophores are at van der Waals contact distances and photoinduced electron transfer becomes ultrafast (Zhong and Zewail 2001). Tryptophan and tyrosine cause similar dynamic quenching of A488. Compared to these amino acids, quenching by methionine and histidine is marginal. In addition, only tryptophan causes considerable static quenching of A488 (Chen, Ahsan et al. 2010). Flavodoxin does not contain histidine residues, has one methionine residue (Met30), three tryptophan residues (i.e., Trp74, Trp128 and Trp167), and five tyrosine residues (i.e., Tyr47, Tyr102, Tyr106, Tyr114 and Tyr133). Of these residues, Trp74 most likely causes folding-induced changes in quenching of A488 fluorescence, because this residue is nearest to Cys69 and shielded from solvent in native A488-apoflavodoxin (Figure 3.1).

Comparison of the denaturant-dependencies of $<\tau_0>/<\tau>$ and F_0/F reveals that the native baselines of both folding curves have slopes that are equally shallow (Figure 3.4D). Thus, addition of denaturant hardly affects A488 fluorescence of native dye-labelled apoflavodoxin. Figure 3.4D shows that random coil A488-apoflavodoxin, which exists above 6 M GuHCl (Nabuurs, Westphal et al. 2008), has similar $<\tau_0>/<\tau>$- and F_0/F-values, which are both larger than the corresponding values that characterise native protein. Thus, dynamic quenching of A488 in random coil protein is larger than in native apoflavodoxin.

Upon decreasing denaturant concentration from 6 to 2 M GuHCl, F_0/F increases considerably, whereas $<\tau_0>/<\tau>$ barely alters (Figure 3.4D). Apoflavodoxin's molten globule forms in this denaturant range, whereas the native state of the protein does not populate yet. Consequently, compared to unfolded protein, only static quenching of A488 is enhanced in this folding intermediate. Figure 3.4D shows that static quenching of A488 exclusively tracks formation of apoflavodoxin's molten globule. Both static and dynamic quenching of A488 decreases considerably upon increasing the population of the native state by lowering GuHCl concentration below 2 M (Figure 3.4D). Clearly, the results of this work show that A488 fluorescence is a sensitive reporter of protein folding.

Acknowledgements

We thank Arie van Hoek for help in acquisition of time-resolved fluorescence data.

References

Alagaratnam, S., G. van Pouderoyen, et al. (2005). "A crystallographic study of Cys69Ala flavodoxin II from *Azotobacter vinelandii*: structural determinants of redox potential." Protein Sci. 14(9): 2284-2295.

Amir, D. and E. Haas (1987). "Estimation of Intramolecular Distance Distributions in Bovine Pancreatic Trypsin-Inhibitor by Site-Specific Labeling and Nonradiative Excitation Energy-Transfer Measurements." Biochemistry 26(8): 2162-2175.

Anfinsen, C. B. (1973). "Principles that govern the folding of protein chains." Science 181(4096): 223-230.

Arai, M. and K. Kuwajima (2000). "Role of the molten globule state in protein folding." Adv. Protein Chem. 53: 209-282.

Bollen, Y. J., M. B. Kamphuis, et al. (2006). "The folding energy landscape of apoflavodoxin is rugged: Hydrogen exchange reveals nonproductive misfolded intermediates." Proc. Natl. Acad. Sci. U.S.A. 103(11): 4095-4100.

Bollen, Y. J., S. M. Nabuurs, et al. (2005). "Last in, first out: The role of cofactor binding in flavodoxin folding." J. Biol. Chem. 280(9): 7836-7844.

Bollen, Y. J., I. E. Sanchéz, et al. (2004). "Formation of on- and off-pathway intermediates in the folding kinetics of *Azotobacter vinelandii* apoflavodoxin." Biochemistry 43(32): 10475-10489.

Bollen, Y. J. and C. P. van Mierlo (2005). "Protein topology affects the appearance of intermediates during the folding of proteins with a flavodoxin-like fold." Biophys. Chem. 114(2-3): 181-189.

Borst, J. W., M. A. Hink, et al. (2005). "Effects of refractive index and viscosity on fluorescence and anisotropy decays of enhanced cyan and yellow fluorescent proteins." J. Fluoresc. 15(2): 153-160.

Bryngelson, J. D., J. N. Onuchic, et al. (1995). "Funnels, pathways, and the energy landscape of protein folding: a synthesis." Proteins Struct. Funct. Bioinf. 21(3): 167-195.

Chen, H., S. S. Ahsan, et al. (2010). "Mechanisms of quenching of Alexa fluorophores by natural amino acids." J. Am. Chem. Soc. 132(21): 7244-7245.

Choi, J., S. Kim, et al. (2011). "Unfolding dynamics of cytochrome c revealed by single-molecule and ensemble-averaged spectroscopy." Phys. Chem. Chem. Phys 13(13): 5651-5658.

Deniz, A. A., M. Dahan, et al. (1999). "Single-pair fluorescence resonance energy transfer on freely diffusing molecules: Observation of Forster distance dependence and subpopulations." Proc. Natl. Acad. Sci. U.S.A. 96(7): 3670-3675.

Deniz, A. A., T. A. Laurence, et al. (2000). "Single-molecule protein folding: Diffusion fluorescence resonance energy transfer studies of the denaturation of chymotrypsin inhibitor 2." Proc. Natl. Acad. Sci. U.S.A. 97(10): 5179-5184.

Dill, K. A. and H. S. Chan (1997). "From Levinthal to pathways to funnels." Nat. Struct. Mol. Biol. 4(1): 10-19.

Dinner, A. R., A. Sali, et al. (2000). "Understanding protein folding via free-energy surfaces from theory and experiment." Trends Biochem. Sci. 25(7): 331-339.

Dobson, C. M. (2003). "Protein folding and misfolding." Nature 426(6968): 884-890.

Eftink, M. R. (1994). "The use of fluorescence methods to monitor unfolding transitions in proteins." Biophys. J. 66(2 Pt 1): 482-501.

Engel, R., A. H. Westphal, et al. (2008). "Macromolecular crowding compacts unfolded apoflavodoxin and causes severe aggregation of the off-pathway intermediate during apoflavodoxin folding." J. Biol. Chem. 283(41): 27383-27394.

Förster, T. (1948). "Zwischenmolekulare Energiewanderung Und Fluoreszenz." Ann. Phys. 2(1-2): 55-75.

Haas, E., E. Katchalski-Katzir, et al. (1978). "Brownian-Motion of Ends of Oligopeptide Chains in Solution as Estimated by Energy-Transfer between Chain Ends." Biopolymers 17(1): 11-31.

Knox, R. S. and H. van Amerongen (2002). "Refractive index dependence of the Förster resonance excitation transfer rate." J. Phys. Chem. B 106(20): 5289-5293.

Lakowicz, J. R. (2006). Principles of fluorescence spectroscopy. New York, Springer.

Laptenok, S. P., N. V. Visser, et al. (2011). "A general approach for detecting folding intermediates from steady-state and time-resolved fluorescence of single-tryptophan-containing proteins." Biochemistry 50(17): 3441-3450.

Nabuurs, S. M., B. J. de Kort, et al. (2009). "Non-native hydrophobic interactions detected in unfolded apoflavodoxin by paramagnetic relaxation enhancement." Eur. Biophys. J. 39: 689-698.

Nabuurs, S. M., A. H. Westphal, et al. (2009). "Topological switching between an α-β parallel protein and a remarkably helical molten globule." J. Am. Chem. Soc. 131: 8290-8295.

Nabuurs, S. M., A. H. Westphal, et al. (2008). "Extensive formation of off-pathway species during folding of an α-β parallel protein is due to docking of (non)native structure elements in unfolded molecules." J. Am. Chem. Soc. 130(50): 16914-16920.

Nabuurs, S. M., A. H. Westphal, et al. (2009). "Non-cooperative formation of the off-pathway molten globule during folding of the α-β parallel protein apoflavodoxin." J. Am. Chem. Soc. 131: 2739-2746.

Nozaki, Y. (1972). "The preparation of guanidine hydrochloride." Methods Enzymol. 26: 43-50.

Ohgushi, M. and A. Wada (1983). "'Molten-globule state': a compact form of globular proteins with mobile side-chains." FEBS Lett. 164(1): 21-24.

Panchuk-Voloshina, N., R. P. Haugland, et al. (1999). "Alexa dyes, a series of new fluorescent dyes that yield exceptionally bright, photostable conjugates." J. Histochem. Cytochem. 47(9): 1179-1188.

Ptitsyn, O. B. (1995). "Molten globule and protein folding." Adv. Protein Chem. 47: 83-229.

Rhoades, E., M. Cohen, et al. (2004). "Two-state folding observed in individual protein molecules." J. Am. Chem. Soc. 126(45): 14686-14687.

Rhoades, E., E. Gussakovsky, et al. (2003). "Watching proteins fold one molecule at a time." Proc. Natl. Acad. Sci. U.S.A. 100(6): 3197-3202.

Schuler, B., E. A. Lipman, et al. (2002). "Probing the free-energy surface for protein folding with single-molecule fluorescence spectroscopy." Nature 419(6908): 743-747.

Sillen, A. and Y. Engelborghs (1998). "The correct use of "average" fluorescence parameters." Photochem. Photobiol. 67(5): 475-486.

Steensma, E., H. A. Heering, et al. (1996). "Redox properties of wild-type, Cys69Ala, and Cys69Ser *Azotobacter vinelandii* flavodoxin II as measured by cyclic voltammetry and EPR spectroscopy." Eur. J. Biochem. 235(1-2): 167-172.

Stryer, L. and R. P. Haugland (1967). "Energy transfer: a spectroscopic ruler." Proc. Natl. Acad. Sci. U.S.A. 58(2): 719-726.

van Mierlo, C. P., W. M. van Dongen, et al. (1998). "The equilibrium unfolding of *Azotobacter vinelandii* apoflavodoxin II occurs via a relatively stable folding intermediate." Protein Sci. 7(11): 2331-2344.

Vendruscolo, M., E. Paci, et al. (2001). "Three key residues form a critical contact network in a protein folding transition state." Nature 409(6820): 641-645.

Visser, N. V., A. H. Westphal, et al. (2008). "Tryptophan-tryptophan energy migration as a tool to follow apoflavodoxin folding." Biophys. J. 95(5): 2462-2469.

Zhong, D. P. and A. H. Zewail (2001). "Femtosecond dynamics of flavoproteins: Charge separation and recombination in riboflavine (vitamin B-2)-binding protein and in glucose oxidase enzyme." Proc. Natl. Acad. Sci. U.S.A. 98(21): 11867-11872.

Chapter 4

Illuminating the off-pathway nature of the molten globule folding intermediate of an α-β parallel protein

Simon Lindhoud, Adrie H. Westphal, Jan Willem Borst, and Carlo P.M. van Mierlo

Abstract

Partially folded protein species transiently form during folding of most proteins. Often, these species are molten globules, which may be on- or off-pathway to the native state. Molten globules are ensembles of interconverting protein conformers that have a substantial amount of secondary structure, but lack virtually all tertiary side-chain packing characteristics of natively folded proteins. Due to solvent-exposed hydrophobic groups, molten globules are prone to aggregation, which can have detrimental effects on organisms. The molten globule observed during folding of the 179-residue apoflavodoxin from *Azotobacter vinelandii* is off-pathway, as it has to unfold before native protein can form. Here, we study folding of apoflavodoxin and characterise its molten globule using fluorescence spectroscopy and Förster Resonance Energy Transfer (FRET). Apoflavodoxin is site-specifically labelled with fluorescent donor and acceptor dyes, utilising dye-inaccessibility of Cys69 in cofactor-bound protein. Donor (i.e., Alexa Fluor 488) is covalently attached to Cys69 in all apoflavodoxin variants used. Acceptor (i.e., Alexa Fluor 568) is coupled to Cys1, Cys131 and Cys178, respectively. Our FRET data show that apoflavodoxin's molten globule forms in a non-cooperative manner and that its N-terminal 69 residues fold last. In addition, striking conformational differences between molten globule and native protein are revealed, because the inter-label distances sampled in the 111-residue C-terminal segment of the molten globule are shorter than observed for native apoflavodoxin. Thus, FRET sheds light on the off-pathway nature of the molten globule during folding of an α-β parallel protein.

(Submitted)

Introduction

Folding of proteins to conformations with proper biological activities is of vital importance for all living organisms. To describe protein folding, the concept of a multidimensional energy landscape or folding funnel arose from a combination of experimental data, theory and simulation (Bryngelson, Onuchic et al. 1995; Dill and Chan 1997; Dinner, Sali et al. 2000; Vendruscolo, Paci et al. 2001; Fersht and Daggett 2002). In this model, proteins descend along a funnel wall describing the free energy of folding, until they reach the native state. Folding energy landscapes usually are rugged and comprise kinetic traps and barriers that pose restrictions on the way to the native state. As a result, partially folded intermediates are formed, which may be on- or off-pathway to the native state. When the intermediate is on-pathway, as is observed for the majority of proteins studied to date, it has native-like topology and is productive for folding. In contrast, when the intermediate is off-pathway, it is trapped in such a manner that the native state cannot be reached without substantial reorganisational events (Jahn and Radford 2008).

The resemblance between early kinetic intermediates and molten globules (Ohgushi and Wada 1983; Ptitsyn, Pain et al. 1990; Christensen and Pain 1991; Arai and Kuwajima 2000) suggests that these molten globules can be considered as models of transient intermediates (Jahn and Radford 2008). Several kinetic studies have revealed involvement of off-pathway intermediates during protein folding (see e.g. (Fernandez-Recio, Genzor et al. 2001; Melo, Chen et al. 2003; Bollen, Sanchéz et al. 2004)). The formation of a kinetically trapped off-pathway molten globule increases the likelihood of protein aggregation. Elucidation of the formation and conformation of molten globules offers potential insights into factors responsible for protein misfolding, aggregation, and, potentially, for numerous devastating pathologies (Dobson 2003; Chiti and Dobson 2006).

Structural characterisation of molten globules is hampered by the often transient nature of their existence, their usually relatively low population at equilibrium, and their aggregation at high protein concentrations (Jaenicke and Seckler 1997). One needs techniques that detect these species with high sensitivity, and thus fluorescence spectroscopy and the phenomenon of Förster Resonance Energy Transfer are very suitable (Stryer and Haugland 1967; Amir, Krausz et al. 1992; Haas 2005). FRET is the distance dependent transfer of electronic excitation energy from a donor fluorophore to an acceptor chromophore through non-radiative dipole-dipole coupling. This phenomenon enables detection of distances between donor and acceptor molecules of typically < 10 nm (Förster 1948; Stryer and Haugland 1967; Lakowicz 2006). The FRET efficiency (E) strongly depends on the distance (r) between a donor and an acceptor molecule, according to Equation 4.1.

$$E = \frac{1}{1 + \left(r / R_0\right)^6} \qquad [4.1]$$

with R_0 being the Förster distance, i.e., the distance at which the energy transfer efficiency is 50 %. Labelling of proteins with bright donor and acceptor dyes strongly facilitates the use of FRET to study protein folding. Here, we employ FRET to study the folding of dye-labelled *A. vinelandii* apoflavodoxin, and to characterise its off-pathway molten globule.

Flavodoxins are monomeric flavoproteins that are involved in electron transfer and contain a non-covalently bound FMN cofactor (Mayhew and Tollin 1992). These proteins adopt the flavodoxin-like topology, also referred to as the doubly-wound or α-β parallel topology. This topology is among the most common topologies in the protein databank, and is shared by many functionally and sequentially unrelated proteins.

We demonstrated previously that kinetic folding of apoflavodoxin occurs spontaneously, involves an energy landscape with two intermediates, and is described by Scheme 4.1 (Bollen, Sanchéz et al. 2004; Bollen, Kamphuis et al. 2006).

$$I_{off} \rightleftharpoons \textit{Unfolded apoflavodoxin} \rightleftharpoons I_{on} \rightleftharpoons \textit{Native apoflavodoxin} \qquad \text{[Scheme 4.1]}$$

Non-covalent binding of FMN to native apoflavodoxin is the last step in flavodoxin folding (Bollen, Nabuurs et al. 2005). Native apoflavodoxin (i.e., flavodoxin without FMN) strongly resembles flavodoxin, except for dynamic disorder in the flavin-binding region (Steensma, Nijman et al. 1998; Steensma and van Mierlo 1998). Intermediate I_{on} lies on the productive folding route from unfolded to native protein, is highly unstable and is therefore not observed during denaturant-induced equilibrium unfolding. Approximately 90% of folding molecules fold via off-pathway intermediate I_{off}, which is a relatively stable species that needs to unfold to produce native protein and thus acts as a trap. Formation of an off-pathway folding species is probably inherent to the folding of proteins with a flavodoxin-like fold (Bollen and van Mierlo 2005), as this species is experimentally observed for other α-β parallel proteins of which the kinetic folding has been investigated (i.e., apoflavodoxin from *Anabaena* (Fernandez-Recio, Genzor et al. 2001), CheY (Kathuria, Day et al. 2008), cutinase (Otzen, Giehm et al. 2007), and UMP/CMP kinase (Lorenz and Reinstein 2008)).

Denaturant-induced equilibrium folding of apoflavodoxin is described by the three-state model of Scheme 4.2 (Bollen, Sanchéz et al. 2004).

$$I_{off} \rightleftharpoons \textit{Unfolded apoflavodoxin} \rightleftharpoons \textit{Native apoflavodoxin} \qquad \text{[Scheme 4.2]}$$

Off-pathway intermediate I_{off} populates significantly at equilibrium (Figure 4.1), enabling characterisation of its properties. This species is molten globule-like: it is compact, its three tryptophans are solvent-exposed, and it has severely broadened NMR resonances due to exchange between different conformers on the micro- to millisecond time scale (van Mierlo, van Dongen et al. 1998; van Mierlo, van den Oever et al. 2000; Bollen, Sanchéz et al. 2004; Engel, Westphal et al. 2008). Elevated apoflavodoxin concentrations and molecular crowding cause severe aggregation of this molten globule (van Mierlo, van den Oever et al. 2000; Engel, Westphal et al. 2008).

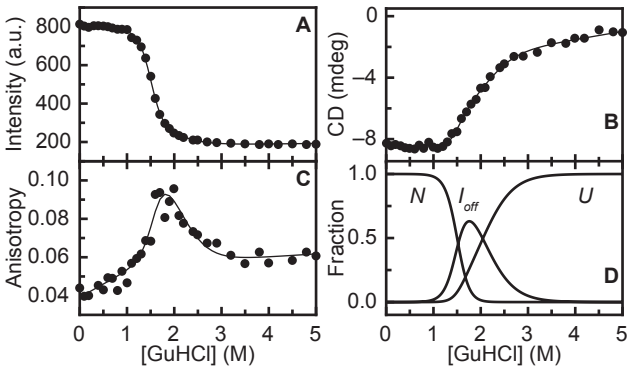

Figure 1.4 Denaturant-dependent equilibrium folding shows involvement of an intermediate during apoflavodoxin folding (Bollen, Sanchéz et al. 2004). (A) Fluorescence emission intensity of tryptophan detected at 340 nm upon excitation at 280 nm. (B) CD signal at 222 nm. (C) Fluorescence anisotropy data detected with a 335 nm cut-off filter, excitation is at 300 nm. Solid lines in panels A to C are the result of a global fit of a three-state model for equilibrium (un)folding. (D) Normalised fractions of native (N), off-pathway intermediate (I_{off}), and unfolded (U) apoflavodoxin as a function of denaturant concentration. Protein concentration is 5.6 μM in 100 mM potassium pyrophosphate, pH 6.0, and data are recorded at 25 °C.

Unfolded apoflavodoxin has four transiently ordered regions. Three of these regions (i.e., Ala41-Gly53, Gln99-Ala122, and Thr160-Gly176) transiently form α-helices and the fourth region (i.e., Glu72-Gly83)) transiently adopts non-native structure, which is neither α-helix nor β-strand (Nabuurs, Westphal et al. 2008). Upon reducing denaturant concentration, the four structured elements in unfolded apoflavodoxin transiently interact and subsequently form the ordered core of the molten globule (Nabuurs, Westphal et al. 2008; Nabuurs, Westphal et al. 2009; Nabuurs, Westphal et al. 2009; Nabuurs and van Mierlo 2010).

In this study, we monitor denaturant-dependent equilibrium folding of doubly dye-labelled apoflavodoxin variants using ensemble fluorescence and FRET. To obtain these proteins, we introduce cysteine residues at appropriate positions into apoflavodoxin. In addition, site-specific labelling with equimolar ratio of donor to acceptor is desired (Ratner, Kahana et al. 2002; Lakowicz 2006), because fluorescence emissions of labels are differently affected by their corresponding local environment. To fulfill this criterion, we utilise specific properties of the cofactor-bound form of the protein. Donor

(i.e., Alexa Fluor 488 C_5 maleimide; A488) is coupled to Cys69, whereas acceptor (i.e., Alexa Fluor 568 C_5 maleimide; A568) is attached to Cys1, Cys131, or Cys178, respectively. These dyes are brightly fluorescent, photostable, and excitable by visible light (Panchuk-Voloshina, Haugland et al. 1999; Schuler, Lipman et al. 2005). The corresponding doubly dye-labelled proteins are called d69-a1, d69-a131, and d69-a178, respectively. Subsequent measurements of fluorescence emission and FRET during apoflavodoxin folding reveal hitherto unknown features of the molten globule folding intermediate of an α-β parallel protein.

Materials and Methods

Protein engineering, expression and purification of flavodoxin variants containing cysteine pairs

Single oligonucleotide site-directed mutagenesis (Shenoy and Visweswariah 2003) was used to generate three variants of *A. vinelandii* (strain ATCC 478) flavodoxin II, which each contain a pair of cysteine residues. All variants have the wild-type cysteine at position 69. Through replacement of the residue at position 1, or position 131, or position 178, flavodoxin variants A001C, D131C, and S178C were generated, respectively. Recombinant and wild-type flavodoxins were expressed in *Escherichia coli* TG2 cells, which grew in Terrific Broth. Each flavodoxin variant was purified according to the well-established procedure developed for wild-type flavodoxin (van Mierlo, van Dongen et al. 1998). Purified proteins have a ratio of absorbance at 280 nm and absorbance at 450 nm (i.e., A280/A450) of about 4.75, demonstrating that all molecules contain stoichiometric amounts of FMN. To avoid oxidation of cysteine thiols, dithiothreitol (DTT) was present during protein purification.

The buffer used in all experiments with purified protein was 100 mM potassium pyrophosphate (KPPi), pH 6.0, unless otherwise mentioned.

Site-specific labelling of Cys001, Cys131, or of Cys178 with acceptor in holoprotein

Acceptor label (i.e., A568; Invitrogen) was added in 2.5-fold molar excess to purified cysteine-pair containing flavodoxin, and after 15 minutes at 22 °C, the reaction was stopped by adding 10-fold molar excess of reduced glutathione (Sigma). Labelling during this short period largely prevents dye labelling of the relatively inaccessible Cys69 (see Chapter 2 of this thesis). Subsequently, by using gel filtration with a P6-DG column (Bio-Rad), dye-labelled and non-labelled flavodoxin were separated from unreacted label, and buffer was exchanged to 20 mM Bis-Tris-HCl (Duchefa), pH 6.0. Singly acceptor-labelled protein was separated from non-labelled flavodoxin and from a small fraction of doubly acceptor-labelled protein, using ion exchange chromatography with a MonoQ 5/5 HR column (Pharmacia). Elution was done in the Bis-Tris-HCl buffer mentioned, using a salt gradient ranging from 0 to 1 M KCl.

Site-specific labelling of Cys69 with donor in unfolded protein

Singly acceptor labelled flavodoxin was unfolded in 6 M guanidine hydrochloride (GuHCl; Fluka), 100 mM KPPi, pH 7.0, to optimise accessibility of Cys69 for labelling. Subsequent addition of 10-fold molar excess of donor label (i.e., A488; Invitrogen) at 22 °C for a period exceeding 60 minutes led to labelling of Cys69. The resulting doubly dye-labelled apoflavodoxin molecules (i.e., d69-a1, d69-a131, or d69-a178) were separated from unreacted label, FMN and GuHCl using gel filtration with a Superdex75 10/30 HR column (Pharmacia). To obtain 'donor-only' protein (i.e., d69-apoflavodoxin), wild-type apoflavodoxin (i.e., protein that contains a single cysteine at position 69) was labelled with A488 using the same procedure to label Cys69 of singly-acceptor labelled protein. All dye-labelled apoflavodoxin was stored in 3 M GuHCl at -20 °C.

Denaturant induced equilibrium (un)folding

To determine the concentration of dye-labelled protein stock, absorption spectra of singly and doubly labelled apoflavodoxin were acquired on an HP-8453 diode array spectrophotometer. Label concentrations were determined using absorption coefficients of 71000 M^{-1} cm^{-1} and 91300 M^{-1} cm^{-1} for A488 and A568, respectively.

For each data point in a denaturant-dependent equilibrium folding series of dye-labelled apoflavodoxin, 50 µL of 1.25 µM protein stock in 2 M GuHCl was diluted into 950 µL of the appropriate GuHCl concentration using a Hamilton syringe. Final protein concentration was 62.5 nM. Samples were at equilibrium, since no change in fluorescence was observed after 5 minutes of incubation. For practical reasons, prior to measurements, samples stood for 16 to 24 hours in the dark at 25 °C.

Steady-state fluorescence measurements of denaturant-dependent equilibrium folding at 25 °C were done on a Cary Eclipse fluorescence spectrophotometer (Varian). Several combinations of excitation and emission wavelengths were used. Tryptophan fluorescence emission was measured at 330 nm, upon excitation at 280 nm. Donor was excited at 450 nm, to avoid direct excitation of the acceptor, and donor fluorescence emission was measured at 515 nm. Acceptor was excited at 580 nm and acceptor fluorescence emission was measured at 630 nm. Sensitised emission of acceptor fluorescence was measured at 630 nm upon excitation of donor at 450 nm. All fluorescence signals were recorded for 7.125 seconds. Excitation and emission slits were set to a width of 5 nm, except for the measurement of tryptophan fluorescence, where the emission slit was set to 10 nm.

To avoid protein adsorbing to glass surfaces, Tween-20 was added to all solutions to a final concentration of 0.0035 % (w/v). This addition does not affect apoflavodoxin, since no change in thermal midpoint of apoflavodoxin unfolding is observed. Refractometry was used to determine the GuHCl concentration in each individual sample (Nozaki 1972).

Time-dependent fluorescence anisotropy

Time resolved fluorescence was acquired using the time-correlated single photon counting technique, as described elsewhere (Borst, Hink et al. 2005). For measurement of donor fluorescence lifetime and anisotropy, excitation was at 450 nm and fluorescence emission was detected using a Schott 512.2 nm (FWHM ~13 nm) interference filter, in combination with a Schott GG475 (475 nm) long pass filter. For measurement of acceptor fluorescence lifetime and anisotropy, excitation was at 575 nm and fluorescence emission was detected using a Balzers 635 nm (FWHM ~13 nm) interference filter, in combination with a Schott RG610 (610 nm) long pass filter. Pulse duration was 0.2 ps, pulse energies were at the pJ level and the repetition rate of excitation pulses was 3.8×10^6 Hz. Samples were kept at 25 °C. Decay curves were collected in 4096 channels of a multi-channel analyser using a channel time spacing of 5.0 ps. Measurements consisted of ten repeated cycles of 10 s duration of parallel ($I_{\parallel}$ (t)) and perpendicularly ($I_{\perp}$ (t)) polarised fluorescence emission. Background fluorescence was measured under the same conditions. For the deconvolution procedure, the dynamic instrumental response function was determined using freshly made solutions of Erythrosine B in H_2O (τ = 80 ps) and pinacyanol in 100% MeOH (τ = 6 ps), both with an OD of 0.1 at the wavelengths used for donor and acceptor excitation, respectively.

The total fluorescence decay I(t) ($I(t) = I_{\parallel}(t) + 2I_{\perp}(t)$) was analysed using a sum of discrete exponentials with lifetimes τ_i and amplitudes α_i. The time-dependent fluorescence anisotropy $r(t)$ ($r(t) = (I_{\parallel}(t) - I_{\perp}(t)) / I(t)$) was calculated from parallel and perpendicular intensity components (van den Berg, van Hoek et al. 2004). Data analysis was done using TRFA data processor (Scientific Software Technologies Center, Minsk).

Results

Site-specific dye-labelling to track protein folding

By site-directed mutagenesis, we designed apoflavodoxin variants A001C, D131C, and S178C, respectively. The introduced cysteines reside in solvent-accessible loops (Figure 4.2), thus enabling dye labelling. All protein variants expressed in *E. coli* contain tightly bound FMN. Tight binding of FMN occurs primarily through a very specific combination and geometry of hydrogen bonds and aromatic interactions with native apoflavodoxin. Consequently, the observation that all apoflavodoxin variants of this study bind FMN tightly implies that the three-dimensional structures of the corresponding flavodoxin are nearly indistinguishable from the one of wild-type flavodoxin. Analogously, the conformations of native apoflavodoxin variants thus are similar.

The introduced cysteines are more accessible than Cys69 (Figure 4.2), allowing site-specific labelling with A568. Under the given experimental conditions hardly any labelling of Cys69 takes

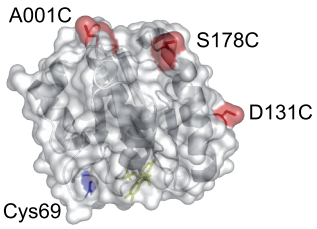

Figure 4.2 In flavodoxin, Cys69 is much less accessible than Cys1, Cys131, and Cys178. The cartoon model shows the surface of flavodoxin in a semi-transparent fashion, with Cys69 in blue, and the other cysteines in red. The FMN cofactor is shown in yellow. The cartoon model and the cysteines were generated with PyMOL (Schrödinger, LLC, Palo Alto, Ca, USA) using the crystal structure of *A. vinelandii* flavodoxin (pdb ID 1YOB (Alagaratnam, van Pouderoyen et al. 2005)).

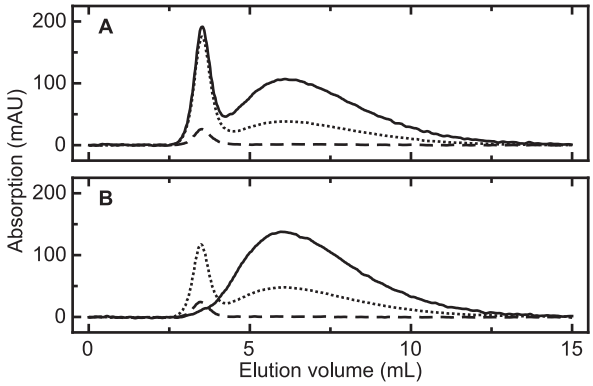

Figure 4.3 Biogel P6DG elution profiles of wild-type and S178C flavodoxin after labelling of these proteins with A568. (A) Flavodoxin variant S178C, which contains cysteine residues at positions 69 and 178, respectively. (B) Wild-type flavodoxin, which contains only cysteine at position 69. Solid lines represent absorption at 578 nm (i.e., due to presence of A568), dashed lines represent absorption at 450 nm (i.e., due to presence of FMN) and dotted lines represent absorption at 280 nm (i.e., due to tryptophan, FMN and A568). Labelling is done as described in Materials and Methods, using identical concentrations of S178C and wild-type flavodoxin. Protein elutes at about 3.5 ml of elution volume, whereas free label elutes at larger elution volumes.

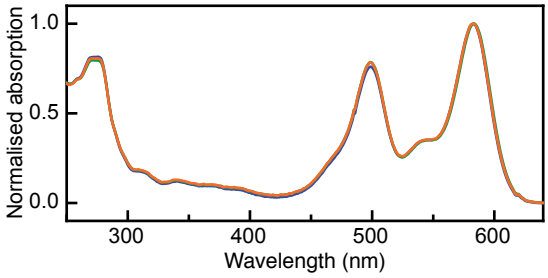

Figure 4.4 Doubly labelled apoflavodoxin has equimolar ratio of donor to acceptor. Normalised absorption spectra of d69-a1 (blue), d69-a131 (green) and d69-a178 (orange) are shown. Based on absorption coefficients of 71000 M^{-1} cm^{-1} and 91300 M^{-1} cm^{-1} for A488 and A568, respectively, the ratio of donor to acceptor is calculated to be equimolar. Dye-labelled proteins are in 3 M GuHCl.

place (Figure 4.3). Subsequent unfolding of each acceptor-labelled variant enables labelling of Cys69 with A488. The degree of doubly dye-labelling is similar, because the absorption spectra of the proteins almost completely overlap (Figure 4.4). Equimolar ratio of donor to acceptor is obtained.

Upon removal of denaturant, GuHCl-unfolded, dye-labelled apoflavodoxin variants autonomously fold to native apoprotein, because apoflavodoxin unfolding is reversible (van Mierlo, van Dongen et al. 1998). Subsequent addition of FMN leads to complete reconstitution of holoprotein (data not shown), and thus, coupling of donor and acceptor dyes does not impede the ability of apoflavodoxin to bind cofactor.

Use of d69-a1 allows tracking of the folding of the N-terminal part of the protein, which consists of β-strands 1, 2 and 3, and α-helices A and B of native apoflavodoxin (Figure 4.5A, B). Use of d69-a131 reports about the folding of residue 69 up to and including residue 131, consisting of β-strands 4 and 5a, and α-helices C and D of native apoflavodoxin (Figure 4.5A, C), and use of d69-a178 additionally informs about the folding of residues 131 up to and including residue 178, consisting of β-strand 5b and C-terminal α-helix E of native protein (Figure 4.5A, D).

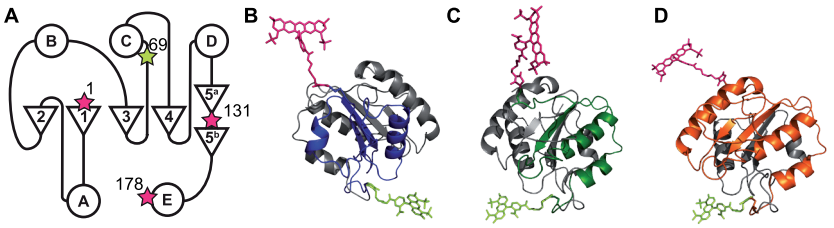

Figure 4.5 Covalent attachment of dye-labels to enable FRET-based probing of folding of various regions of apoflavodoxin. In all protein variants, donor label (i.e., A488) is attached to residue 69. (A) Positions of dye labels within the topology of flavodoxin. A488 is represented by a bright green star and acceptor label (i.e., A568) by a pink star. (B) Cartoon representation of d69-a1, showing in blue the backbone that intervenes residues 1 and 69. (C) d69-a131, with the backbone intervening residues 69 and 131 in green. (D) d69-a178, with the backbone intervening residues 69 and 178 in orange. A488 is shown in bright green, and A568 in pink. Cartoons are generated with PyMOL (Schrödinger, LLC, Palo Alto, Ca, USA) using the crystal structure of *A. vinelandii* flavodoxin (pdb ID 1YOB (Alagaratnam, van Pouderoyen et al. 2005)) and the molecular structures of A488 and A568, as provided by Invitrogen.

Folding of dye-labelled apoflavodoxins involves a stable intermediate

Participation of a folding intermediate is observed during folding of apoflavodoxin that is labelled with a donor and an acceptor label, as the following data show. Figures 4.6A to 4.6C present fluorescence emission intensities of tryptophan, A488, and of A568 during denaturant-dependent equilibrium folding of doubly dye-labelled protein. Fluorescence emission intensities of donor (i.e., A488 (Figure 4.6B)) and of acceptor (i.e., A568 (Figure 4.6C)) reports biphasic unfolding curves for d69-a131 and d69-a178. This biphasic behaviour demonstrates population of a stable intermediate during folding of both proteins.

Compared to native and unfolded protein, the intermediate has lower fluorescence emission intensities of donor as well as of acceptor. Use of FRET enables further characterisation of this intermediate, as discussed below. Unfolding curves of d69-a1 show no clear biphasic pattern (Figures 4.6B, C). Nevertheless, a stable intermediate populates during its folding, because the transition revealed by fluorescence emission intensities of tryptophans (Figure 4.6A) and the transitions revealed by fluorescence emission intensities of A488 and A568 do not coincide. This non-coincidence of unfolding transitions is a hallmark of the involvement of a folding

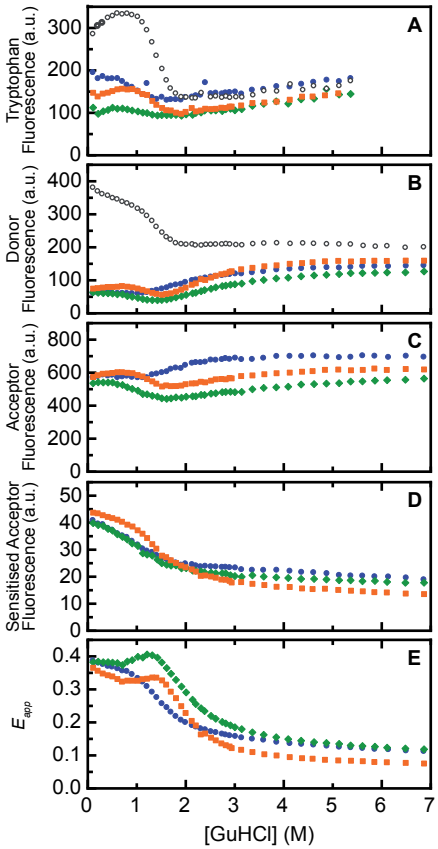

Figure 4.6 The denaturant-dependence of fluorescence signals of doubly dye-labelled apoflavodoxin reveals properties of apoflavodoxin's folding intermediate. Shown are fluorescence data of 'donor-only' protein (open circles), d69-a1 (blue circles), d69-a131 (green diamonds) and of d69-a178 (orange squares). Protein concentration is 62.5 nM. (A) Fluorescence emission intensity of tryptophan at 330 nm with excitation at 280 nm. (B) Fluorescence emission intensity of donor (A488) at 515 nm with excitation at 450 nm. (C) Fluorescence emission intensity of acceptor (A568) at 630 nm with excitation at 580 nm. (D) Sensitised fluorescence emission intensity of acceptor at 630 nm with excitation at 450 nm. (E) Apparent FRET efficiency (E_{app}), calculated by using data of panels (B) and (D) and equation 4.3. Standard deviations of the fluorescence signals shown vary between 1 to 3 % of the measured signal intensities.

intermediate. In conclusion, folding of all three doubly dye-labelled apoflavodoxin variants involves a stable folding intermediate.

Fluorescence of tryptophans of doubly dye-labelled apoflavodoxin has a complex dependency on denaturant due to FRET between the three tryptophan residues of apoflavodoxin (i.e., Trp74, Trp128, and Trp167) (Visser, Westphal et al. 2008), and because FRET occurs between tryptophans and donor as well as acceptor labels (see below). Similarly, FRET between donor and acceptor labels influences fluorescence emission of donor as a function of denaturant concentration. Due to the complex dependence of fluorescence intensity on denaturant concentration when FRET is occurring, and because this dependence is not quantitatively predictable owing to the strong distance dependence of fluorescence intensity (Eftink 1994; Huang, Settanni et al. 2008), we can not use fluorescence signals to calculate thermodynamic parameters of doubly dye-labelled native proteins and corresponding folding intermediates.

Attachment of dye labels to apoflavodoxin will have some impact on the thermodynamic stabilities of the different folding species. Indeed, comparison of Figures 4.1A and 4.6A shows that coupling of donor and acceptor to apoflavodoxin destabilises native apoprotein, because the corresponding folding transition shifts to lower concentration GuHCl. Similarly, upon mutating various amino acid residues of apoflavodoxin, stabilities of the corresponding native apoproteins decrease (van Mierlo, van Dongen et al. 1998; Nabuurs, Westphal et al. 2009; Laptenok, Visser et al. 2011). Yet, just as observed here for doubly dye labelled protein, folding still occurs according to a three-state model, because this is a typical feature of proteins with a flavodoxin-like fold (Bollen and van Mierlo 2005).

Fluorescence of dye-labelled apoflavodoxin in the native and unfolded state

Due to FRET, tryptophan fluorescence of native protein decreases considerably upon covalent attachment of A488 to Cys69 (R_0 ~ 27 Å, data not shown). Upon subsequent covalent coupling of A568 to 'donor-only' apoflavodoxins, tryptophan fluorescence of native protein diminishes even further (Figure 4.6A), because A568 functions as additional acceptor for FRET (R_0 ~ 26 Å). The distance between C^{α} of residue 131 and the most nearby tryptophan (i.e., C^{7a} of Trp128) is 8.7 Å, whereas the distance between C^{α} of residue 1 and its most nearby tryptophan (i.e., C^{7a} of Trp167) is 18.3 Å. In case of d69-a178, 14.8 Å separates C^{α} of residue 178 and its most nearby tryptophan (i.e., C^{7a} of Trp167) (Table 4.1). Correspondingly, in their native states, d69-a131 has the lowest tryptophan fluorescence, whereas d69-a1 has the highest emission (Figure 4.6A).

Table 4.1 Distances between residues used in dye-labeling and tryptophans of native apoflavodoxin.

From/To	Trp74	Trp128	Trp167
Cys1	21.3 Å	24.3 Å	18.3 Å
Cys69	12.8 Å	26.4 Å	24.5 Å
Cys131	25.3 Å	8.7 Å	15.2 Å
Cys178	26.1 Å	19.3 Å	14.8 Å

The distances reported are between C7a of the tryptophan indicated and Ca of the residue to be dye-labeled, as measured by using PyMol (Schrödinger, LLC, Palo Alto, Ca, USA) and the crystal structure of A. vinelandii *flavodoxin (pdb ID 1YOB (Alagaratnam, van Pouderoyen et al. 2005)).*

Tryptophan fluorescence data show that the unfolded baselines of the folding curves of 'donor-only' apoflavodoxin and d69-a1 coincide. Hence, in unfolded protein no FRET from tryptophans to A568 occurs, as apparently their spatial separation exceeds twice the corresponding Förster distance. In case of unfolded d69-a131 and d69-a178, FRET plays a role, because their tryptophan fluorescence is lower than that of 'donor-only' apoflavodoxin (Figure 4.6A). FRET from tryptophans to acceptor is similar in these unfolded proteins, because their unfolded baselines coincide.

To quantify FRET between A488 and A568 during denaturant-dependent equilibrium folding of doubly dye-labelled apoflavodoxin, we use equation 4.2:

$$E = 1 - \frac{I_{DA}}{I_D} \qquad [4.2]$$

where I_{DA} and I_D are the fluorescence emission intensities of donor label in presence and in absence of acceptor, respectively. We obtained I_D by measuring the denaturant dependency of fluorescence emission of 'donor-only' protein (i.e., d69-apoflavodoxin) at 515 nm, which appears to track folding of this protein (Figure 4.6B). Upon attaching acceptor label to native 'donor-only' apoflavodoxin, fluorescence intensity of donor A488 severely decreases, as comparison of native baselines in Figure 4.6B shows. This decrease is due to FRET from A488 to A568. Whereas at zero molar denaturant this FRET between both dyes is similarly efficient for d69-a1 and d69-a131, it is less efficient in case of d69-a178. Upon unfolding of doubly dye-labelled protein above 2 M GuHCl, donor fluorescence increases and levels off at high concentrations of denaturant (Figure 4.6B). Fluorescence emission intensity of A488 of fully unfolded protein at 6.9 M GuHCl decreases from d69-a178, d69-a1 to

d69-a131. This order is consistent with the number of amino acid residues in between donor and acceptor in these proteins, which decreases from 108, to 67, and to 61 residues, respectively.

Changes in fluorescence emission intensity of directly excited acceptor upon (un)folding of apoflavodoxin (Figure 4.6C) are due to changes in quenching of this dye, which also happens for A488 in case of 'donor-only' apoflavodoxin (Figure 4.6B). When a fluorophore is in proximity of tryptophan, photon induced electron transfer towards tryptophan can occur and as a result fluorescence of the dye involved diminishes due to static quenching (Chen, Ahsan et al. 2010; Mansoor, Dewitt et al. 2010). Due to this quenching, A568 fluorescence of unfolded apoflavodoxin decreases from d69-a1, to d69-a178, and to d69-a131, respectively. This order reflects the number of amino acid residues in between acceptor and nearest tryptophan in the primary sequence of the protein (i.e., 72, 10, and 2 residues, respectively). In case of native protein, Trp74 and Trp167 are in the protein interior, whereas Trp128 is located at the protein surface (Visser, Westphal et al. 2008). Consequently, in native protein, quenching of acceptor in d69-a131 is more efficient than in case of the other two doubly dye-labelled apoflavodoxins, for which A568 is about equally fluorescent (Figure 4.6C).

Changes in quenching upon formation of apoflavodoxin's molten globule cause the dip in fluorescence emission intensity of A568 of d69-a131, and of d69-a178 at ~1.7 M GuHCl (Figure 4.6C). Upon formation of this intermediate, tryptophans become solvent exposed (Bollen, Sanchéz et al. 2004; Nabuurs, Westphal et al. 2009), which leads to increased quenching of A568. Remarkably, in case of d69-a1, Figure 4.6C shows that A568 fluorescence rises upon increasing denaturant concentration. This observation reveals molecular details of apoflavodoxin's folding intermediate, as shown below.

FRET tracks folding of dye-labelled apoflavodoxin

By using fluorescence of donor label in presence and in absence of acceptor (i.e., I_{DA} and I_{D}, respectively (Figure 4.6B)), and subsequent application of equation 4.2, we determine FRET efficiencies (E) of native and unfolded doubly dye-labelled apoflavodoxins. Table 4.2 reports these values for native protein at 0.1 M GuHCl (i.e., at the lowest concentration denaturant used) and for unfolded protein at 6.9 M GuHCl, at which apoflavodoxin behaves as a random coil (Nabuurs, Westphal et al. 2008). FRET efficiencies range from 0.80 to 0.83 for native doubly dye-labelled apoflavodoxins. Using R_0 of 53.1 ± 0.5 (Engel, Westphal et al. 2008), we calculate that the corresponding inter-dye distances range from 40 ± 2 to 42 ± 2 Å, which is in reasonable agreement with the molecular dimensions of native apoflavodoxin. Unfolded apoflavodoxins are characterised by much lower FRET efficiencies, as the average distances between donor and acceptor labels are increased compared to the distances in native protein. FRET efficiencies range from 0.20, to 0.27, to 0.37, for unfolded d69-a178,

unfolded d69-a1, and for unfolded d69-a131, respectively. This increase correlates with the inter-residue separations of both dyes in the primary sequences of these unfolded proteins.

Table 4.2 FRET efficiencies of native and unfolded doubly dye-labeled apoflavodoxins.

Protein variant	Fluorescence of native protein (a.u.)	FRET efficiency of native protein	Fluorescence of unfolded protein (a.u.)	FRET efficiency of unfolded protein
d69	382.15 ± 5.17		201.69 ± 3.18	
d69-a1	62.84 ± 1.85	0.84 ± 0.03	145.99 ± 2.55	0.27 ± 0.01
d69-a131	63.45 ± 1.93	0.83 ± 0.03	126.86 ± 2.88	0.37 ± 0.01
d69-a178	74.89 ± 2.61	0.80 ± 0.03	159.51 ± 2.49	0.20 ± 0.01

Fluorescence emission intensity is of donor (A488) at 515 nm with excitation at 450 nm. Fluorescence of native protein is determined at 0.1 M GuHCl (i.e., at the lowest concentration denaturant used), whereas fluorescence of unfolded protein is determined at 6.9 M GuHCl.

The doubly dye-labelled apoflavodoxins enable monitoring of FRET efficiencies during folding. Attachment of acceptor label to 'donor-only' protein affects the thermodynamic stabilities of apoflavodoxin's folding species. Consequently, in the transition regions of unfolding of 'donor-only' and doubly dye-labelled proteins the populations of these species differ. As a result, donor fluorescence of 'donor-only' protein (i.e., I_D) and of doubly dye-labelled protein (i.e., I_{DA}) cannot be used to determine the exact FRET efficiencies of doubly dye-labelled apoflavodoxin species according to equation 4.2. Therefore, we utilised the measured donor fluorescence intensities of doubly dye-labelled protein, and acquired the emission of acceptor upon excitation of donor, to calculate the apparent FRET efficiency (E_{app}) at various denaturant concentrations, according to Equation 4.3.

$$E_{app} = \frac{I_{FRET}}{I_{FRET} + I_{DA}} \qquad [4.3]$$

where I_{FRET} is the sensitised fluorescence emission intensity of acceptor (i.e., emission of acceptor upon excitation of donor). With identical fluorescence quantum yields of donor and acceptor and identical detection efficiencies of both fluorescence signals, E_{app} equals E.

Figure 4.6D shows the denaturant-dependence of IFRET (i.e., fluorescence emission intensity of acceptor A568 at 630 nm with excitation of donor A488 at 450 nm) for all doubly dye-labelled apoflavodoxins. Application of equation 4.3 to the data of Figures 4.6B and 4.6D yields Figure 4.6E, which shows the corresponding E_{app}. Clearly, because the E_{app}-values are significantly lower than

the corresponding *E*-values mentioned previously, considerable differences between fluorophore quantum yields and/or detection efficiencies of donor and acceptor dyes exist, causing downscaling of E_{app} compared to *E*. Indeed, fluorescence quantum yields of A488 and A568 are 0.84 and 0.63, respectively (Invitrogen). In addition, whereas we measure fluorescence emission of A488 at its emission maximum of 515 nm, we acquire fluorescence emission of A568 at 630 nm, to avoid simultaneous detection of donor fluorescence. Fluorescence intensity of A568 at 630 nm is only ~ 50 % of its emission maximum, and thus E_{app} becomes even further reduced.

Changes in E_{app} track folding of dye-labelled apoflavodoxin (Figure 4.6E). In case of d69-a131 and d69-a178, a hump in the corresponding unfolding curves highlights the presence of a folding intermediate. Remarkably, despite that folding of d69-a1 involves a stable intermediate, as discussed, no such hump is observed for this protein (Figure 4.6E).

Dependence of Förster distance on folding state

To further assess the molecular source of the hump in the unfolding curve of d69-a131 and of d69-a178 (Figure 4.6E), one needs to address the effects of changing from one folding state to another has on the parameters that comprise the Förster equation:

$$R_0 = 0.211\left(Q_D n^{-4} \kappa^2 J(\lambda)\right)^{1/6} \qquad [4.4]$$

where Q_D is the quantum yield of donor fluorescence in absence of acceptor, *n* the refractive index of the medium that separates donor from acceptor (Knox and van Amerongen 2002), κ^2 the orientation factor for the relevant transition dipole moments, and *J* the integrated spectral overlap of acceptor absorbance and donor fluorescence spectra (M^{-1} cm^3).

Upon changing the folding state, Q_D in equation 4.4 possibly alters. Figure 4.6B suggests that native 'donor-only' apoflavodoxin has a Q_D-value higher than that of the corresponding unfolded protein or folding intermediate. Consequently, these latter protein states would have R_0-values that are lower than the one associated with native protein. For example, decreasing Q_D from 0.84 to 0.5 results in a drop of R_0 from 53.1 Å to 48.7 Å (Engel, Westphal et al. 2008). In the hypothetical situation that the distance between donor and acceptor dyes remains unaltered upon switching folding states, but Q_D diminishes, both folding intermediate and unfolded protein would show less FRET than native protein. However, Figure 4.6E reports increased FRET for folding intermediate compared to FRET for native and unfolded protein.

The refractive index of the medium that separates donor from acceptor alters by changing denaturant concentration and thus *n* in equation 4.4 changes. With refractometry we determined that the refractive index of buffer (i.e., 100 mM KPPi, pH 6.0) is 1.337, whereas the refractive

index of buffer with 6.9 M GuHCl is 1.451. The interior of native protein has a refractive index of ~ 1.6 (Toptygin, Savtchenko et al. 2002), and consequently the refractive index of protein lies somewhere between approximately 1.3 and 1.6, since the medium is a mixture of buffer, GuHCl and protein. A reasonable estimate for the refractive index of hydrated protein (~50 % protein and ~50 % water), which separates donor from acceptor label in apoflavodoxin, is a value of ~ 1.5 (Knox and van Amerongen 2002; Vörös 2004). Upon adding denaturant, n slightly increases and thus R_0 decreases. Consequently, again in the hypothetical situation that donor and acceptor dyes would remain fixed upon switching folding states, both folding intermediate and unfolded protein would give rise to slightly less FRET than native protein. Figure 4.6E clearly shows that this situation is not the case for folding intermediate.

Assessing the effects a change of folding state has on κ^2, and thus on R_0, is difficult to achieve. The dipole orientation factor κ^2 equals:

$$\kappa^2 = \left(\cos\theta_T - 3\cos\theta_D\cos\theta_A\right)^2 \qquad [4.5]$$

in which θ_T represents the angle between donor emission dipole and acceptor absorption dipole, and θ_D and θ_A are the angles between these dipoles and the vector that connects donor and acceptor. In case of donor and acceptor pairs having unrestricted flexibility, κ^2 equals 2/3.

Despite that the dyes are attached to apoflavodoxin via flexible linkers, dye-reorientation might be restricted by interactions of the fluorophores with the protein surface. These interactions may differ between folding states. To assess κ^2 associated with these states, we measured time-resolved fluorescence anisotropy to determine the reorientation rates of A488 and A568, using 'donor-only' and doubly dye-labelled protein at increasing concentrations denaturant (see Materials and Methods). The anisotropy decay (r_t) of a dye-labelled native protein exhibiting slow overall rotation with time constant Φ_{prot} and amplitude β_2, and fast reorientation of the attached dye with time constant for internal reorientation Φ_{dye} and amplitude β_1, is described by the following model (Szabo 1984):

$$r_t = \left\{\beta_1 \exp\left(-t/\Phi_{dye}\right) + \beta_2\right\}\exp\left(-t/\Phi_{prot}\right) \qquad [4.6]$$

where the sum of the amplitudes is the fundamental anisotropy (i.e., $r_0 = r_t(t=0)$). This model excellently describes anisotropy decay of dye-labelled apoflavodoxin at each concentration of denaturant used (Figure 4.7). Note that upon unfolding, overall rotation of the protein decreases, while concomitantly flexibility of the polypeptide increases considerably. As a result, for unfolded protein, Φ_{prot} reports the combined local dynamics of the label and of the amino acid to which the dye is covalently coupled. Taking the measured anisotropy data one can calculate a second-rank

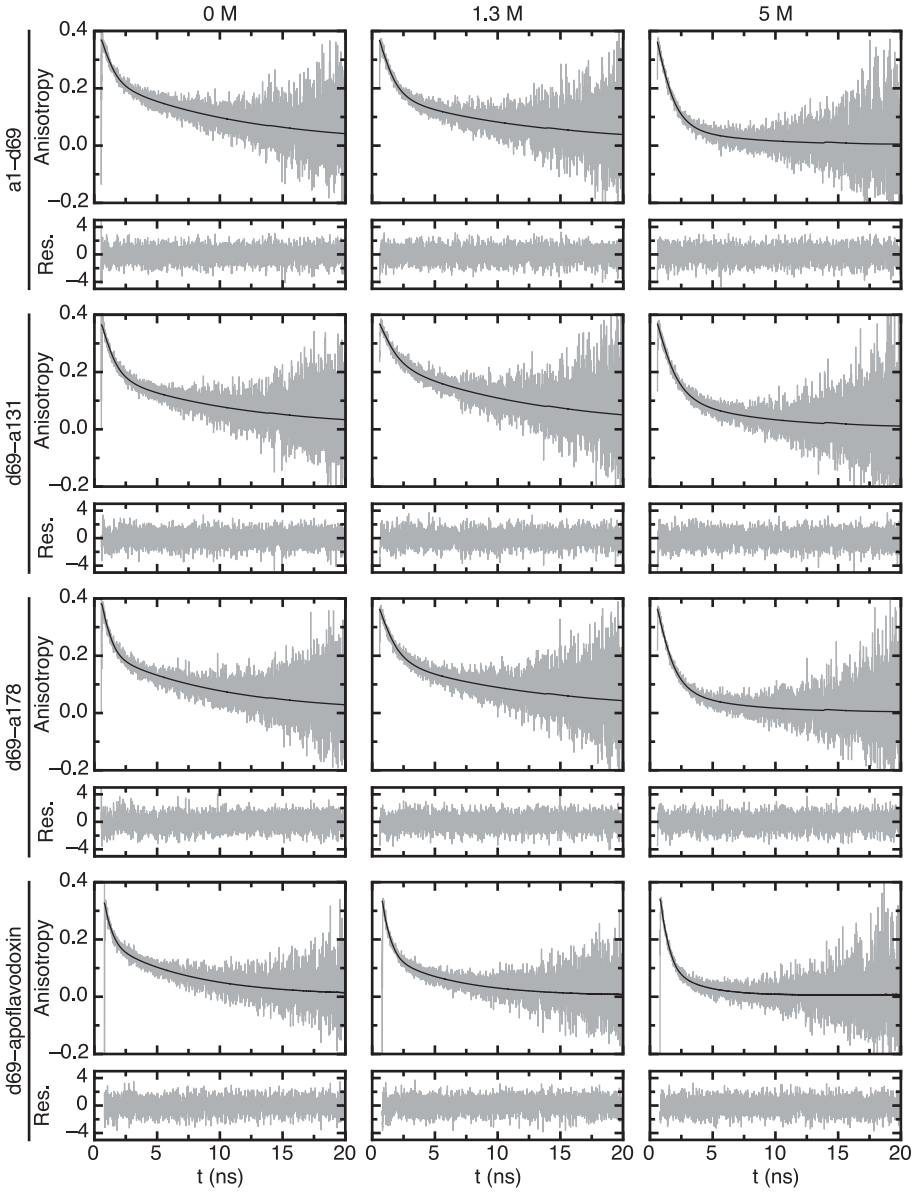

Figure 4.7 Examples of experimental fluorescence anisotropy decay curves (grey lines) and associated bi-exponential fits (black lines) obtained for A568 of doubly dye-labelled apoflavodoxins and for A488 of d69-apoflavodoxin. Shown are anisotropy decays obtained for protein in 0 M, 1.3 M and 5 M guanidine hydrochloride, respectively. Weighted residuals are shown to illustrate the quality of the fits.

order parameter *S* for the reorienting fluorophores that are attached to apoflavodoxin, according to (Szabo 1984):

$$S^2 = \beta_2 / r_0 \qquad [4.7]$$

Thus, when the dye does not reorient with respect to protein (i.e., dye motion is fully restricted) *S* equals 1. The rate of dye reorientation is given by the diffusion coefficient $D_\perp$ of internal motion, which is calculated according to (Szabo 1984):

$$D_\perp = \left(1 - S^2\right) \Big/ \left(6\Phi_{dye}\right) \qquad [4.8]$$

Figure 4.8 shows the rates of dye reorientation of A488 in 'donor-only' apoflavodoxin, as well as of A568 in doubly dye-labelled apoflavodoxin variants. The value of $D_\perp$ for all denaturant concentrations used is well above 50 MHz (Figure 4.8) and shows that the dye labels exhibit flexibility. Consequently, during our measurements, donor emission and acceptor excitation dipoles are randomly oriented towards one another, which justifies the assumption that $\kappa^2 = 2/3$ at all denaturant concentrations used.

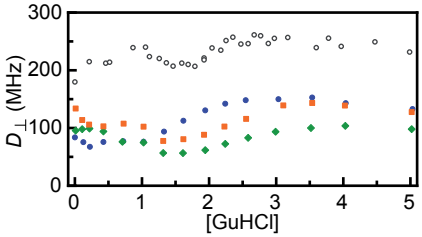

Figure 4.8 Denaturant-dependencies of the reorientation rates of dye labels attached to apoflavodoxins. Shown are the $D_\perp$ data of A488 of 'donor-only' protein (open circles), and of A568 of d69-a1 (blue circles), d69-a131 (green diamonds) and d69-a178 (orange squares), respectively.

Finally, upon changing folding state, the spectral overlap integral *J* of the Förster equation might alter. This integral equals:

$$J(\lambda) = \int_0^\infty F_D(\lambda)\varepsilon_A(\lambda)\lambda^4 \, d\lambda \qquad [4.9]$$

where $f_D(\lambda)$ is the normalised fluorescence emission spectrum of donor, and $\varepsilon_A(\lambda)$ is the normalised absorption spectrum of acceptor weighted by the corresponding molar extinction coefficient. Figure 4.9 shows that upon adding 6.9 M GuHCl to apoflavodoxin, both the emission spectrum of donor as well as the excitation spectrum of acceptor shift to the red by about 3 to 4 nm, and concomitantly εA increases by about 11 %. This combined effect causes a 14 % increase in the

integrated spectral overlap and thus leads to a slightly larger Förster distance (i.e., R_0 increases 2.3 % and changes from 53.1 to 54.3 Å).

In conclusion, upon switching between folding states, changes in parameters of the Förster equation are such that they cannot account for the observed hump in the E_{app} unfolding curves of d69-a131 and d69-a178. These humps must thus reflect shortening of separation between donor and acceptor upon conversion of native protein to folding intermediate. Upon this transition, no such shortening happens in the N-terminal part of apoflavodoxin, because no accompanying hump exists in the E_{app} unfolding curve of d69-a1.

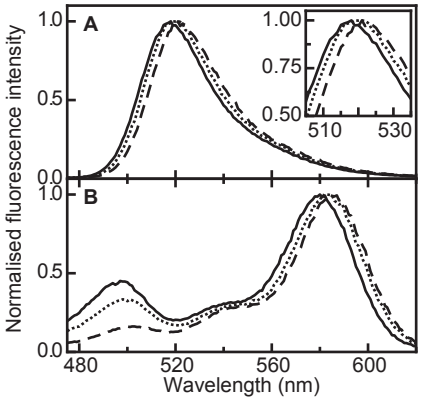

Figure 4.9 Upon adding denaturant, apoflavodoxin's donor emission spectrum and acceptor excitation spectrum shift to the red. (A) Normalised emission spectra of 'donor-only' apoflavodoxin. The inset zooms in on the fluorescence emission maximum, which shifts from 518 to 521 nm upon adding 6.9 M GuHCl. (B) Normalised excitation spectrum of acceptor of d69-a178. GuHCl concentrations are 0.1 M (solid line), 1.7 M (dotted line) and 6.9 M (dashed line), respectively.

Discussion

Exploiting the dye-inaccessibility of Cys69 in cofactor-bound flavodoxin, we obtained a homogeneous population of doubly dye-labelled protein molecules with donor attached to Cys69 and acceptor at desired positions. In this study, we track folding of ensembles of site-specifically dye-labelled apoflavodoxin molecules by fluorescence emission intensities and apparent FRET efficiencies.

Molecular properties of apoflavodoxin's off-pathway folding intermediate

Fluorescence emission intensity and E_{app} data of the three doubly dye-labelled apoflavodoxins reveal hitherto unknown features of the off-pathway molten globule of apoflavodoxin. The hump observed in the E_{app} data of denaturant-dependent folding of d69-a131 and d69-a178 (Figure 4.6E) implies that donor and acceptor are less separated in the interconverting ensemble of conformers

that represents I_{off}, than they are in native apoflavodoxin. Concomitantly, fluorescence emission intensity of A568 drops (Figure 4.6C), revealing exposure of hydrophobic side chains of tryptophan and tyrosine residues in the folding intermediate, which both act as fluorescence quenchers of acceptor label (with tryptophan being the dominant quencher). Exposure of hydrophobic side chains probably causes a slight decrease in reorientation rate of A568, as Figure 4.8 suggests. The C-terminal part of the molten globule, involving residues 69 to 178, must thus be rather compact and differs considerably from native protein. This part of the molten globule has a midpoint of unfolding of ~ 2 M GuHCl.

Folding of apoflavodoxin's molten globule is non-cooperative

In case of d69-a1, where E_{app} monitors folding of the N-terminal 69 residues of the protein, no hump exists in the corresponding denaturant-dependent folding curve (Figure 4.6E). Despite the absence of this hump, apoflavodoxin's folding intermediate does populate in between ~ 0.8 to ~ 3.0 M GuHCl, as the non-coincidence of the unfolding transitions of d69-a1 in Figures 4.6A-C demonstrates. Hence, the observed decrease of E_{app} in this denaturant range implies that the N-terminal 69 residues of the folding intermediate unfold above 0.8 M GuHCl. This conclusion is supported by fluorescence emission intensity of A568, which also shows no hump during denaturant-dependent equilibrium folding of the protein (Figure 4.6C). In native d69-a1, due to its vicinity and partial solvent accessibility, Tyr47 quenches fluorescence of A568. At about 1 M GuHCl, where folding intermediate is also present, this quenching sustains, implying that the N-terminal part of this intermediate must be structured at relatively low concentrations of GuHCl. Increasing denaturant concentration leads to increased fluorescence of A568, because the N-terminal part of the molten globule unfolds and because unfolded d69-a1 becomes populated. Unfolding of the N-terminal part of the molten globule thus occurs at lower denaturant concentration than happens for its C-terminal part. This observation shows that folding of apoflavodoxin's molten globule is non-cooperative.

Unfolding of transiently ordered regions in unfolded apoflavodoxin

The data of Figure 4.6 imply that the unfolded state of apoflavodoxin, which is fully populated at about 3 M GuHCl, expands upon increasing denaturant concentration. Upon adding denaturant, E_{app} diminishes for all three dye-labelled unfolded proteins (Figure 4.6E), because the average separation between donor and acceptor dyes increases. In addition, fluorescence of A488 and A568 increases (Figure 4.6B, C), due to less efficient energy transfer and because less quenching of both dyes by tryptophan and tyrosine residues occurs, as the average distances between these residues and dye labels increase. This expansion of unfolded protein with increasing denaturant reflects unfolding of transiently ordered regions that exist in unfolded apoflavodoxin at about

3 M GuHCl. At 6 M GuHCl, the protein behaves as random coil (Nabuurs, Westphal et al. 2008; Nabuurs, Westphal et al. 2009).

FRET data show that the conformations of molten globule and native apoflavodoxin differ drastically

NMR spectroscopy shows that upon lowering denaturant concentration, structure formation within virtually all parts of unfolded apoflavodoxin precedes folding to the molten globule state. This folding transition is non-cooperative and involves a series of distinct transitions. Four structured elements in unfolded apoflavodoxin transiently interact and subsequently form the ordered core of the molten globule. This ordered core is gradually extended upon decreasing denaturant concentration (Nabuurs, Westphal et al. 2008; Nabuurs, Westphal et al. 2009; Nabuurs, Westphal et al. 2009; Nabuurs and van Mierlo 2010). NMR spectroscopy detects formation of apoflavodoxin's molten globule in an indirect manner through disappearance of resonances of unfolded protein. Resonances of the molten globule cannot be detected by this technique, because they are broadened beyond detection due to exchange between different conformers on the micro- to millisecond time scale (Engel, Westphal et al. 2008; Nabuurs, Westphal et al. 2009). In contrast, in the study presented here we directly detect features of this molten globule by measuring fluorescence emission and FRET of the dye labels that are covalently attached to the protein. These fluorescence data show that upon decreasing denaturant concentration, the C-terminal 111 residues of the molten globule fold first, leading to a conformation that differs drastically from the one of the C-terminal part of native protein. The N-terminal part of the molten globule species is still unfolded and upon lowering denaturant concentration this protein part becomes structured, as the data of Figure 4.6 imply. This study shows that the conformations of molten globule and native protein differ considerably. Hence, to produce native α-β parallel protein, the molten globule needs to unfold, explaining why this folding species is off-pathway during folding of apoflavodoxin.

Acknowledgements

We thank Arie van Hoek and Antonie Visser for help in acquisition and analysis of time-resolved fluorescence data.

References

Alagaratnam, S., G. van Pouderoyen, et al. (2005). "A crystallographic study of Cys69Ala flavodoxin II from *Azotobacter vinelandii*: structural determinants of redox potential." Protein Sci. 14(9): 2284-2295.

Amir, D., S. Krausz, et al. (1992). "Detection of local structures in reduced unfolded bovine pancreatic trypsin inhibitor." Proteins 13(2): 162-173.

Arai, M. and K. Kuwajima (2000). "Role of the molten globule state in protein folding." Adv. Prot. Chem. 53: 209-282.

Bollen, Y. J., M. B. Kamphuis, et al. (2006). "The folding energy landscape of apoflavodoxin is rugged: Hydrogen exchange reveals nonproductive misfolded intermediates." Proc. Natl. Acad. Sci. U.S.A. 103(11): 4095-4100.

Bollen, Y. J., S. M. Nabuurs, et al. (2005). "Last in, first out: The role of cofactor binding in flavodoxin folding." J. Biol. Chem. 280(9): 7836-7844.

Bollen, Y. J., I. E. Sanchéz, et al. (2004). "Formation of on- and off-pathway intermediates in the folding kinetics of *Azotobacter vinelandii* apoflavodoxin." Biochemistry 43(32): 10475-10489.

Bollen, Y. J. and C. P. van Mierlo (2005). "Protein topology affects the appearance of intermediates during the folding of proteins with a flavodoxin-like fold." Biophys. Chem. 114(2-3): 181-189.

Borst, J. W., M. A. Hink, et al. (2005). "Effects of refractive index and viscosity on fluorescence and anisotropy decays of enhanced cyan and yellow fluorescent proteins." J. Fluorescence 15(2): 153-160.

Bryngelson, J. D., J. N. Onuchic, et al. (1995). "Funnels, pathways, and the energy landscape of protein folding: a synthesis." Proteins 21(3): 167-195.

Chen, H., S. S. Ahsan, et al. (2010). "Mechanisms of quenching of Alexa fluorophores by natural amino acids." J. Am. Chem. Soc. 132(21): 7244-7245.

Chiti, F. and C. M. Dobson (2006). "Protein misfolding, functional amyloid, and human disease." Annu. Rev. Biochem. 75: 333-366.

Christensen, H. and R. H. Pain (1991). "Molten globule intermediates and protein folding." Eur. Biophys. J. 19(5): 221-229.

Dill, K. A. and H. S. Chan (1997). "From Levinthal to pathways to funnels." Nat. Struct. Mol. Biol. 4(1): 10-19.

Dinner, A. R., A. Sali, et al. (2000). "Understanding protein folding via free-energy surfaces from theory and experiment." Trends Biochem. Sci. 25(7): 331-339.

Dobson, C. M. (2003). "Protein folding and misfolding." Nature 426(6968): 884-890.

Eftink, M. R. (1994). "The use of fluorescence methods to monitor unfolding transitions in proteins." Biophys. J. 66(2 Pt 1): 482-501.

Engel, R., A. H. Westphal, et al. (2008). "Macromolecular crowding compacts unfolded apoflavodoxin and causes severe aggregation of the off-pathway intermediate during apoflavodoxin folding." J. Biol. Chem. 283(41): 27383-27394.

Fernandez-Recio, J., C. G. Genzor, et al. (2001). "Apoflavodoxin folding mechanism: an alpha/beta protein with an essentially off-pathway intermediate." Biochemistry 40(50): 15234-15245.

Fersht, A. R. and V. Daggett (2002). "Protein folding and unfolding at atomic resolution." Cell 108(4): 573-582.

Förster, T. (1948). "Zwischenmolekulare Energiewanderung Und Fluoreszenz." Ann. Phys. 2(1-2): 55-75.

Haas, E. (2005). "The study of protein folding and dynamics by determination of intramolecular distance distributions and their fluctuations using ensemble and single-molecule FRET measurements." ChemPhysChem 6(5): 858-870.

Huang, F., G. Settanni, et al. (2008). "Fluorescence resonance energy transfer analysis of the folding pathway of Engrailed Homeodomain." Protein Eng. Des. Sel. 21(3): 131-146.

Jaenicke, R. and R. Seckler (1997). "Protein misassembly *in vitro*." Adv. Prot. Chem. 50: 1-59.

Jahn, T. R. and S. E. Radford (2008). "Folding versus aggregation: polypeptide conformations on competing pathways." Arch. Biochem. Biophys. 469(1): 100-117.

Kathuria, S. V., I. J. Day, et al. (2008). "Kinetic traps in the folding of beta alpha-repeat proteins: CheY initially misfolds before accessing the native conformation." J. Mol. Biol. 382(2): 467-484.

Knox, R. S. and H. van Amerongen (2002). "Refractive index dependence of the Förster resonance excitation transfer rate." J. Phys. Chem. B 106(20): 5289-5293.

Lakowicz, J. R. (2006). Principles of fluorescence spectroscopy, Springer Verlag.

Laptenok, S. P., N. V. Visser, et al. (2011). "A general approach for detecting folding intermediates from steady-state and time-resolved fluorescence of single-tryptophan-containing proteins." Biochemistry 50(17): 3441-3450.

Lorenz, T. and J. Reinstein (2008). "The influence of proline isomerization and off-pathway intermediates on the folding mechanism of eukaryotic UMP/CMP Kinase." J. Mol. Biol. 381(2): 443-455.

Mansoor, S. E., M. A. Dewitt, et al. (2010). "Distance mapping in proteins using fluorescence spectroscopy: the tryptophan-induced quenching (TrIQ) method." Biochemistry 49(45): 9722-9731.

Mayhew, S. G. and G. Tollin (1992). General properties of flavodoxins. Chemistry and biochemistry of flavoenzymes. F. Müller. Boca Raton, Florida, CRC press. 3: 389-426.

Melo, E. P., L. Chen, et al. (2003). "Trehalose favors a cutinase compact intermediate off-folding pathway." Biochemistry 42(24): 7611-7617.

Nabuurs, S. M. and C. P. van Mierlo (2010). "Interrupted hydrogen/deuterium exchange reveals the stable core of the remarkably helical molten globule of α-β parallel protein flavodoxin." J. Biol. Chem. 285: 4165-4172.

Nabuurs, S. M., A. H. Westphal, et al. (2009). "Topological switching between an α-β parallel protein and a remarkably helical molten globule." J. Am. Chem. Soc. 131: 8290-8295.

Nabuurs, S. M., A. H. Westphal, et al. (2008). "Extensive formation of off-pathway species during folding of an alpha-beta parallel protein is due to docking of (non)native structure elements in unfolded molecules." J. Am. Chem. Soc. 130(50): 16914-16920.

Nabuurs, S. M., A. H. Westphal, et al. (2009). "Non-cooperative formation of the off-pathway molten globule during folding of the α-β parallel protein apoflavodoxin." J. Am. Chem. Soc. 131: 2739-2746.

Nozaki, Y. (1972). The preparation of guanidine hydrochloride. New York, Academic Press.

Ohgushi, M. and A. Wada (1983). "'Molten-globule state': a compact form of globular proteins with mobile side-chains." FEBS Lett. 164(1): 21-24.

Otzen, D. E., L. Giehm, et al. (2007). "Aggregation as the basis for complex behaviour of cutinase in different denaturants." Biomed. Biochim. Acta 1774(2): 323-333.

Panchuk-Voloshina, N., R. P. Haugland, et al. (1999). "Alexa dyes, a series of new fluorescent dyes that yield exceptionally bright, photostable conjugates." J. Histochem. Cytochem. 47(9): 1179-1188.

Ptitsyn, O. B., R. H. Pain, et al. (1990). "Evidence for a molten globule state as a general intermediate in protein folding." FEBS Lett. 262(1): 20-24.

Ratner, V., E. Kahana, et al. (2002). "A general strategy for site-specific double labeling of globular proteins for kinetic FRET studies." Bioconjugate Chem. 13(5): 1163-1170.

Schuler, B., E. A. Lipman, et al. (2005). "Polyproline and the "spectroscopic ruler" revisited with single-molecule fluorescence." Proc. Natl. Acad. Sci. U.S.A. 102(8): 2754-2759.

Shenoy, A. R. and S. S. Visweswariah (2003). "Site-directed mutagenesis using a single mutagenic oligonucleotide and DpnI digestion of template DNA." Anal. Biochem. 319: 735-336.

Steensma, E., M. J. Nijman, et al. (1998). "Apparent local stability of the secondary structure of *Azotobacter vinelandii* holoflavodoxin II as probed by hydrogen exchange: implications for redox potential regulation and flavodoxin folding." Protein Sci. 7(2): 306-317.

Steensma, E. and C. P. van Mierlo (1998). "Structural characterisation of apoflavodoxin shows that the location of the stable nucleus differs among proteins with a flavodoxin-like topology." J. Mol. Biol. 282(3): 653-666.

Stryer, L. and R. P. Haugland (1967). "Energy transfer: a spectroscopic ruler." Proc. Natl. Acad. Sci. U.S.A. 58(2): 719-726.

Szabo, A. (1984). "Theory of Fluorescence Depolarization in Macromolecules and Membranes." J. Chem. Phys. 81(1): 150-167.

Toptygin, D., R. S. Savtchenko, et al. (2002). "Effect of the solvent refractive index on the excited-state lifetime of a single tryptophan residue in a protein." J. Phys. Chem. B 106(14): 3724-3734.

van den Berg, P. A., A. van Hoek, et al. (2004). "Evidence for a novel mechanism of time-resolved flavin fluorescence depolarization in glutathione reductase." Biophys. J. 87(4): 2577-2586.

van Mierlo, C. P., J. M. van den Oever, et al. (2000). "Apoflavodoxin (un)folding followed at the residue level by NMR." Protein Sci. 9(1): 145-157.

van Mierlo, C. P., W. M. van Dongen, et al. (1998). "The equilibrium unfolding of *Azotobacter vinelandii* apoflavodoxin II occurs via a relatively stable folding intermediate." Protein Sci. 7(11): 2331-2344.

Vendruscolo, M., E. Paci, et al. (2001). "Three key residues form a critical contact network in a protein folding transition state." Nature 409(6820): 641-645.

Visser, N. V., A. H. Westphal, et al. (2008). "Tryptophan-tryptophan energy migration as a tool to follow apoflavodoxin folding." Biophys. J. 95(5): 2462-2469.

Vörös, J. (2004). "The density and refractive index of adsorbing protein layers." Biophys. J. 87(1): 553-561.

Chapter 5

Single-molecule FRET reveals non-cooperative folding of a molten globule

Simon Lindhoud, Menahem Pirchi[1], Adrie H. Westphal, Gilad Haran[1], Carlo P.M. van Mierlo

Abstract

Molten globules are ensembles of interconverting conformers that have a substantial amount of secondary structure but lack the tertiary side-chain packing characteristics of native proteins. Exposed hydrophobic groups render molten globule folding intermediates prone to aggregation, which can have detrimental effects on organisms. Illuminating how unfolded proteins form molten globules furthers our understanding about protein folding and aggregation. Here, we use single-molecule Förster Resonance Energy Transfer (smFRET) to investigate in a direct and model free manner formation of the off-pathway molten globule during folding of α-β parallel protein apoflavodoxin. This protein has been site-specifically labelled with donor fluorophore on position 69 and acceptor fluorophore on position 131 or 178, respectively. We observe a unimodal smFRET efficiency distribution at all stages of denaturant-dependent apoflavodoxin folding. smFRET shows that the conformation of the C-terminal part of apoflavodoxin's molten globule, involving residues 69 to 178, differs considerably from native protein. In addition, smFRET exposes that formation of this folding intermediate is strongly favoured. Upon folding of the molten globule, the unimodal smFRET efficiency distribution gradually shifts to larger FRET value due to progressive extension of its ordered core. This non cooperative compaction happens during folding of every single molten globule molecule.

1. Chemical Physics Department, Weizmann Institute of Science, Rehovot, Israel

Introduction

Folding of proteins to their functional conformation is of vital importance for all living organisms, and hence attracts considerable attention. Improvements in experimental techniques and enhancements in computing power during the past two decades have revolutionised our understanding of the mechanisms of protein folding *in vitro*. Proteins may fold along a myriad of different routes within a multidimensional energy landscape or folding funnel, which represents the conformational entropy versus the free energy (Bryngelson, Onuchic et al. 1995; Dill and Chan 1997; Dinner, Sali et al. 2000; Vendruscolo, Paci et al. 2001; Fersht and Daggett 2002; Thirumalai, O'Brien et al. 2010). Energy landscapes can be rugged, allowing formation of partially folded intermediates, which may be on- or off-pathway to the native state. When the intermediate is on-pathway, it has native-like topology and is productive for folding. In contrast, when the intermediate is off-pathway it is trapped in such a manner that the native state cannot be reached without substantial reorganisational events (Jahn and Radford 2008).

Early kinetic folding intermediates often resemble molten globules. Molten globules are commonly occurring folding intermediates that have exposed hydrophobic patches, which render them prone to aggregation (Ohgushi and Wada 1983; Christensen and Pain 1991; Ptitsyn 1995; Pande and Rokhsar 1998; Arai and Kuwajima 2000; Baldwin, Frieden et al. 2010). Several kinetic studies have revealed involvement of off-pathway intermediates during folding (see e.g. (Fernandez-Recio, Genzor et al. 2001; Melo, Chen et al. 2003; Bollen, Sanchéz et al. 2004)). Formation of a kinetically trapped off-pathway molten globule increases the probability of protein aggregation.

Elucidation of how unfolded proteins form molten globules furthers our understanding about protein folding and offers potential insights into factors responsible for protein misfolding, aggregation, and, potentially, for numerous devastating pathologies (Dobson 2003; Chiti and Dobson 2006). Studies of molten globule folding intermediates are hampered by the, often, transient nature of their existence, their usually low presence at equilibrium, and their conformational heterogeneity. Investigation of the formation of these species requires methods that detect them with high sensitivity and that avoid measurement of ensemble-averaged information. smFRET is well suited for this purpose, because it is able to directly illuminate conformational heterogeneity within an ensemble, by detecting freely diffusing dye-labelled proteins one at a time (Deniz, Dahan et al. 1999). FRET is the distance dependent transfer of electronic excitation energy from a donor fluorophore to an acceptor chromophore through non-radiative dipole-dipole coupling. This phenomenon occurs for distances of typically < 10 nm (Förster 1948; Fersht and Daggett 2002;

Lakowicz 2006). The FRET efficiency (*E*) strongly depends on the distance (*r*) between a donor and an acceptor molecule, according to Equation 5.1

$$E = \frac{1}{1 + \left(r / R_0\right)^6} \qquad [5.1]$$

with R_0 being the Förster distance, i.e., the distance at which the energy transfer efficiency is 50 %. By using single-molecule fluorescence detection methods it is possible to elucidate specific structural and dynamic aspects of the evolution of individual members of an equilibrium ensemble. Experiments employing smFRET have proven powerful for direct (i.e., model free) quantitative determination of steady state populations of folding states corresponding to folded and unfolded proteins, and folding intermediates. These experiments provide information about the structural distributions within folding states and about the kinetics of exchange between these states (Gopich and Szabo 2007; Gopich and Szabo 2010; Chung, Gopich et al. 2011). For instance, smFRET measurements enable characterisation of the collapse an unfolded protein undergoes prior to folding to its native state (Schuler, Lipman et al. 2002; Sherman and Haran 2006; Ziv and Haran 2009).

In this study, we employ smFRET to study the folding of doubly dye-labelled *Azotobacter vinelandii* apoflavodoxin, and monitor formation of its off-pathway molten globule. Flavodoxins are monomeric, single domain, flavoproteins that are involved in electron transfer and contain a non-covalently bound flavin mononucleotide (FMN) cofactor (Mayhew and Tollin 1992). These proteins adopt the flavodoxin-like topology, also referred to as the doubly-wound or α-β parallel topology. This topology is among the most common topologies in the protein databank, and is shared by many functionally and sequentially unrelated proteins.

Kinetic folding of apoflavodoxin (i.e., flavodoxin without FMN) occurs spontaneously and involves an energy landscape with two intermediates, as described by (Bollen, Sanchéz et al. 2004):

$$I_{off} \rightleftharpoons \textit{Unfolded apoflavodoxin} \rightleftharpoons I_{on} \rightleftharpoons \textit{Native apoflavodoxin} \qquad \text{[Scheme 5.1]}$$

Non-covalent binding of FMN to native apoflavodoxin is the last step in flavodoxin folding (Bollen, Nabuurs et al. 2005). Native apoflavodoxin strongly resembles flavodoxin, except for dynamic disorder in the flavin-binding region (Steensma, Nijman et al. 1998; Steensma and van Mierlo 1998). Intermediate I_{off} is an off-pathway molten globule that needs to unfold to produce native protein and thus acts as a trap. Approximately 90 % of unfolded molecules swiftly, but temporarily, form this molten globule upon lifting denaturing conditions. Intermediate I_{on} lies on the productive folding route, is highly unstable and is therefore not observed during denaturant-dependent

equilibrium folding of apoflavodoxin, which has therefore been described by the three-state model (van Mierlo, van Dongen et al. 1998; Bollen, Sanchéz et al. 2004):

$$I_{off} \rightleftharpoons \textit{Unfolded apoflavodoxin} \rightleftharpoons \textit{Native apoflavodoxin} \qquad \text{[Scheme 5.2]}$$

Molten globule I_{off} is compact, has solvent-exposed tryptophans and, in contrast to both native and unfolded apoflavodoxin, has severely broadened NMR resonances due to exchange between different conformers on the micro- to millisecond time scale (van Mierlo, van Dongen et al. 1998; van Mierlo, van den Oever et al. 2000; Bollen, Sanchéz et al. 2004; Engel, Westphal et al. 2008; Nabuurs, Westphal et al. 2009). Elevated apoflavodoxin concentration and molecular crowding cause severe aggregation of this folding species (van Mierlo, van den Oever et al. 2000; Engel, Westphal et al. 2008). Formation of an off-pathway intermediate is an intrinsic feature of proteins with the α-β parallel topology (Bollen and van Mierlo 2005).

NMR spectroscopy shows that unfolded apoflavodoxin is random coil at 6.0 M guanidine hydrochloride (GuHCl). Under less denaturing conditions, unfolded apoflavodoxin forms four transiently ordered regions (Bollen, Sanchéz et al. 2004; Nabuurs, Westphal et al. 2008). Three of these regions (i.e., Ala41-Gly53, Gln99-Ala122, and Thr160-Gly176) transiently form α-helices and the fourth region (i.e., Glu72-Gly83)) transiently adopts non-native structure, which is neither α-helix nor β strand. The four structured elements in unfolded apoflavodoxin transiently interact and form the ordered core of the molten globule (Nabuurs, Westphal et al. 2009; Nabuurs, Westphal et al. 2009). Apoflavodoxin's molten globule folds in a non cooperative manner, whereas folding of native apoflavodoxin is highly cooperative (van Mierlo, van den Oever et al. 2000;

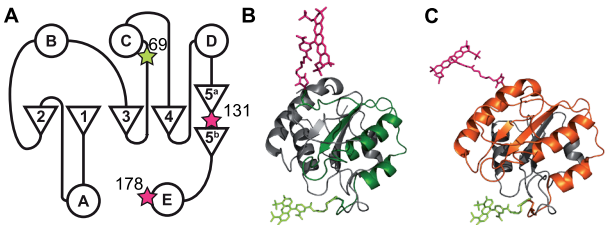

Figure 5.1 Covalent attachment of dye labels to enable FRET-based probing of apoflavodoxin folding. In both protein variants, donor label (i.e., A488) is attached to residue 69. (A) Position of dye labels within the topology of apoflavodoxin. A bright green star represents A488 and a pink star represents acceptor label (i.e., A568). (B) Cartoon representation of d69-a131, showing in green the protein backbone between residues 69 and 131. (C) Cartoon representation of d69-a178, showing in orange the protein backbone between residues 69 and 178. A488 is shown in bright green and A568 in pink. Cartoons are generated using the crystal structure of *A. vinelandii* flavodoxin (pdb ID 1YOB (Alagaratnam, van Pouderoyen et al. 2005)) and the molecular structures of A488 and A568, as provided by Invitrogen.

Nabuurs, Westphal et al. 2009). Ensemble FRET data strengthen this molecular picture of apoflavodoxin folding (Lindhoud, Westphal et al. 2012 (Submitted)).

For the purpose of FRET characterisation of apoflavodoxin folding, we introduced cysteine residues into the protein. Subsequently, apoflavodoxin has been site-specifically labelled with fluorescent donor and acceptor dyes (Figure 5.1A) (Lindhoud, Westphal et al. 2012 (Submitted)). Donor fluorophore (i.e., Alexa Fluor 488 C_5 maleimide (A488)) is covalently attached to Cys69. Acceptor fluorophore (i.e., Alexa Fluor 568 C_5 maleimide (A568)) is coupled to Cys131 (Figure 5.1B) or Cys178 (Figure 5.1C), respectively. The corresponding doubly dye-labelled proteins are called d69-a131 and d69-a178, respectively (Lindhoud, Westphal et al. 2012 (Submitted)). We demonstrated that measuring of ensemble FRET tracks denaturant-dependent folding of d69-a131 and d69-a178 (Lindhoud, Westphal et al. 2012 (Submitted)). The biphasic nature of the corresponding folding curves shows formation of apoflavodoxin's off-pathway molten globule (Figure 5.2) (Lindhoud, Westphal et al. 2012 (Submitted)). This intermediate folding state populates down to about 0.7 M GuHCl. Below 0.7 M GuHCl, both d69-a131 and d69-a178 are native.

Here, we report the use of smFRET to follow in a model free manner formation of apoflavodoxin's off-pathway molten globule. We show that a unimodal FRET efficiency distribution, the centre of which shifts to larger value upon decreasing denaturant concentration, describes molten globule formation of both d69-a131 and d69-a178. Clearly, smFRET detects progressive compaction during folding of apoflavodoxin's molten globule.

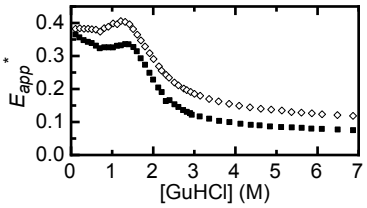

Figure 5.2 Monitoring of ensemble FRET tracks denaturant-dependent folding of d69-a131 and d69- a178. Data of d69-a131 are shown as open diamonds and data of d69-a178 are shown as black squares, respectively. The apparent FRET efficiency (E_{app}^*) is calculated according to ($E_{app}^* = I_{FRET}/(I_{FRET}+I_{DA})$), where IFRET is sensitised fluorescence emission of acceptor (i.e. emission of acceptor upon excitation of donor), and I_{DA} is fluorescence emission of donor label in presence of acceptor, respectively. Protein concentration is 62.5 nM. I_{DA} is measured at 515 nm and I_{FRET} is measured at 630 nm, both upon excitation of donor at 450 nm. Data are taken from (Lindhoud, Westphal et al. 2012 (Submitted))

Materials and Methods

Single-molecule fluorescence of diffusing doubly dye-labelled apoflavodoxin

By site-directed mutagenesis, we designed two apoflavodoxin variants that contain a pair of cysteine residues. Both variants contain the wild-type cysteine at position 69, and through replacement of the residue at position 131 or 178, apoflavodoxin variants D131C and S178C were generated, respectively. Protein engineering, expression, purification, and subsequent site specific labelling of apoflavodoxin with A488 (Invitrogen) on position 69 and with A568 (Invitrogen) either on position 131 or position 178, with equimolar ratio of donor to acceptor, are described elsewhere (Lindhoud et al., submitted). Upon removal of denaturant, both doubly dye-labelled protein variants autonomously fold to native apoprotein, because denaturant-induced apoflavodoxin unfolding is reversible (van Mierlo, van Dongen et al. 1998; Lindhoud, Westphal et al. 2012 (Submitted)).

The buffer used in all denaturant-dependent folding experiments was 100 mM potassium pyrophosphate (Sigma), pH 6.0. Buffer and GuHCl stock were incubated with granulated active charcoal (Scharlau Chemie) during 48 hours, and subsequently filtered through a 0.2 µm cellulose acetate filter (Whatman), prior to addition of Tween-20 (Sigma-Ultra). Buffer and GuHCl stock were mixed to obtain the appropriate denaturant concentration series, and dye-labelled protein was added to all samples to a final concentration of 15 pM. The concentration of dye-labelled protein stock was determined using an absorption coefficient of 71000 M^{-1} cm^{-1} for A488. All samples were at equilibrium after 5 minutes (Lindhoud, Westphal et al. 2012 (Submitted)) and contain 0.0035 % Tween-20. Refractometry was used to determine the GuHCl concentration in each individual sample (Nozaki 1972).

Sample cells for single-molecule measurements were constructed of 24 × 50 mm and 18 × 18 mm HF-cleaned microscopy coverslips, which are separated by two parafilm spacers. Prior to loading with d69-a131 or d69-a178 in the desired concentration of denaturant, sample cells were washed with 800 µL of the corresponding denaturant solution. After loading, the cell was sealed with high vacuum silicone grease (Merck).

A single-molecule spectrometer, as described in (Pirchi, Ziv et al. 2011), was used to detect fluorescence of diffusing dye-labelled apoflavodoxin molecules in the sample cell at ambient temperature. Excitation was done with the 488 nm laser line of an argon-laser at an output of 50 µW. Photons of each sample were collected during a 1-hour period. Signal detection was done in time-stamping mode, i.e., by registering the time lag between consecutive photons arriving at the detectors.

Data treatment and analysis

A burst search algorithm, as described in (Sherman and Haran 2006), was used to select fluorescence bursts that have a total photon count of at least 50, with an inter-photon arrival time of maximally 50 µs. The apparent FRET efficiency (E_{app}) of each burst was calculated according to:

$$E_{app} = \frac{n_A - \gamma n_D}{n_A + n_D} \qquad [5.2]$$

in which n_A and n_D are the number of photons detected in acceptor and donor channel, respectively, and γ describes the number of donor photons detected in the acceptor channel. We determined that γ = 7 %, using 'donor-only' protein, in which A488 is covalently attached to wild-type apoflavodoxin (i.e., protein that contains a single cysteine at position 69). This singly dye-labelled protein we refer to as A488-apoflavodoxin.

A common observation in smFRET experiments is that a fluorophore bleaches while dye-labelled protein traverses through the confocal spot. This bleaching affects E_{app}. To identify bursts of photons during which such bleaching occurs, we determined the difference in E_{app} between the first and last 30% of photons of the burst involved. When the absolute value of this difference exceeds 0.5 E_{app}-units as selection criterion, the burst was discarded (supporting information Figure S5.1). Apparent FRET efficiencies of duplicate measurements were accumulated and used to construct histograms, which show the numbers of bursts observed within bins of E_{app}. A sum of Gaussian distribution functions was fitted to the histogram obtained at a particular concentration denaturant, according to:

$$N\left(E_{app}\right) = \sum_{i=1}^{n} A_i \exp\left(-\frac{\left(E_{app} - \varepsilon_i\right)^2}{2\sigma_i^2}\right) \qquad [5.3]$$

in which N is the number of bursts within a specific bin of apparent FRET efficiency, and A_i is the amplitude, ε_i the centre, and σ_i the width of the i^{th} Gaussian distribution. The width and centre of the distribution observed at zero FRET efficiency, which is due to missing or bleached acceptor, are fixed to $\sigma = 0.03$ and $\varepsilon = 0$, respectively.

Results and Discussion

Observation of a unimodal smFRET efficiency distribution during apoflavodoxin equilibrium folding

When folded and unfolded dye-labelled proteins are characterised by sufficiently different FRET efficiencies and do not exchange on the timescale of detection, smFRET reports the presence of both species separately. Examples of these observations include smFRET detected folding of acyl-CoA-binding protein (Laurence, Kong et al. 2005), adenylate kinase (Sherman, Itkin et al. 2008) chymotrypsin inhibitor 2 (Deniz, Laurence et al. 2000; Laurence, Kong et al. 2005) cold-shock protein (Schuler, Lipman et al. 2002), immunity protein Im9 (Tezuka-Kawakami, Gell et al. 2006), protein A (Huang, Sato et al. 2007), protein L (Sherman and Haran 2006), and ribonuclease H (Kuzmenkina, Heyes et al. 2005;

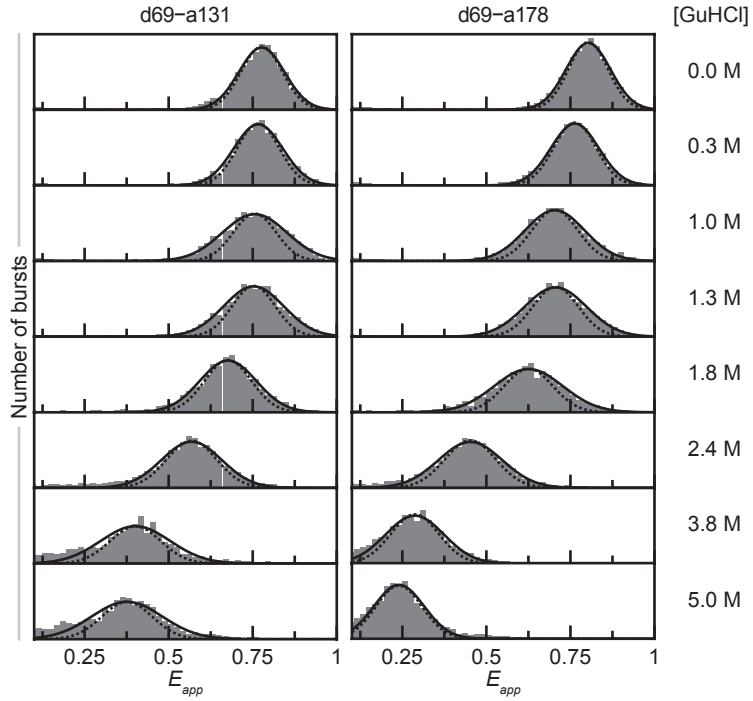

Figure 5.3 A unimodal Gaussian distribution describes smFRET efficiency histograms of d69-a131 and d69-a178 at all concentrations denaturant. The left-hand column shows the denaturant-dependence of smFRET data of d69-a131 and the right-hand column shows the corresponding data of d69-a178. GuHCl concentration is indicated on the left-hand side. Vertical grey bars show the numbers of bursts observed within a bin of apparent FRET efficiency. Bursts of photons during which bleaching occurs are not taken into account, as described in Materials and Methods. Solid lines show the results of fitting Gaussian distribution function equation 5.3 to the data. Dotted lines indicate shot-noise limited distributions according to equation 5.4. Histograms are normalised to the total number of burst obtained. The complete series of denaturant-dependent histograms obtained is shown in supporting information Figure S5.2.

Kuzmenkina, Heyes et al. 2006). During denaturant-dependent equilibrium folding of these proteins, changes in relative populations of the unfolded and the folded state happen. Consequently, one observes bimodal smFRET efficiency distributions in the transition region of folding of these proteins.

To assess in a model-free and direct manner the denaturant-dependent populations of apoflavodoxin's folding states, we determined smFRET efficiencies of d69-a131 and d69-a178 at GuHCl concentrations ranging from 5 to 0 M. This range covers the full equilibrium folding transition of apoflavodoxin. Figure 5.3 shows a selection of smFRET histograms obtained (the complete series of denaturant-dependent histograms is available as supporting information Figure S5.2).

At all concentrations denaturant a single Gaussian distribution describes the smFRET efficiency distribution of d69-a131 and d69-a178 (Figure 5.3). The centre of this distribution shifts from low E_{app} for unfolded protein at 5.0 M GuHCl, where donor and acceptor are well separated, to large E_{app} for native protein. No distinct smFRET distributions corresponding to unfolded protein, molten globule and native protein are observed in the transition region of apoflavodoxin equilibrium folding.

smFRET Detects native, molten globule and unfolded apoflavodoxin

Figure 5.4 shows how the centre of the smFRET efficiency distribution of unfolded apoflavodoxin shifts upon lowering denaturant concentration, as well as corresponding changes in width of this distribution (i.e., it presents the denaturant-dependencies of ε and σ of equation 5.3). Clearly, smFRET depends biphasically on denaturant concentration, just as ensemble FRET shows. The presence of the hump in the folding curves is due to molten globule formation. Consequently, donor and acceptor

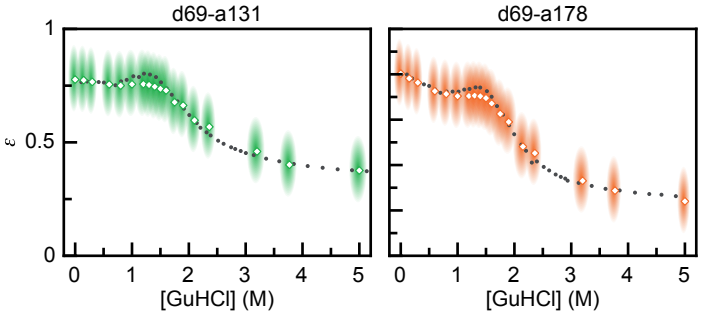

Figure 5.4 Usage of smFRET enables detection of formation of apoflavodoxin's molten globule. Shown is the denaturant-dependency of the centre of the Gaussian distribution function that describes an smFRET efficiency distribution (i.e., ε; open diamonds) and of the corresponding width (i.e., σ; shaded areas) for d69-a131 (green) and d69-a178 (orange). Grey dots show the apparent FRET efficiencies obtained from ensemble FRET measurements (Lindhoud, Westphal et al. 2012 (Submitted)), which are scaled to match smFRET data. This scaling is required, because of differing detection efficiencies between single-molecule and ensemble FRET measurements. The denaturant-dependency of ε is biphasic, and thus smFRET shows formation of the molten globule during apoflavodoxin folding.

are less separated in the interconverting ensemble of conformers that represents apoflavodoxin's off-pathway intermediate than they are in native apoflavodoxin. The C-terminal part of this molten globule, involving residues 69 to 178, must be rather compact and differs considerably from native protein (Lindhoud, Westphal et al. 2012 (Submitted)). Thus, smFRET detects native and unfolded protein, as well as formation of the molten globule.

Comparison of the denaturant-dependence of the width of an smFRET distribution with the corresponding shot-noise limited width provides further proof for detection of formation of apoflavodoxin's molten globule. Dotted lines in Figure 5.3 show shot-noise limited E_{app} distributions, as approximated by using equation 5.4 (Nir, Michalet et al. 2006)

$$\sigma^* = (1+\gamma)\sqrt{\frac{\left(\frac{\varepsilon+\gamma}{1+\gamma}\right)\left(1-\left(\frac{\varepsilon+\gamma}{1+\gamma}\right)\right)}{n}} \qquad [5.4]$$

in which σ^* is the shot-noise limited width of a particular FRET efficiency distribution (with ε as centre), and n is the minimum number of photons used to calculate the FRET efficiency of a burst ($n = 50$). As mentioned in Materials and Methods, $\gamma = 7$ %. Figure 5.5 shows the denaturant-dependence of the ratio of the width of an smFRET distribution (σ) to the corresponding shot-noise limited width (σ^*). Upon diminishing of the fraction of native proteins by increasing GuHCl concentration above 0.7 M and thereby populating apoflavodoxin's molten globule state, the smFRET efficiency distribution of apoflavodoxin broadens (i.e., σ/σ^* becomes larger). Such broadening can be due to fluorescence quenching and/or bleaching of either of the fluorophores involved (Nir, Michalet et al. 2006; Kalinin, Sisamakis et al. 2010). Indeed, quenching of donor and acceptor is most profound for apoflavodoxin's molten globule (Lindhoud, Westphal et al. 2012 (Submitted)). Furthermore, due to the microsecond to millisecond conformational dynamics within apoflavodoxin's molten globule

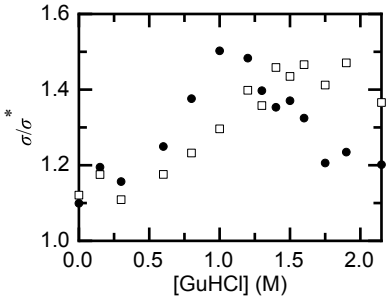

Figure 5.5. Denaturant-dependence of the width of an smFRET distribution of apoflavodoxin compared to its shot-noise limited width. The vertical axis shows the width of an smFRET efficiency distribution (σ) divided by its corresponding shot-noise limited width (σ^*). Filled circles show data of d69-a131, whereas open squares show those of d69-a178.

ensemble the corresponding smFRET efficiency distributions can also broaden beyond shot-noise limits. Thus, the increase in σ/σ^* further substantiates that smFRET detects formation of the molten globule during apoflavodoxin folding.

Upon molten globule folding, apoflavodoxin's smFRET efficiency distribution shifts considerably

In contrast to the non-cooperative folding of apoflavodoxin's molten globule, formation of native apoflavodoxin is highly cooperative with a transition region of equilibrium folding of about 1 M GuHCl (Steensma and van Mierlo 1998; van Mierlo, van den Oever et al. 2000; Bollen, Sanchéz et al. 2004; Nabuurs, Westphal et al. 2009). Both d69-a131 and d69-a178 are native up to 0.7 M GuHCl (Lindhoud, Westphal et al. 2012 (Submitted)). Due to their highly cooperative folding, above 1.7 M GuHCl the native states of d69-a131 and d69-a178 are not populated. Hence, above this denaturant concentration native protein does not contribute to smFRET efficiency.

Figure 5.3 shows that upon going from 5.0 to 1.8 M GuHCl, the smFRET distributions of unfolded d69-a131 and d69-a178 shift from ε-values of 0.35 and 0.23, respectively, to 0.68 and 0.63, respectively. This considerable shift of the centre of the smFRET efficiency distribution, and corresponding reduction of distance between donor and acceptor is thus due to non-cooperative formation of apoflavodoxin's molten globule. Upon further lowering GuHCl concentration the native state of apoflavodoxin populates and the fraction of proteins that are molten globule diminishes.

Exchange between unfolded and molten globule protein

Observation of unimodal smFRET efficiency distributions down to 1.7 M GuHCl, where native apoflavodoxin needs not to be considered, can arise from exchange between unfolded and molten globule conformers, causing collapse of the peaks in the corresponding histograms. Prime determinants for whether this phenomenon happens are the FRET efficiencies that characterise each conformer involved and the rates of transitions between these conformers. Simulations show that bimodal smFRET efficiency distributions can collapse into a unimodal distribution when the rate of exchange between conformers exceeds the timespan of observation the molecule involved (i.e., the observation window) over one order of magnitude (Gopich and Szabo 2010). In case of apoflavodoxin, Fluorescence Correlation Spectroscopy-analysis of photon trajectories obtained at various GuHCl concentrations shows that its diffusion through the laser spot lasts 0.1 to 1 ms (data not shown).

If unfolded protein would be present down to 1.7 M GuHCl, exchange between this species and apoflavodoxin's molten globule could give rise to observation of unimodal smFRET efficiency distributions. Kinetics of exchange between unfolded apoflavodoxin and molten

globule in absence of denaturant has been described by the following model and rate constants (Bollen, Sanchéz et al. 2004):

$$I_{off} \underset{417\ s^{-1}}{\overset{0.73\ s^{-1}}{\rightleftharpoons}} U \qquad \text{[Scheme 5.3]}$$

The rate constants for exchange between unfolded protein and molten globule depend on denaturant concentration ([*D*]) according to:

$$k_{ij} = k^{0}_{ij} \exp\left(m_{ij}\left[D\right] / RT\right) \qquad [5.5]$$

with k_{ij}^{0} the rate constant at zero concentration denaturant, m_{ij} the denaturant dependencies of rate constants $k_{loff\text{-}U}$ and $k_{U\text{-}loff}$, which are 0.576 ± 0.002 kcal mol^{-1} M^{-1} and -1.256 ± 0.002 kcal mol^{-1} M^{-1}, respectively (Bollen, Sanchéz et al. 2004). Hence, according to the above model, between for example 3.4 and 1.7 M GuHCl $k_{loff\text{-}U}$ ranges from 20.18 × 10^{-3} ms^{-1} to 1.21 × 10^{-3} ms^{-1}, respectively, and $k_{U\text{-}loff}$ ranges from 0.30 × 10^{-3} ms^{-1} to 11.18 × 10^{-3} ms^{-1}, respectively. Thus, compared to the 0.1 to 1 ms observation window of our smFRET experiments, exchange between unfolded apoflavodoxin and molten globule is slow. Consequently, if both species co-exist in the transition region of equilibrium folding, as the three-state model of equilibrium folding of apoflavodoxin suggests, they would likely give rise to bimodal smFRET efficiency distributions. However, Figure 5.3 does not show such bimodality. This observation implies that if unfolded and molten globule apoflavodoxin co-exist, they would be characterised by remarkably similar FRET efficiencies. However, NMR data reveal that this situation is not the case, as discussed below.

Only the molten globule state populates in the transition region of folding down to 1.7 M GuHCl

Recently, we used NMR spectroscopy as an alternative model-free approach to study apoflavodoxin folding. The NMR approach shows that resonances of unfolded protein disappear upon lowering denaturant concentration (Nabuurs, Westphal et al. 2009). This disappearance is due to non-cooperative formation of apoflavodoxin's molten globule. Resonances of the ordered core of the molten globule are not observed by NMR spectroscopy, because they are broadened beyond detection due to exchange between different conformers on the micro- to millisecond time scale (van Mierlo, van den Oever et al. 2000; Nabuurs, Westphal et al. 2009). Hence, by following the disappearance of NMR resonances of amino acid residues of unfolded apoflavodoxin upon lowering concentration denaturant, formation of apoflavodoxin's molten globule is detected in an indirect manner. These resonances disappear as a series of distinct sigmoidal transitions with fitted midpoints ranging between 2.7 and 1.5 M GuHCl. Upon lowering denaturant concentration, first the

ordered core of the molten globule forms (Nabuurs, Westphal et al. 2009; Nabuurs and van Mierlo 2010).

We conclude that once a residue of unfolded apoflavodoxin is no longer observed by NMR spectroscopy upon lowering denaturant concentration, and thus has undergone a folding transition, it has become part of the molten globule, and consequently the unfolded state of apoflavodoxin no longer populates. Note however, that unstructured parts of the molten globule species still have dynamical and conformational properties typical for unfolded protein and thus give rise to sharp NMR resonances (Nabuurs, Westphal et al. 2009). Upon further lowering denaturant concentration these resonances also disappear, because the structured core of apoflavodoxin's molten globule extends (Nabuurs, Westphal et al. 2009).

In the transition region of folding down to 1.7 M GuHCl, only the molten globule state populates. As a consequence, in this denaturant range we obtain unimodal smFRET efficiency histograms (Figure 5.3), which track folding of apoflavodoxin's molten globule.

Non-cooperative compaction during folding of every single molten globule molecule

Our smFRET data show that the apparent FRET efficiency of unfolded apoflavodoxin slightly increases upon decreasing GuHCl concentration, because the average separation between donor and acceptor dyes decreases in the unfolded baseline (Figure 5.4). Collapse of unfolded protein upon decreasing denaturant concentration has been observed by smFRET for several proteins (see e.g., (Schuler, Lipman et al. 2002; Kuzmenkina, Heyes et al. 2006; Sherman and Haran 2006; Hoffmann, Kane et al. 2007; Mukhopadhyay, Krishnan et al. 2007; Ziv and Haran 2009)). In case of apoflavodoxin, this limited compaction of unfolded protein with decreasing denaturant concentration coincides with formation of transiently ordered regions within unfolded protein (Nabuurs, Westphal et al. 2008; Nabuurs, Westphal et al. 2009).

Upon further lowering of denaturant concentration, smFRET shows that each unfolded apoflavodoxin molecule forms a molten globule species, which is accompanied by a considerable increase in apparent FRET efficiency. Clearly, formation of this folding intermediate is strongly favoured. Most importantly, upon folding of this molten globule, the unimodal smFRET efficiency distribution gradually shifts to larger FRET value due to progressive extension of its ordered core (Figure 5.4). This non-cooperative compaction happens during folding of every single molten globule molecule.

Non-native docking of helices in apoflavodoxin's molten globule prevents formation of the parallel β-sheet of native apoflavodoxin (Nabuurs, Westphal et al. 2008; Nabuurs, de Kort et al. 2009; Nabuurs, Westphal et al. 2009; Nabuurs, Westphal et al. 2009; Nabuurs and van Mierlo 2010). Hence,

to produce native α-β parallel protein, the molten globule needs to unfold, explaining why this folding species is off-pathway during folding of apoflavodoxin. The smFRET data of this study show that formation and concomitant compaction of the molten globule are strongly favoured. Consequently, during kinetic folding of unfolded apoflavodoxin molecules, they swiftly form this molten globule upon lifting denaturing conditions.

Supporting Information

Figure S5.1 Bursts during which bleaching occurs are discarded by using as selection criterion the difference in apparent FRET efficiency between the first and last 30 % of photons of the particular burst involved. Data in A, B, C and D correspond to d69-a131, whereas data in E, F, G and H correspond to d69-a178. Data in A, B, E and F are obtained at 0 M GuHCl, whereas data in C, D, G and H are obtained at 5 M GuHCl. Scatter plots (A, C, E and G) show apparent FRET efficiencies of the first 30 % (abscissa) and last 30 % (ordinate) of photons of the fluorescence burst involved. Differences in apparent FRET efficiencies between these parts of the bursts are plotted as histograms (B, D, F and H). Bursts are discarded when the absolute value of this difference exceeds 0.5 (i.e., hatched areas).

Figure S5.2 Denaturant-dependence of smFRET efficiency histograms of d69-a131 and d69-a178. The left-hand column shows the denaturant-dependence of smFRET data of d69-a131 and the right-hand column shows the corresponding data of d69-a178. GuHCl concentration is indicated in each panel. Stair plots show the numbers of bursts observed within bins of apparent FRET efficiencies. Vertical grey bars show smFRET histograms after discarding burst during which dye bleaching occurs (for selection of these burst, see Materials and Methods and Figure S5.1). Smooth lines show the results of fitting the Gaussian distribution function of equation 3 to the histograms. The width and centre of the distribution at zero FRET efficiency are fixed to $\sigma = 0.03$ and $\varepsilon = 0$, respectively. The relatively low amplitude of this peak testifies of a robust procedure for site-specific doubly dye labelling of apoflavodoxin.

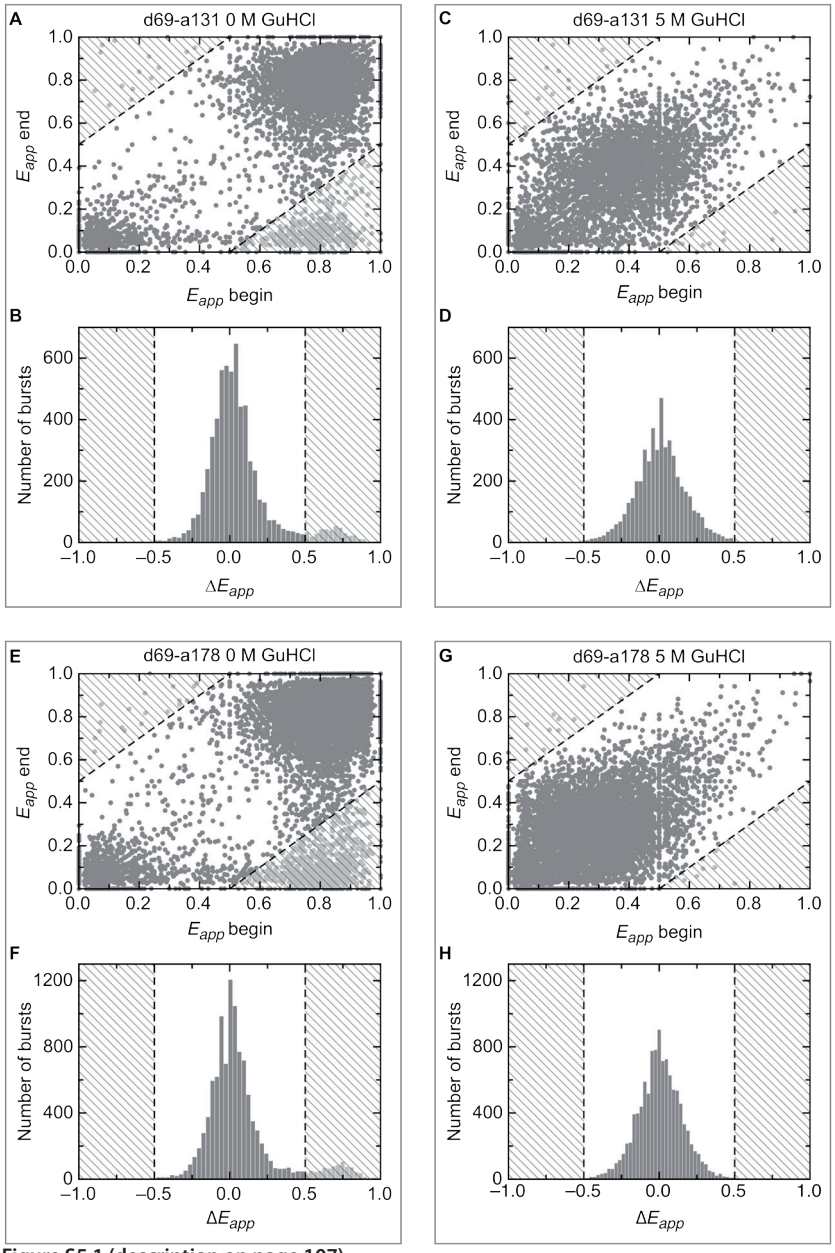

Figure S5.1 (description on page 107)

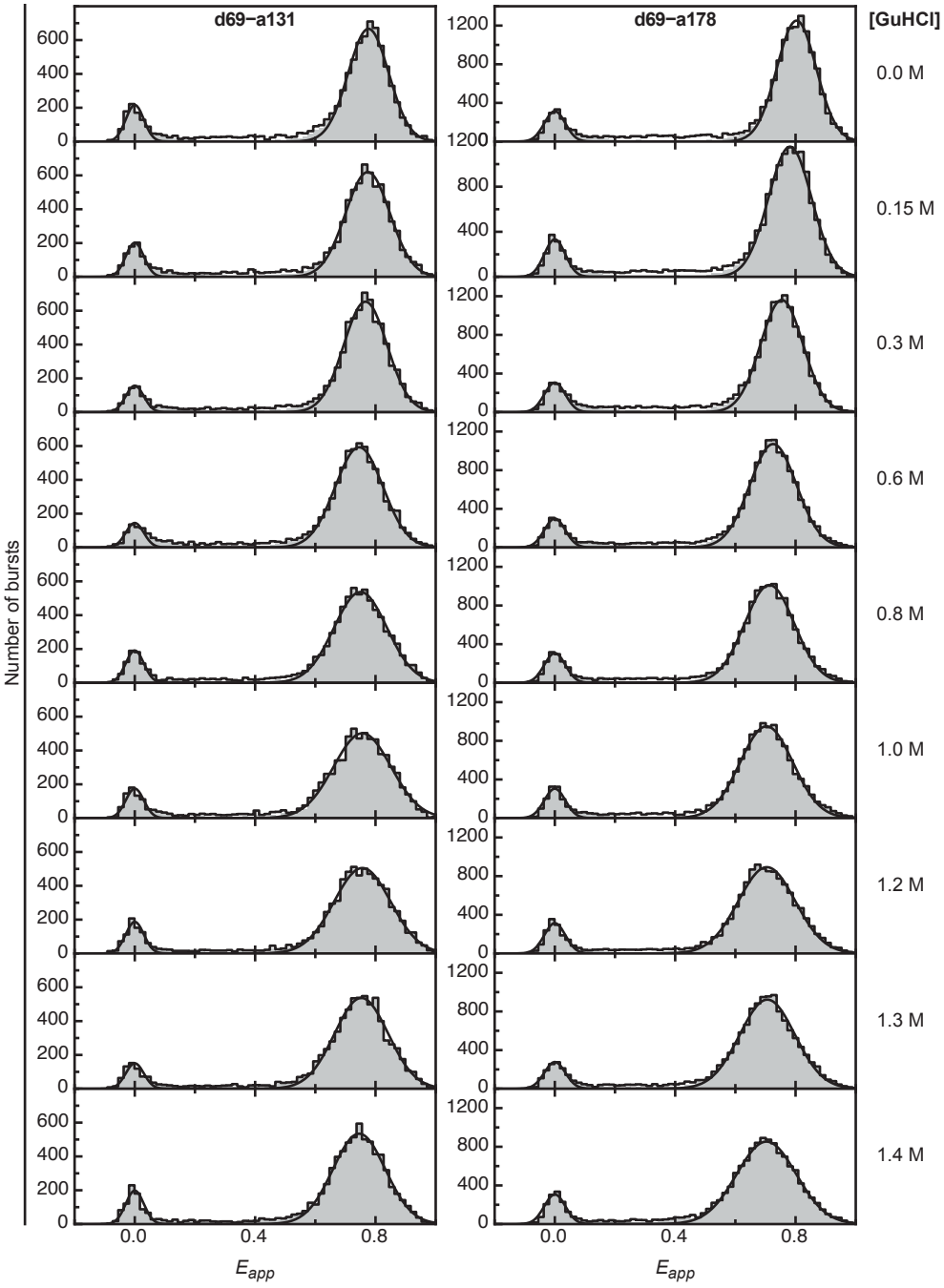

Figure S5.2 Denaturant-dependence of smFRET efficiency histograms of d69-a131 and d69-a178
(description on page 107)

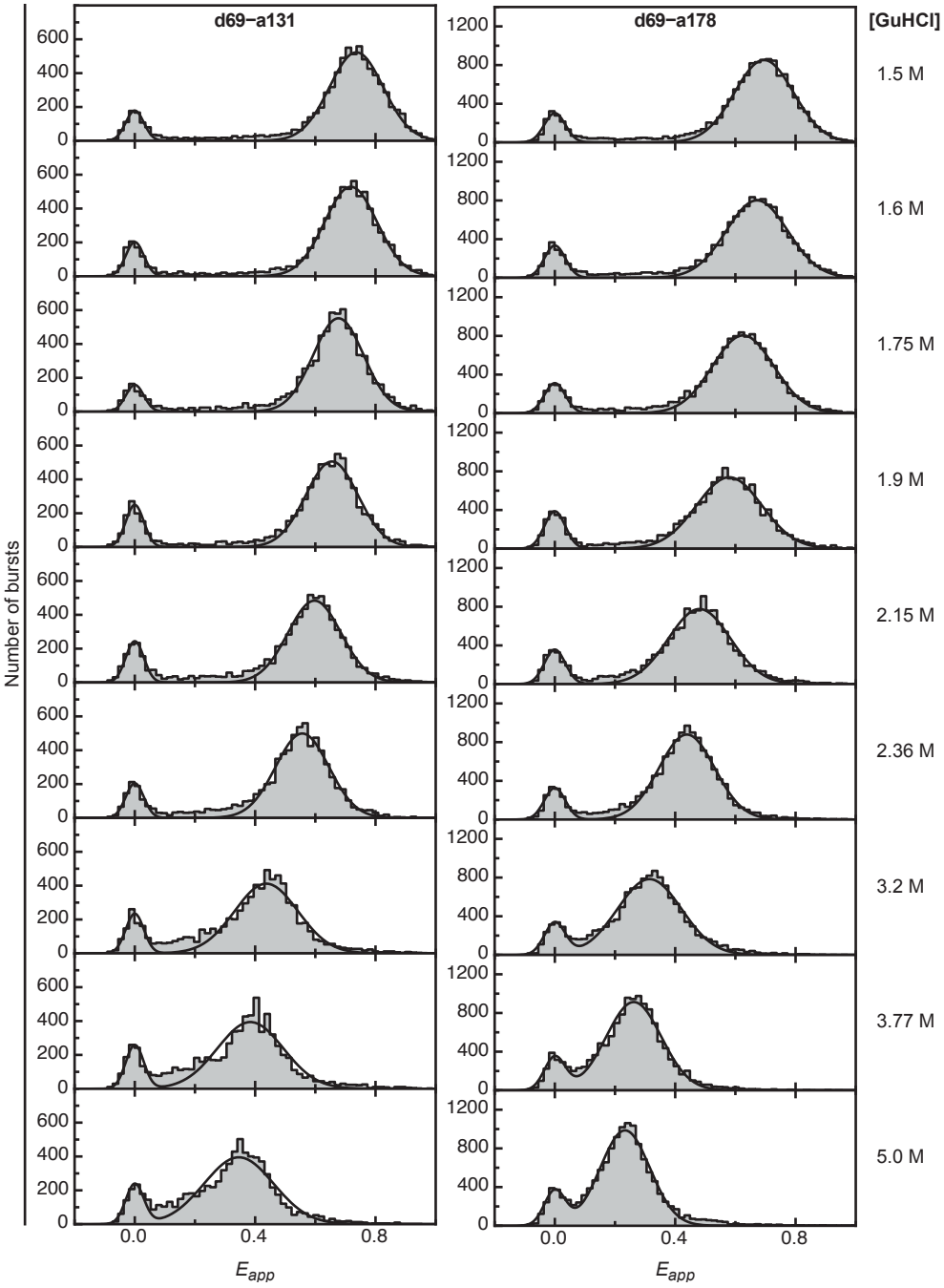

Figure S5.2 (continued) Denaturant-dependence of smFRET efficiency histograms of d69-a131 and d69-a178 (description on page 107)

References

Alagaratnam, S., G. van Pouderoyen, et al. (2005). "A crystallographic study of Cys69Ala flavodoxin II from *Azotobacter vinelandii*: structural determinants of redox potential." Protein Sci. 14(9): 2284-2295.

Arai, M. and K. Kuwajima (2000). "Role of the molten globule state in protein folding." Adv. Protein Chem. 53: 209-282.

Baldwin, R. L., C. Frieden, et al. (2010). "Dry molten globule intermediates and the mechanism of protein unfolding." Proteins Struct. Funct. Bioinf. 78(13): 2725-2737.

Bollen, Y. J., I. E. Sanchéz, et al. (2004). "Formation of on- and off-pathway intermediates in the folding kinetics of *Azotobacter vinelandii* apoflavodoxin." Biochemistry 43(32): 10475-10489.

Bollen, Y. J. and C. P. van Mierlo (2005). "Protein topology affects the appearance of intermediates during the folding of proteins with a flavodoxin-like fold." Biophys. Chem. 114(2-3): 181-189.

Bollen, Y. J. M., S. M. Nabuurs, et al. (2005). "Last in, first out." J. Biol. Chem. 280(9): 7836-7844.

Bryngelson, J. D., J. N. Onuchic, et al. (1995). "Funnels, pathways, and the energy landscape of protein folding: a synthesis." Proteins Struct. Funct. Bioinf. 21(3): 167-195.

Chiti, F. and C. M. Dobson (2006). "Protein misfolding, functional amyloid, and human disease." Annu. Rev. Biochem. 75: 333-366.

Christensen, H. and R. H. Pain (1991). "Molten globule intermediates and protein folding." Eur. Biophys. J. 19(5): 221-229.

Chung, H. S., I. V. Gopich, et al. (2011). "Extracting rate coefficients from single-molecule photon trajectories and FRET efficiency histograms for a fast-folding protein." J. Phys. Chem. A 115(16): 3642-3656.

Deniz, A. A., M. Dahan, et al. (1999). "Single-pair fluorescence resonance energy transfer on freely diffusing molecules: observation of Forster distance dependence and subpopulations." Proc. Natl. Acad. Sci. U.S.A. 96(7): 3670-3675.

Deniz, A. A., T. A. Laurence, et al. (2000). "Single-molecule protein folding: Diffusion fluorescence resonance energy transfer studies of the denaturation of chymotrypsin inhibitor 2." Proc. Natl. Acad. Sci. U.S.A. 97(10): 5179-5184.

Dill, K. A. and H. S. Chan (1997). "From Levinthal to pathways to funnels." Nat. Struct. Mol. Biol. 4(1): 10-19.

Dinner, A. R., A. Sali, et al. (2000). "Understanding protein folding via free-energy surfaces from theory and experiment." Trends Biochem. Sci. 25(7): 331-339.

Dobson, C. M. (2003). "Protein folding and misfolding." Nature 426(6968): 884-890.

Engel, R., A. H. Westphal, et al. (2008). "Macromolecular crowding compacts unfolded apoflavodoxin and causes severe aggregation of the off-pathway intermediate during apoflavodoxin folding." J. Biol. Chem. 283(41): 27383-27394.

Fernandez-Recio, J., C. G. Genzor, et al. (2001). "Apoflavodoxin folding mechanism: an alpha/beta protein with an essentially off-pathway intermediate." Biochemistry 40(50): 15234-15245.

Fersht, A. R. and V. Daggett (2002). "Protein folding and unfolding at atomic resolution." Cell 108(4): 573-582.

Förster, T. (1948). "Zwischenmolekulare Energiewanderung Und Fluoreszenz." Ann. Phys. 2(1-2): 55-75.

Gopich, I. V. and A. Szabo (2007). "Single-molecule FRET with diffusion and conformational dynamics." J. Phys. Chem. B 111(44): 12925-12932.

Gopich, I. V. and A. Szabo (2010). "FRET efficiency distributions of multistate single molecules." J. Phys. Chem. B 114(46): 15221-15226.

Hoffmann, A., A. Kane, et al. (2007). "Mapping protein collapse with single-molecule fluorescence and kinetic synchrotron radiation circular dichroism spectroscopy." Proc. Natl. Acad. Sci. U.S.A. 104(1): 105-110.

Huang, F., S. Sato, et al. (2007). "Distinguishing between cooperative and unimodal downhill protein folding." Proc. Natl. Acad. Sci. U.S.A. 104(1): 123-127.

Jahn, T. R. and S. E. Radford (2008). "Folding versus aggregation: polypeptide conformations on competing pathways." Arch. Biochem. Biophys. 469(1): 100-117.

Kalinin, S., E. Sisamakis, et al. (2010). "On the origin of broadening of single-molecule FRET efficiency distributions beyond shot noise limits." J. Phys. Chem. B 114(18): 6197-6206.

Kuzmenkina, E. V., C. D. Heyes, et al. (2005). "Single-molecule Förster resonance energy transfer study of protein dynamics under denaturing conditions." Proc. Natl. Acad. Sci. U.S.A. 102(43): 15471-15476.

Kuzmenkina, E. V., C. D. Heyes, et al. (2006). "Single-molecule FRET study of denaturant induced unfolding of RNase H." J. Mol. Biol. 357(1): 313-324.

Lakowicz, J. R. (2006). Principles of Fluorescence Spectroscopy. New York, Springer.

Laurence, T. A., X. X. Kong, et al. (2005). "Probing structural heterogeneities and fluctuations of nucleic acids and denatured proteins." Proc. Natl. Acad. Sci. U.S.A. 102(48): 17348-17353.

Lindhoud, S., A. H. Westphal, et al. (2012 (Submitted)). "Illuminating the off-pathway nature of the molten globule folding intermediate of an α-β parallel protein."

Mayhew, S. G. and G. Tollin (1992). General properties of flavodoxins. Chemistry and biochemistry of flavoenzymes. F. Müller. Boca Raton, Florida, CRC press. 3: 389-426.

Melo, E. P., L. Chen, et al. (2003). "Trehalose favors a cutinase compact intermediate off-folding pathway." Biochemistry 42(24): 7611-7617.

Mukhopadhyay, S., R. Krishnan, et al. (2007). "A natively unfolded yeast prion monomer adopts an ensemble of collapsed and rapidly fluctuating structures." Proc. Natl. Acad. Sci. U.S.A. 104(8): 2649-2654.

Nabuurs, S. M., B. J. de Kort, et al. (2009). "Non-native hydrophobic interactions detected in unfolded apoflavodoxin by paramagnetic relaxation enhancement." Eur. Biophys. J. 39: 689-698.

Nabuurs, S. M. and C. P. van Mierlo (2010). "Interrupted hydrogen/deuterium exchange reveals the stable core of the remarkably helical molten globule of α-β parallel protein flavodoxin." J. Biol. Chem. 285: 4165-4172.

Nabuurs, S. M., A. H. Westphal, et al. (2009). "Topological switching between an α-β parallel protein and a remarkably helical molten globule." J. Am. Chem. Soc. 131: 8290-8295.

Nabuurs, S. M., A. H. Westphal, et al. (2008). "Extensive formation of off-pathway species during folding of an α-β parallel protein is due to docking of (non)native structure elements in unfolded molecules." J. Am. Chem. Soc. 130(50): 16914-16920.

Nabuurs, S. M., A. H. Westphal, et al. (2009). "Non-cooperative formation of the off-pathway molten globule during folding of the α-β parallel protein apoflavodoxin." J. Am. Chem. Soc. 131: 2739-2746.

Nir, E., X. Michalet, et al. (2006). "Shot-noise limited single-molecule FRET histograms: comparison between theory and experiments." J. Phys. Chem. B 110(44): 22103-22124.

Nozaki, Y. (1972). The preparation of guanidine hydrochloride. New York, Academic Press.

Ohgushi, M. and A. Wada (1983). "'Molten-globule state': a compact form of globular proteins with mobile side-chains." FEBS Lett. 164(1): 21-24.

Pande, V. S. and D. S. Rokhsar (1998). "Is the molten globule a third phase of proteins?" Proc. Natl. Acad. Sci. U.S.A. 95(4): 1490-1494.

Pirchi, M., G. Ziv, et al. (2011). "Single-molecule fluorescence spectroscopy maps the folding landscape of a large protein." Nat. Commun. 2: 493.

Ptitsyn, O. B. (1995). "Molten globule and protein folding." Adv. Protein Chem. 47: 83-229.

Schuler, B., E. A. Lipman, et al. (2002). "Probing the free-energy surface for protein folding with single-molecule fluorescence spectroscopy." Nature 419(6908): 743-747.

Sherman, E. and G. Haran (2006). "Coil-globule transition in the denatured state of a small protein." Proc. Natl. Acad. Sci. U.S.A. 103(31): 11539-11543.

Sherman, E., A. Itkin, et al. (2008). "Using fluorescence correlation spectroscopy to study conformational changes in denatured proteins." Biophys. J. 94(12): 4819-4827.

Steensma, E., M. J. Nijman, et al. (1998). "Apparent local stability of the secondary structure of *Azotobacter vinelandii* holoflavodoxin II as probed by hydrogen exchange: implications for redox potential regulation and flavodoxin folding." Protein Sci. 7(2): 306-317.

Steensma, E. and C. P. van Mierlo (1998). "Structural characterisation of apoflavodoxin shows that the location of the stable nucleus differs among proteins with a flavodoxin-like topology." J. Mol. Biol. 282(3): 653-666.

Tezuka-Kawakami, T., C. Gell, et al. (2006). "Urea-induced unfolding of the immunity protein Im9 monitored by spFRET." Biophys. J. 91(5): L42-L44.

Thirumalai, D., E. P. O'Brien, et al. (2010). "Theoretical Perspectives on Protein Folding." Annu. Rev. Biophys. 39: 159-183.

van Mierlo, C. P., J. M. van den Oever, et al. (2000). "Apoflavodoxin (un)folding followed at the residue level by NMR." Protein Sci. 9(1): 145-157.

van Mierlo, C. P., W. M. van Dongen, et al. (1998). "The equilibrium unfolding of *Azotobacter vinelandii* apoflavodoxin II occurs via a relatively stable folding intermediate." Protein Sci. 7(11): 2331-2344.

van Mierlo, C. P. M., J. M. P. van den Oever, et al. (2000). "Apoflavodoxin (un)folding followed at the residue level by NMR." Protein Sci. 9(1): 145-157.

Vendruscolo, M., E. Paci, et al. (2001). "Three key residues form a critical contact network in a protein folding transition state." Nature 409(6820): 641-645.

Ziv, G. and G. Haran (2009). "Protein folding, protein collapse, and Tanford's transfer model: lessons from single-molecule FRET." J. Am. Chem. Soc. 131(8): 2942-2947.

Chapter 6

Summary and General discussion

Simon Lindhoud and Carlo P.M. van Mierlo

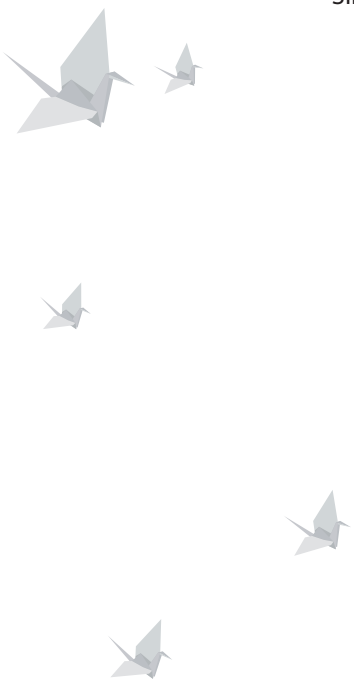

Summary

This thesis entitled 'Visualisation and Characterisation of Apoflavodoxin Folding' describes work that has been carried out to illuminate folding of a flavoprotein. The protein under investigation, i.e. flavodoxin, adopts the widely prevalent α-β parallel topology. Flavodoxin is a 179-residue monomeric protein that contains a tightly, but non-covalently, bound flavin mononucleotide (FMN) cofactor. Apoflavodoxin's denaturant-dependent equilibrium folding has been described by the three-state model (van Mierlo, van Dongen et al. 1998; Bollen, Sanchéz et al. 2004):

$$I_{off} \rightleftharpoons \textit{Unfolded apoflavodoxin} \rightleftharpoons I_{on} \rightleftharpoons \textit{Native apoflavodoxin} \quad \text{[Scheme 6.1]}$$

Off-pathway folding intermediate I_{off} is a relatively stable, molten globule-like folding species (Engel, Westphal et al. 2008). Formation of such an off-pathway folding intermediate appears to be a characteristic feature of proteins with α-β parallel topologies (Bollen and van Mierlo 2005).

Cofactor binding protects flavodoxin against oxidative stress

Binding of FMN to native apoflavodoxin is the last step in folding of flavodoxin (Bollen, Nabuurs et al. 2005). With FMN bound to the apoprotein, flavodoxin functions as an electron carrier. In addition to the well-known properties of cofactors as functional moieties, cofactors have as secondary function stabilisation of proteins against denaturation. A previously unknown property of cofactors is that they can protect proteins against potentially harmful effects of oxidative stress, as demonstrated in this thesis (**Chapter 2**). Flavodoxin contains two potentially oxidation-sensitive residues (i.e., Met30 and Cys69). Under influence of hydrogen peroxide-induced oxidative stress, methionine forms methionine sulphoxide, and cysteine consecutively forms sulphenic, sulphinic and sulphonic acid states. The sulphenic acid can react with another cysteine to form a disulphide. Whereas Met30 is buried in the solvent inaccessible protein interiors of flavodoxin and apoflavodoxin, Cys69 resides in a functionally important loop at the surface near the FMN binding site of both proteins. Use of a combination of analytical anion-exchange chromatography, analytical gel-filtration, liquid chromatography coupled with mass spectrometry and native mass spectrometry revealed that Met30 is insensitive to hydrogen peroxide induced oxidation in both apoflavodoxin and flavodoxin. However, in apoprotein Cys69 is susceptible to covalent modification, and rapidly becomes oxidised in presence of hydrogen peroxide. This oxidation results in formation of cysteine sulphenic acid and subsequent covalent dimerisation of apoflavodoxin. In addition, Cys69 becomes irreversibly oxidised to sulphinic and sulphonic acid. In flavodoxin covalent modification of this residue is slowed down compared to apoflavodoxin. Strikingly, oxidising conditions have rather limited effect on flavodoxin, because no oxidation of Cys69 beyond cysteine sulphenic acid state is observed. Apparently, in flavodoxin the sulphenic acid form of Cys69 is stabilised through

intramolecular interaction. Clearly, cofactor binding protects flavodoxin against oxidative stress (Figure 6.1).

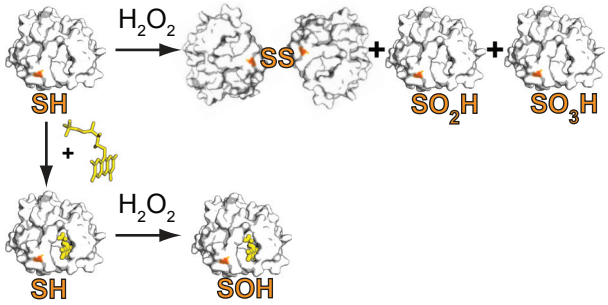

Figure 6.1 Cofactor binding protects flavodoxin against oxidative stress. Hydrogen peroxide-mediated oxidation of apoflavodoxin results in formation of covalently linked protein dimers, as well as consecutive formation of sulphinic acid state (SO_2H) and sulphonic acid state (SO_3H) of Cys69. In contrast, addition of H_2O_2 to flavodoxin (FMN is shown in yellow) only leads to formation of Cys69 sulphenic acid state (SOH).

Fluorescence quenching of an Alexa dye tracks conformational changes during protein folding

Thus far, insight into apoflavodoxin's molten globule has been mainly obtained by methods that either indirectly detect this folding species or infer its properties by employing fitting of a three-state model for protein folding. Illuminating the formation and conformational properties of apoflavodoxin's molten globule requires use of methods that efficiently and directly detect this folding species, and are able to elucidate the heterogeneity of the protein folding process. (Single-molecule) fluorescence spectroscopy and Förster Resonance Energy Transfer (FRET) are well suited for this purpose.

Labelling of apoflavodoxin molecules with fluorescent donor and acceptor probes facilitates visualisation of their folding by fluorescence spectroscopy and FRET. Ideally, only changes in inter-dye distances result in changes of donor fluorescence in FRET experiments. However, fluorescent probes are generally sensitive to changes in their local environments. Folding-induced conformational changes potentially affect fluorescence properties of dyes that are attached to a protein. Alteration of donor fluorescence quantum yield affects R_0 of a FRET pair, and thus influences the range of distances that can be determined by measuring FRET efficiencies. Hence, folding-induced changes in fluorescent properties of fluorophores must be characterised first to facilitate interpretation of FRET.

The first step taken in visualisation of apoflavodoxin folding was labelling of Cys69 with a FRET donor fluorophore (i.e., Alexa Fluor 488; A488, which is a commonly used donor) (**Chapter 3**). Subsequently, denaturant-dependent equilibrium folding of A488 labelled apoflavodoxin (A488-apoflavodoxin) was monitored using tryptophan fluorescence intensity, A488

fluorescence intensity and circular dichroism at 222 and 225 nm. Fitting of a three-state model for protein folding to the data obtained reveals that attachment of A488 predominantly destabilises native protein, while preserving apoflavodoxin's three-state folding characteristics.

Compared to native A488-apoflavodoxin, fluorescence of A488 is quenched in both molten globule and unfolded protein. Diminishing of fluorescence intensity can be attributed to dynamic and/or static quenching processes. Only dynamic quenching is characterised by reduction of the fluorescence lifetime of the fluorophore involved. In case of static quenching, which involves formation of a non-fluorescent ground-state complex between fluorophore and quencher, such alteration of fluorescence lifetime is not observed. Comparison of the denaturant dependencies of A488 fluorescence intensity and lifetime revealed that upon formation of molten globule, both static and dynamic quenching increase (Figure 6.2). Interaction of A488 with tryptophan residues likely causes this static and dynamic quenching. In case of molten globule and unfolded apoflavodoxin, tryptophans are solvent exposed and can interact with the dye label. In contrast, solvent accessibility of tryptophans is considerably lower in native protein. Clearly, fluorescence intensity of A488 tracks folding of A488-apoflavodoxin.

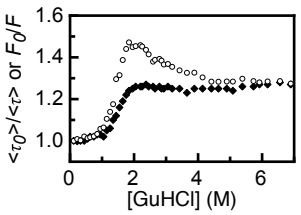

Figure 6.2 Quenching of A488 fluorescence tracks folding of A488-apoflavodoxin. Denaturant-dependence of F_0/F (open dots); F is fluorescence intensity at a given concentration denaturant and F_0 is fluorescence intensity in absence of denaturant. Denaturant-dependence of $<\tau_0>/<\tau>$ (filled diamonds); $<\tau>$is average fluorescence lifetime at a given concentration denaturant and $<\tau_0>$ is average fluorescence lifetime in absence of denaturant.

Illuminating the off-pathway nature of the molten globule folding intermediate of an α-β parallel protein

Characterisation of folding-induced conformational changes within different parts of apoflavodoxin is achieved by labelling the protein with a suitable donor and acceptor FRET pair (**Chapter 4**). Site-directed mutagenesis was used to introduce a cysteine residue either on position 1, 131 or 178 of apoflavodoxin. Labelling with donor and acceptor is preferably site-specific, because folding-induced changes in local environments of these dyes affect their fluorescence properties. Exploiting the inaccessibility of Cys69 in the cofactor bound form of the protein (Figure 6.3A), selective labelling of Cys1, Cys131 or Cys178 with acceptor label Alexa Fluor 568 (A568) was achieved. Purification of singly labelled protein and subsequent removal of cofactor enabled labelling of

Cys69 with donor A488. Apoflavodoxin molecules thus obtained are site-specifically labelled with donor label on Cys69, and acceptor label either on Cys1, Cys131 or Cys178 (i.e., a1-d69-, d69-a131-, and d69-a178-apoflavodoxin, respectively) (Figure 6.3).

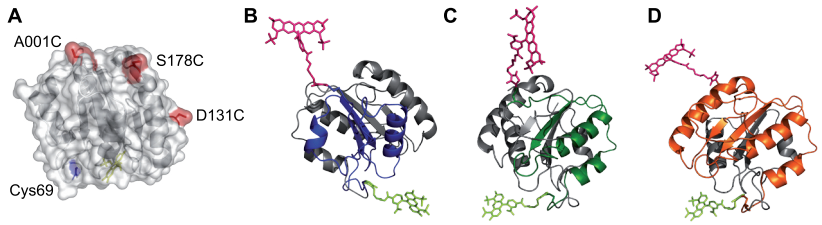

Figure 6.3 Covalent attachment of dye-labels to enable FRET-based probing of apoflavodoxin folding. (A) In flavodoxin, Cys69 is much less accessible than Cys1, Cys131, and Cys178, enabling site-specific labelling with thiol-reactive fluorescent probes. This model shows the surface of flavodoxin in a semi-transparent fashion, with Cys69 in blue, and the other cysteines in red. The FMN cofactor is shown in yellow. (B) Cartoon representation of d69-a1, showing in blue the backbone that intervenes residues 1 and 69. (C) d69-a131, with the backbone intervening residues 69 and 131 in green. (D) d69-a178, with the backbone intervening residues 69 and 178 in orange. A488 is shown in bright green, and A568 in pink. Cartoons are generated with PyMOL (Schrödinger, LLC, Palo Alto, Ca, USA) using the crystal structure of *A. vinelandii* flavodoxin (pdb ID 1YOB (Alagaratnam, van Pouderoyen et al. 2005)) and the molecular structures of A488 and A568, as provided by Invitrogen.

Fluorescence intensities of tryptophan residues, and of donor and acceptor label of doubly dye-labelled apoflavodoxin were monitored as function of concentration denaturant. This monitoring shows that the N-terminal 69 residues of apoflavodoxin's molten globule forms fold last. In addition, employment of FRET as a qualitative spectroscopic ruler revealed striking conformational differences between molten globule and native protein. Shorter inter-label distances are sampled within the 111-residue C-terminal segment of the ensemble of molten globule-like conformers than in native apoflavodoxin (Figure 6.4). Thus, ensemble FRET sheds light on the off-pathway nature of the molten globule during folding of an α-β parallel protein.

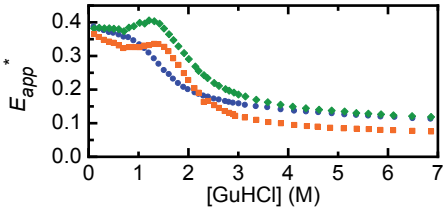

Figure 6.4 Monitoring of ensemble FRET tracks denaturant-dependent folding of doubly dye-labelled apoflavodoxin. Data corresponding to a1-d69-, d69-a131- and d69-a178-apoflavodoxin are shown in blue, green and orange, respectively. The apparent FRET efficiency (E_{app}^*) is calculated according to ($E_{app}^* = I_{FRET}/(I_{FRET}+I_{DA})$), where I_{FRET} is sensitised fluorescence emission of acceptor (i.e. emission of acceptor upon excitation of donor), and I_{DA} is fluorescence emission of donor label in presence of acceptor, respectively. Protein concentration is 62.5 nM. I_{DA} is measured at 515 nm and I_{FRET} is measured at 630 nm, both upon excitation of donor at 450 nm.

Single-molecule FRET reveals non-cooperative folding of a molten globule

Ensemble averaging obscures measurements of conformational heterogeneity in for example molten globule states. Still, fitting of models for protein folding to ensemble-averaged folding curves can give insight into denaturant-dependent equilibrium populations of discernable folding states. To obtain full insight into folding-related conformational heterogeneity necessitates use of direct and model-free detection methods, with single molecule fluorescence spectroscopy and FRET (smFRET) as prominent examples.

Doubly dye-labelled protein variants d69-a131-apoflavodoxin (Figure 6.3C) and d69-a178-apoflavodoxin (Figure 6.3D) report different FRET efficiencies in their native, molten globule and unfolded states. Thus, these protein variants are suitable to elucidate protein folding by smFRET (**Chapter 5**). smFRET efficiencies were recorded for thousands of individual protein molecules at denaturant concentrations ranging in between 0 and 5 M guanidine hydrochloride (GuHCl), and corresponding smFRET efficiency histograms were constructed (Figure 6.5). Remarkably, at all denaturant concentrations used, a single smFRET efficiency distribution is observed in each histogram.

smFRET efficiency distributions of native and molten globule apoflavodoxin overlap at denaturant concentrations where both folding states significantly populate. Starting with unfolded apoflavodoxin, smFRET exposes that upon lowering of denaturant concentration formation of the molten globule folding intermediate is strongly favoured. Upon folding of the molten globule, the unimodal smFRET efficiency distribution gradually shifts to larger FRET value due to progressive extension of its ordered core. This non-cooperative compaction happens during folding of every single molten globule molecule. Consequently, during kinetic folding of unfolded apoflavodoxin molecules, they swiftly form this molten globule upon lifting denaturing conditions.

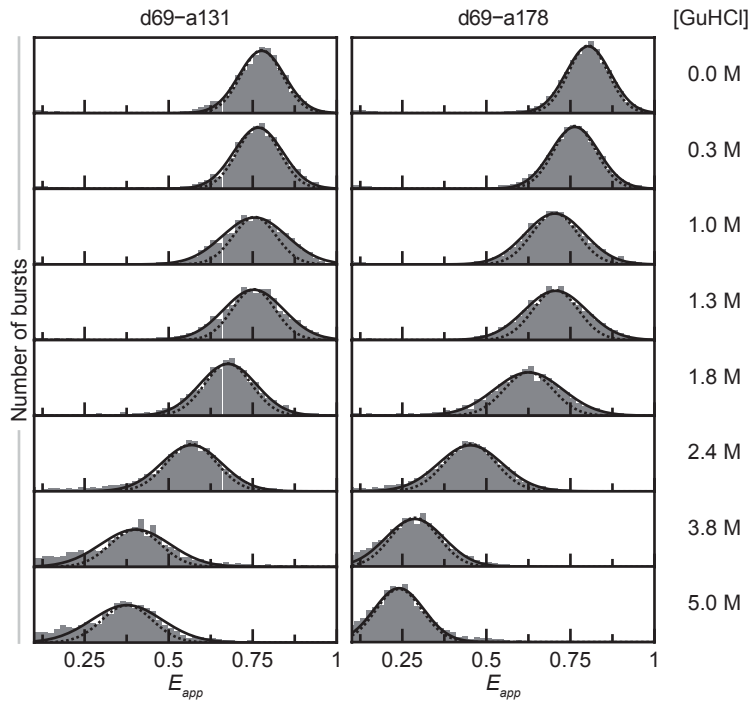

Figure 6.5 A unimodal Gaussian distribution describes smFRET efficiency histograms of d69-a131 and d69-a178 at all concentrations denaturant. The left-hand column shows the denaturant-dependence of smFRET data of d69-a131 and the right-hand column shows the corresponding data of d69-a178. GuHCl concentration is indicated on the left-hand side. Vertical grey bars show the numbers of bursts observed within a bin of apparent FRET efficiency. Bursts of photons during which bleaching occurs are not taken into account, as described in Materials and Methods. Solid lines show the results of fitting Gaussian distribution function equation 5.3 to the data. Dotted lines indicate shot-noise limited distributions according to equation 5.4. Histograms are normalised to the total number of burst obtained. The complete series of denaturant-dependent histograms obtained is shown in supporting information Figure S5.2.

General discussion

Folding of small single-domain proteins of less than 100 amino acid residues has been studied extensively and is generally well described by two-state equilibrium behaviour, in which only unfolded and native protein needs to be taken into account (Jackson 1998). Folding of larger proteins is complex and involves population of partially folded intermediate states, like molten globules (Brockwell and Radford 2007). These folding species have loosely packed cores and exposed hydrophobic residues, which render them prone to aggregation (Ohgushi and Wada 1983; Ptitsyn, Pain et al. 1990; Christensen and Pain 1991; Arai and Kuwajima 2000).

Denaturant-dependent folding of apoflavodoxin involves formation of a relatively stable off-pathway molten globule (Bollen, Sanchéz et al. 2004; Nabuurs, Westphal et al. 2008; Nabuurs, Westphal et al. 2009; Nabuurs, Westphal et al. 2009; Nabuurs and van Mierlo 2010). Protein molecules that adopt this non-native conformation must unfold considerably before the native state can be attained. Thus far, insight into formation of apoflavodoxin's molten globule has been obtained predominantly by use of methods that either indirectly detect this folding species or require use of a three-state model for protein folding. Here, use of site-specifically doubly-dye labelled apoflavodoxin molecules, and (single-molecule) fluorescence spectroscopy and FRET illuminates molecular features of apoflavodoxin's molten globule. These approaches enable direct and sensitive detection of this folding intermediate.

In light of the findings presented in this thesis, the three-state description of apoflavodoxin folding requires revision. Indeed, three states can be distinguished in apoflavodoxin folding curves: (i) native apoflavodoxin, which folds cooperatively in the denaturant range between ~2 to ~1 M GuHCl, (ii) molten globule apoflavodoxin, which is the sole species up to ~ 1.7 M GuHCl, and (iii) unfolded apoflavodoxin, which exists at high concentrations of GuHCl. The three-state model for protein folding treats the observed transition from unfolded to molten globule as being first order (i.e., at the corresponding denaturation midpoint both states populate equally).

This thesis shows that between about 2 to 3.4 M GuHCl, all apoflavodoxin equilibrium data report conformational changes within the molten globule species, rather than reporting exchange between molten globule and unfolded state. As a consequence, thermodynamic analysis of the corresponding folding data by using a three-state model seems inappropriate. Remarkably, however, independent measurement of apoflavodoxin stability by model-free, native-state hydrogen-deuterium exchange (Bollen, Kamphuis et al. 2006)) yields a free energy difference between native and unfolded apoflavodoxin similar to the value extracted by using the three-state model for folding (Bollen, Sanchéz et al. 2004). Thus, also the free energy difference between molten globule and unfolded state, as extracted by using a three-state model for protein folding,

must be approximately correct. Note however, that use of this three-state model of equilibrium folding affected previously extracted kinetic parameters of apoflavodoxin folding and our current understanding of apoflavodoxin's folding landscape. During analysis of apoflavodoxin folding kinetics, it was assumed that the transition from unfolded to molten globule is a single first order transition. Hence, transition midpoints obtained by apoflavodoxin equilibrium folding were fixed during analysis of apoflavodoxin folding kinetics. However, this thesis shows that the observed 'transition' between unfolded and molten globule apoflavodoxin actually reflects conformational changes within this molten globule species. As a consequence, backward and forward rate constants that describe the molten globule to unfolded state equilibrium have previously been incorrectly determined.

Folding of the molten globule involves increasingly compact interconverting intermediate conformations. In order to get a better understanding of apoflavodoxin's folding energy landscape, it is necessary to reassess kinetic apoflavodoxin folding by using model free approaches that are able to detect each folding species with similar efficiency. Therefore, it would be very interesting to study conformational interchange within apoflavodoxins molten globule and exchange between native, molten globule and unfolded conformations by recording smFRET trajectories of single molecules at several concentrations denaturant. This approach is well suited for resolving folding dynamics in presence of a multitude of intermediate conformations (Pirchi, Ziv et al. 2011).

This thesis shows that visualisation and characterisation of apoflavodoxin folding by employing site-specific dye labelling, fluorescence spectroscopy and (single-molecule) FRET enables direct detection of molten globule folding. Use of these methodologies demonstrates that folding of the C-terminal part of apoflavodoxin's molten globule precedes folding of its N-terminal part, and shows that the conformations of molten globule and native apoflavodoxin differ drastically. Most importantly, smFRET provides direct insight into non-cooperative molten globule folding, and shows that formation of this intermediate is strongly favoured. Upon folding, apoflavodoxin's molten globule gradually compacts due to progressive extension of its ordered core. This gradual compaction during folding of molten globules is likely a general phenomenon for proteins with a flavodoxin-like topology, and possibly happens during folding of many other proteins as well.

References

Alagaratnam, S., G. van Pouderoyen, et al. (2005). "A crystallographic study of Cys69Ala flavodoxin II from *Azotobacter vinelandii*: structural determinants of redox potential." Protein Sci. 14(9): 2284-2295.

Arai, M. and K. Kuwajima (2000). "Role of the molten globule state in protein folding." Adv. Protein. Chem. 53: 209-282.

Bollen, Y. J., I. E. Sanchéz, et al. (2004). "Formation of on- and off-pathway intermediates in the folding kinetics of *Azotobacter vinelandii* apoflavodoxin." Biochemistry 43(32): 10475-10489.

Bollen, Y. J. and C. P. van Mierlo (2005). "Protein topology affects the appearance of intermediates during the folding of proteins with a flavodoxin-like fold." Biophys. Chem. 114(2-3): 181-189.

Bollen, Y. J. M., M. B. Kamphuis, et al. (2006). "The folding energy landscape of apoflavodoxin is rugged: Hydrogen exchange reveals nonproductive misfolded intermediates." Proc. Natl. Acad. Sci. U.S.A. 103(11): 4095-4100.

Bollen, Y. J. M., S. M. Nabuurs, et al. (2005). "Last in, first out." J. Biol. Chem. 280(9): 7836-7844.

Brockwell, D. J. and S. E. Radford (2007). "Intermediates: ubiquitous species on folding energy landscapes?" Curr. Opin. Struct. Biol. 17(1): 30-37.

Christensen, H. and R. H. Pain (1991). "Molten Globule Intermediates and Protein Folding." Eur. Biophys. J. 19(5): 221-229.

Engel, R., A. H. Westphal, et al. (2008). "Macromolecular crowding compacts unfolded apoflavodoxin and causes severe aggregation of the off-pathway intermediate during apoflavodoxin folding." J. Biol. Chem. 283(41): 27383-27394.

Jackson, S. E. (1998). "How do small single-domain proteins fold?" Fold Des. 3(4): R81-R91.

Nabuurs, S. M. and C. P. van Mierlo (2010). "Interrupted hydrogen/deuterium exchange reveals the stable core of the remarkably helical molten globule of α-β parallel protein flavodoxin." J. Biol. Chem. 285(6): 4165-4172.

Nabuurs, S. M., A. H. Westphal, et al. (2009). "Topological switching between an α-β parallel protein and a remarkably helical molten globule." J. Am. Chem. Soc. 131: 8290-8295.

Nabuurs, S. M., A. H. Westphal, et al. (2008). "Extensive formation of off-pathway species during folding of an α-β parallel protein is due to docking of (non)native structure elements in unfolded molecules." J. Am. Chem. Soc. 130(50): 16914-16920.

Nabuurs, S. M., A. H. Westphal, et al. (2009). "Non-cooperative formation of the off-pathway molten globule during folding of the α-β parallel protein apoflavodoxin." J. Am. Chem. Soc. 131: 2739-2746.

Ohgushi, M. and A. Wada (1983). "'Molten-globule state': a compact form of globular proteins with mobile side-chains." FEBS Lett. 164(1): 21-24.

Pirchi, M., G. Ziv, et al. (2011). "Single-molecule fluorescence spectroscopy maps the folding landscape of a large protein." Nat. Comm. 2.

Ptitsyn, O. B., R. H. Pain, et al. (1990). "Evidence for a molten globule state as a general intermediate in protein folding." FEBS Lett. 262(1): 20-24.

van Mierlo, C. P., W. M. van Dongen, et al. (1998). "The equilibrium unfolding of *Azotobacter vinelandii* apoflavodoxin II occurs via a relatively stable folding intermediate." Protein Sci. 7(11): 2331-2344.

Chapter 7

Nederlandse samenvatting

Eiwitten zijn betrokken bij vrijwel alle processen die essentieel zijn voor het functioneren en voortbestaan van organismen. Deze moleculen zijn onvertakte ketens van aminozuren, waarvan de volgorde en het aantal verschilt per eiwit, en kunnen hun functie alleen uitvoeren als ze zijn opgevouwen tot de stabiele en correcte driedimensionale structuur. De ontvouwen toestand van een eiwit is het startpunt voor deze vouwing. Het eiwit vouwingsproces is complex, omdat eiwitten talloze vouwingsroutes kunnen volgen om de functionele structuur te bereiken. Op deze routes worden gedeeltelijk gevouwen structuren gevormd, en structuren die conflicteren met de correct gevouwen functionele structuur van het eiwit. Deze 'intermediaire' en verkeerd gevouwen structuren kunnen de neiging hebben tot samenklonteren. De vorming van zulke aggregaten speelt een rol bij onder andere de ziekte van Alzheimer, de ziekte van Parkinson, de ziekte van Huntington, diabetes type 2, en de gekkekoeienziekte. Het bestuderen van vouwings-intermediairen geeft inzicht in de vorming van deze moleculen en daarmee in de factoren die een rol spelen bij het ontstaan van verkeerd gevouwen eiwitmoleculen en eiwitaggregaten.

Apoflavodoxine vouwing

Dit proefschrift getiteld "Visualisation and Characterisation of Apoflavodoxin Folding" (vrij vertaald: zichtbaar maken en ophelderen van apoflavodoxine vouwing) beschrijft werk dat is uitgevoerd om het vouwingsproces van het eiwit apoflavodoxine uit de bacterie *Azotobacter vinelandii* beter te begrijpen. Kennis die verkregen wordt over de vouwing van dit eiwit geeft inzicht in de vouwing van een grote groep eiwitten die qua structuur op apoflavodoxine lijken, maar hieraan verder niet verwant zijn. De vouwing van apoflavodoxine laat zich beschrijven door het volgende drietoestandenmodel:

$$I_{off} \rightleftharpoons \textit{Ontvouwen apoflavodoxine} \rightleftharpoons \textit{Gevouwen apoflavodoxine}$$

Vouwingsintermediair I_{off} bevat structuur die conflicteert met de functionele eiwit structuur, en vormt 'off-pathway', d.w.z. dat deze structuur via een andere route gevormd wordt dan correct gevouwen apoflavodoxine. Moleculen die deze vorm aannemen zullen eerst (gedeeltelijk) moeten ontvouwen voordat ze de juiste vouwingsweg kunnen inslaan. Deze off-pathway intermediair lijkt op een zogenaamde 'molten globule'. Een molten globule eiwit bevat een aanzienlijke hoeveelheid structuur, maar heeft niet de compacte pakking van een correct gevouwen eiwit. De molten globule van apoflavodoxine is relatief stabiel, wat ophelderen van eigenschappen van dit molecuul mogelijk maakt. Echter, met de technieken die tot dusver zijn gebruikt om inzicht te verkrijgen in de vouwing van apoflavodoxine kunnen we de karakteristieken van deze intermediair alleen indirect ontrafelen. Daarnaast wordt het bestuderen van zulke moleculen bemoeilijkt door hun tijdelijke bestaan, hun neiging tot aggregeren en hun instabiele structuur. Het verder ophelderen van eigenschappen van

deze vouwingsintermediair vraagt om het gebruik van technieken die individuele eiwitmoleculen detecteren en kunnen onderscheiden van andere moleculen. Hiervoor is enkel-molecuul fluorescentie spectroscopie in combinatie met 'Förster Resonance Energy Transfer' (FRET) uitermate geschikt.

Fluorescentie en FRET

Om te kunnen begrijpen hoe we met fluorescentie spectroscopie de vouwing van eiwitten kunnen bestuderen moeten we eerst weten wat fluorescentie is. Fluorescentie is het proces waarbij een molecuul licht uitstraalt nadat het is aangeslagen door het absorberen van energie in de vorm van een pakketje licht (een foton). De golflengte (kleur), en daarmee de energie, van het uitgestraalde licht is afhankelijk van de eigenschappen van het fluorescente molecuul. Het uitgestraalde foton heeft ook altijd een lagere energie dan de door het molecuul geabsorbeerde energie. De tijd tussen het absorberen van de energie en het uitzenden van licht bedraagt enkele nanoseconden. Als er in deze korte tijd een ander fluorescent molecuul in de buurt is van het aangeslagen molecuul, dan kan het aangeslagen molecuul haar energie afstaan aan het andere molecuul; dit proces wordt FRET genoemd. We noemen dan het aangeslagen molecuul de donor, en het molecuul waaraan de energie wordt afgestaan de acceptor.

De kans dat FRET optreedt (de FRET-efficiëntie) is afhankelijk van een aantal factoren. Allereerst is er de fluorescentie efficiëntie van de donor, d.w.z. de verhouding tussen het aantal keren dat een donor een foton absorbeert, en het aantal keren dat de donor de opgenomen energie weer kwijtraakt door het uitzenden van een foton. Hoe hoger de fluorescentie efficiëntie van de donor, hoe groter de kans dat de energie kan worden afgestaan aan de acceptor. Dit is echter ook afhankelijk van de eigenschappen van de acceptor. Deze kan namelijk alleen als acceptor functioneren als de energie die benodigd is om dit molecuul aan te slaan overeenkomt met de energie van de door de donor uitgezonden fotonen. Het is hier belangrijk om te weten dat FRET plaats vindt zonder dat de donor een foton uitzendt! Naast deze eigenschappen van de donor en acceptor spelen ook de oriëntatie van deze moleculen ten opzichte van elkaar, en de samenstelling van het medium tussen deze moleculen speelt een rol. Tot slot is de afstand tussen donor en de acceptor een bepalende factor voor de kans dat FRET kan plaatsvinden. Door deze sterke afstandsafhankelijkheid kan FRET als spectroscopische meetlat gebruikt worden. Deze meetlat rapporteert over afstanden op de nanometer lengteschaal, wat overeenkomt met de grootteverschillen tussen gevouwen en ontvouwen eiwitten.

Het labelen van eiwitmoleculen met sterk fluorescente donor en acceptor moleculen maakt het mogelijk om met behulp van enkel-molecuul fluorescentie spectroscopie, de afstand tussen donor en acceptor per individueel molecuul te registreren. Als we dit voor duizenden moleculen

doen verkrijgen we inzicht in het aantal vouwingstoestanden dat vormt en hun populaties, omdat de afstand tussen donor en acceptor gerelateerd is aan de vouwingstoestand van het molecuul. Daarnaast is het mogelijk om enkel-molecuul fluorescentie te gebruiken om de vouwing van eiwitmoleculen in de tijd te volgen.

Er bestaan verschillende strategieën om eiwitten te voorzien van een donor en een acceptor label. De meest specifieke methode hiervoor is koppelen van een label aan het aminozuur cysteine. Met behulp van DNA-modificatie technologie, kunnen we eiwitten creëren waar we op specifieke plaatsen cysteine residuen inbouwen. Zodoende kunnen we de donor en acceptor op verschillende posities in het eiwit inbouwen. Hiervoor zijn echter wel twee cysteine residuen nodig, die we selectief zouden willen labelen. Dit is alleen mogelijk als er condities gevonden worden waarin de reactiviteit van deze cysteine residuen verschilt.

Binding van de FMN-cofactor binding beschermt flavodoxine tegen oxidatieve stress

Apoflavodoxine bevat van nature een cysteine residu op positie 69 (Cys69). In **hoofdstuk 2** worden experimenten beschreven om te bepalen hoe de reactiviteit van dit aminozuur kan worden beïnvloed. In de cel bindt apoflavodoxine een flavine mononucleotide (FMN) cofactor. In combinatie met deze cofactor wordt het eiwit flavodoxine genoemd. Met dit aan vitamine B2 verwante molecuul vervult flavodoxine in de cel een rol in elektronen transport. FMN kan alleen binden aan gevouwen apoflavodoxine, en dit is dan ook de laatste stap in het vouwingsproces van flavodoxine.

Naast de bekende werking van cofactoren als functioneel onderdeel van een eiwit, heeft het binden van cofactoren ook tot gevolg dat de stabiliteit van een eiwit toeneemt. Verder kunnen cofactoren mogelijk ook een rol spelen bij het beschermen van een eiwit tegen oxidatieve stress. Organismen worden voortdurend blootgesteld aan oxidatieve stress, en de gevolgen hiervan zijn gekoppeld aan een verscheidenheid aan ziektes. Oxidatieve condities, zoals de aanwezigheid van waterstofperoxide, kunnen leiden tot covalente modificatie van de aminozuren cysteine en methionine.

Cys69 bevindt zich in flavodoxine in de nabijheid van de cofactor. Het induceren van oxidatieve stress met behulp van waterstofperoxide leidt noch in flavodoxine noch in apoflavodoxine tot modificatie van het enkele methionine residu in flavodoxine. Echter, het effect van waterstofperoxide op Cys69 in apoflavodoxine en in flavodoxine verschilt sterk. In apoflavodoxine wordt deze cysteine snel irreversibel geoxideerd, terwijl in flavodoxine deze cysteine nauwelijks reageert met waterstofperoxide. Het blijkt dat de FMN cofactor Cys69 beschermt tegen oxidatie en andere covalente modificaties (Figuur 7.1).

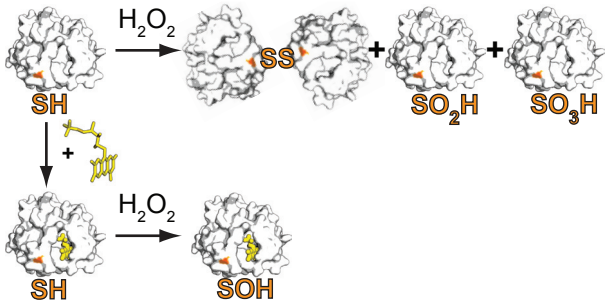

Figuur 7.1 Cofactor binding beschermt flavodoxine tegen oxidatieve stress. Oxidatie van apoflavodoxine met behulp van waterstofperoxide leidt tot de vorming van eiwit dimeren, sulfinylering (SO_2H) en sulfonylering (SO_3H) van Cys69. Daarentegen leidt toevoeging van waterstofperoxide aan flavodoxine (de FMN cofactor is geel weergegeven) slechts tot sulfenylering (SOH) van dit cysteine residu.

Fluorescentie van een Alexa Fluor label rapporteert over apoflavodoxine vouwing.

Om te kunnen begrijpen hoe de FRET-efficiëntie verandert als functie van de vouwingstoestand van het eiwit, moeten vouwing gerelateerde veranderingen van fluorescentie van het donor-label bepaald worden. Dit is de eerste stap in het zichtbaar maken van apoflavodoxine vouwing. In **hoofdstuk 3** wordt beschreven hoe donor-label Alexa Fluor 488 (A488) aan Cys69 van apoflavodoxine gekoppeld wordt. Met behulp van guanidine hydrochloride (GuHCl) worden veranderingen in de vouwingstoestand van het eiwit geïnduceerd. Door onder andere de fluorescentie intensiteit van het donor-label te bepalen bij verschillende GuHCl concentraties blijkt dat dit label drie toestanden rapporteert tijdens de vouwing van apoflavodoxine. Dit is in overeenstemming met het drietoestandenmodel dat wordt gebruikt om vouwing van apoflavodoxine te beschrijven.

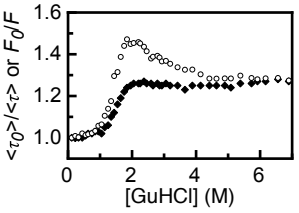

Figuur 7.2 Fluorescentie van een Alexa Fluor label rapporteert over apoflavodoxine vouwing. Denaturant-afhankelijkheid van F_0/F (open stippen); F is de fluorescentie- intensiteit bij een bepaalde concentratie denaturant en F_0 is de fluorescentie-intensiteit in afwezigheid van denaturant. Denaturant-afhankelijkheid van $\langle\tau_0\rangle/\langle\tau\rangle$ (gevulde ruiten); $\langle\tau\rangle$ is de gemiddelde fluorescentie levensduur bij een bepaalde concentratie denaturant en $\langle\tau_0\rangle$ is de gemiddelde fluorescentie levensduur in afwezigheid denaturant.

Metingen van de fluorescentie levensduur (de tijd dat het molecuul in de aangeslagen toestand verblijft) geven inzicht in waarom de fluorescentie intensiteit van het donor-label de vouwing van apoflavodoxine weergeeft. Tijdens de paar nanoseconden dat de aangeslagen toestand bestaat,

zijn er allerlei processen die competitie aangaan met het uitzenden van een foton. Kortstondige interacties met moleculen die de fluorescentie kunnen uitdoven hebben tot gevolg dat het molecuul gemiddeld gezien korter in de aangeslagen toestand verblijft en leveren dus een verkorting van de fluorescentie levensduur op. Bij gevolg verlaagt hierdoor ook de fluorescentie intensiteit. Dit proces wordt dynamische quenching genoemd. Interacties die langer duren dan de fluorescentie levensduur leveren wel een verlaging van de fluorescentie intensiteit op, maar geen verlaging van de fluorescentielevensduur. Dit proces wordt statische quenching genoemd. Verschillen in veranderingen van de fluorescentie-intensiteit en levensduur als functie van de GuHCl concentratie laten zien dat bij A488 (gekoppeld aan Cys69) zowel statische als dynamisch quenching processen een rol spelen in veranderingen van de fluorescentie-intensiteit van de donor (Figuur 7.2). Quenching van A488 ontstaat door interactie met zijketens van het aminozuur tryptofaan, die in de gevouwen toestand zijn opgeborgen in het eiwit en daarom niet in contact kunnen komen met het label. Wanneer de pakking van het eiwit verdwijnt door ontvouwing, kunnen deze aminozuren interacties aangaan met het label. De mogelijkheden tot deze interacties verschillen dus per vouwingstoestand, en daardoor worden de aan vouwing gerelateerde verschillen in fluorescentie-intensiteit van A488 geobserveerd.

Het ophelderen van het off-pathway karakter van de molten globule vouwingsintermediair van apoflavodoxine

Het plaatsen van een acceptor-label op een met een donor gelabeld eiwit, maakt het mogelijk om FRET te gebruiken om eiwitvouwing te bestuderen. Hiervoor moet in apoflavodoxine een extra cysteine residu worden geïntroduceerd. **Hoofdstuk 4** beschrijft het maken van 3 apoflavodoxine varianten, waar op plaats 1, plaats 131 of plaats 178 een cysteine residu is ingebouwd. Gebruikmakend van de bescherming van Cys69 door de cofactor in flavodoxine kan acceptor-label Alexa Fluor 568 (A568 specifiek op de nieuwe cysteine worden gekoppeld. Vervolgens kan, na het verwijderen van de cofactor, A488 aan Cys69 worden gekoppeld. Met de op deze manier verkregen moleculen kan de vouwing van verschillende delen van het apoflavodoxine worden gevolgd (Figuur 7.3). De variant met acceptor op Cys1 en donor op Cys69 (a1-d69) rapporteert over de afstand tussen aminozuren 1 en 69 (Figuur 7.3B). De variant met donor op Cys69 en acceptor op Cys131 (d69-a131) geeft informatie over de afstand tussen aminozuren 69 en 131 (Figuur 7.3C). Het eiwit dat gelabeld is met donor op Cys69 en acceptor op Cys178 (d69-a178) geeft inzicht in de afstand tussen aminozuren 69 en 178 (Figuur 7.3D).

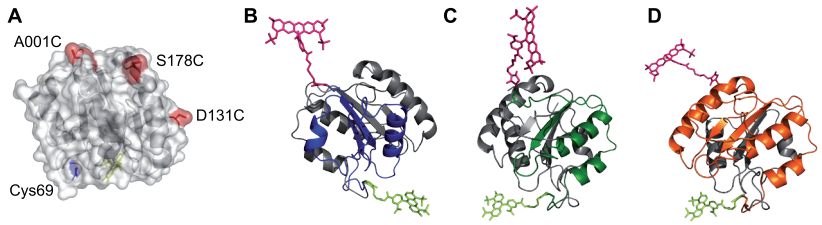

Figuur 7.3 Covalente koppeling van fluorescente labels teneinde apoflavodoxine vouwing te kunnen volgen met behulp van FRET. (A) In flavodoxine is Cys69 minder toegankelijk dan Cys1, Cys131, en Cys178, wat selectief labelen mogelijk maakt. Dit model geeft het eiwitoppervlak van flavodoxine half-transparant weer, Cys69 is blauw, en de overige cysteine residuen zijn rood gekleurd. De FMN cofactor wordt geel weergegeven. (B) Cartoon-weergave van d69-a1, het deel van het eiwit tussen residuen 1 en 69 is blauw gekleurd. (C) Cartoon-weergave van a131-d69, het deel van het eiwit tussen residuen 69 en 131 is groen gekleurd. (D) Cartoon-weergave van a178-d69, het deel van het eiwit tussen residuen 69 en 178 is oranje gekleurd.

Verschillende ensemble fluorescentie signalen (d.w.z., signalen die afkomstig zijn van veel moleculen tegelijkertijd) zijn gemeten tijdens de denaturant-geïnduceerde vouwing van apoflavodoxine. Gebruikmakend van FRET als spectroscopische meetlat zien we dat de verschillende delen van het eiwit bij verschillende denaturant concentraties de molten globule vormen. Allereerst vormt de kern van de molten globule in het gebied tussen Cys69 en Cys178. Pas als deze kern zich gevormd heeft, vouwt het deel tussen aminozuur 1 en 69. Deze observaties komen overeen met het beeld dat is ontstaan uit eerdere experimenten die hebben laten zien dat overal binnen het ontvouwen eiwit structuurvorming optreedt alvorens het de molten globule vormt. *Voor het eerst wordt naast vorming, ook het vouwen van de molten globule waargenomen.* Het blijkt dat residuen 69 en 131, en 69 en 178 dichter bij elkaar komen in de molten globule, dan in het correct gevouwen eiwit. De kern van de molten globule moet dus eerst ontvouwen voordat het eiwit naar de functionele structuur vouwt, wat verklaart waarom deze intermediair off-pathway is.

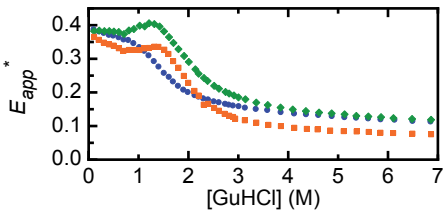

Figuur 7.4 Denaturant-afhankelijke vouwing van dubbel gelabeld apoflavodoxine, bestudeerd door middel van FRET. Data afkomstig van a1-d69-, d69-a131- en d69-a178-apoflavodoxine worden respectievelijk weergegeven in blauw, groen en oranje. Details worden beschreven in hoofdstuk 4.

Enkel-molecuul fluorescentie onthult geleidelijke vorming van een molten globule

Het meten van signalen van verschillende moleculen tegelijkertijd levert informatie op, waarin de binnen deze populatie bestaande heterogeniteit verborgen blijft. Desalniettemin kan het analyseren van zulke data met behulp van wiskundige modellen inzicht geven in deze heterogeniteit (zie bijvoorbeeld hoofdstuk 3). Directe opheldering van heterogeniteit die bestaat binnen de populatie apoflavodoxine moleculen wordt bereikt door bij verschillende denaturant concentraties de FRET-efficiëntie van duizenden *individuele* eiwit moleculen te registreren (**hoofdstuk 5**). Deze FRET-efficiënties kunnen worden weergegeven als histogrammen, die laten zien hoe vaak een bepaalde FRET-efficiëntie geregistreerd is. In het geval van eiwitten die alleen populaties gevouwen en ontvouwen moleculen vormen, worden in deze histogrammen doorgaans twee pieken geobserveerd. De piek die correspondeert met het gevouwen eiwit ligt bij een hoge FRET efficiëntie. De andere piek komt van het ontvouwen eiwit en wordt gevonden bij een lage FRET efficiëntie. Het verlagen van de denaturant concentratie heeft tot gevolg dat er meer gevouwen eiwit wordt gevormd en dat de hoeveelheid ontvouwen eiwit afneemt. Histogrammen van apoflavodoxine bij een hoge concentratie GuHCl laten een piek zien bij lage FRET efficiëntie, corresponderend met ontvouwen eiwit. Verlagen van de denaturant concentratie leidt aanvankelijk tot vorming van de molten globule, waarna ook gevouwen apoflavodoxine ontstaat. Opmerkelijk genoeg wordt dit niet gezien als het toenemen en afnemen van pieken bij een verschillende FRET efficiëntie, maar als een verschuiving van de piek in het histogram naar hogere waarden. *Enkel-molecuul fluorescentie en FRET laten daarmee direct zien hoe de molten globule van apoflavodoxine geleidelijk compacter wordt.*

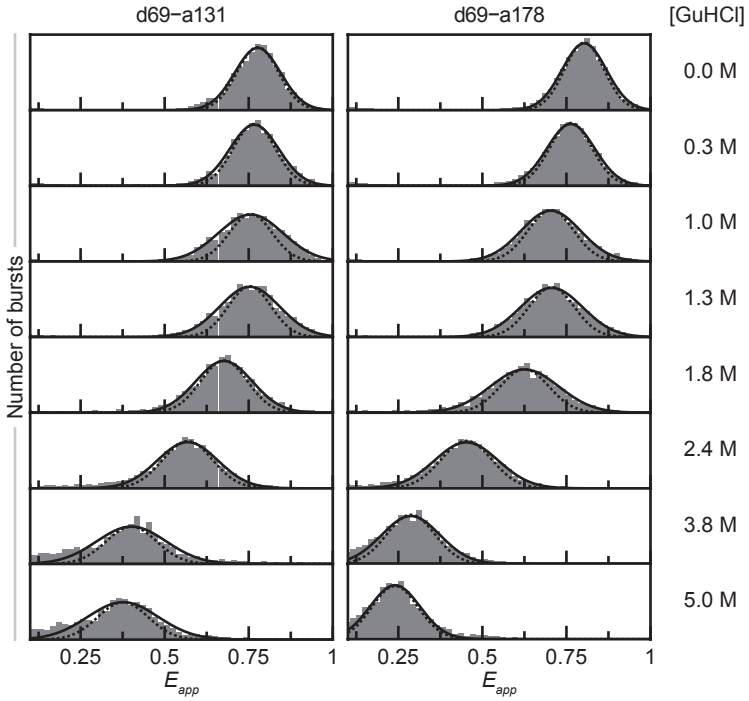

Figuur 6.5 Enkel-molecuul-FRET histogrammen laten een enkele distributie zien bij elke gebruikte denaturant concentraties. Links: denaturant-afhankelijkheid van enkel-molecuul-FRET histogrammen van d69-a131. Rechts: denaturant-afhankelijkheid van enkel-molecuul-FRET histogrammen van d69-a178. Details worden beschreven in hoofdstuk 5.

Dankwoord

Daar is het boekje dan, klaar! De afgelopen 5 jaar zijn er veel momenten geweest waarop ik me niet kon voorstellen dat dit ooit zou gebeuren. Gelukkig zijn er ook mooie tijden om op terug te kijken. Het is maar de vraag of zonder een 'beetje' hulp van collega's, vrienden en familie dit proefschrift ooit af was gekomen. Ik heb van jullie op het persoonlijke vlak en het professionele vlak veel steun mogen ontvangen.

Allereerst wil ik mijn co-promotor Carlo van Mierlo bedanken. Ongeveer 5 jaar geleden sprak jij je vertrouwen in mij uit en mocht ik in jouw groep aan mijn promotieonderzoek beginnen. Tijdens mijn project heb ik heel wat tegenslagen te verduren gehad, maar gelukkig kon jij dat relativeren en wist je me altijd moed in te spreken. Door die motiverende woorden kon ik doorzetten, en uiteindelijk mooie resultaten behalen. Ik denk met plezier terug aan de fikse discussies die we hadden, maar waar geen onvertogen woord viel. Je hebt me veel vrijheid gegeven en stuurde me bij waar nodig. Ik waardeer het zeer dat je mij de ruimte hebt gegeven om mijzelf te ontwikkelen. Bedankt voor deze leerzame periode.

Willem van Berkel, je werd in de laatste fase van mijn onderzoek mijn promotor, maar speelde daarvoor al een rol in mijn promotieonderzoek. Je aanstekelijke enthousiasme, kennis en aangename persoonlijkheid maakten het voor mij erg plezierig om met je samen te werken. Het is mij een waar genoegen en een eer om jou als mijn promotor te hebben.

Sacco de Vries, aanvankelijk zou jij tijdens mijn promotie op het podium zitten, maar stond je plaats af aan Willem. Ik kijk met veel plezier terug op de reis naar Barcelona. Bedankt!

Beste Adrie, je hebt het vijf jaar lang met mij op een kamer volgehouden! Dat is een prestatie waar ik alleen maar respect voor kan hebben! Je bent een onuitputtelijke bron van kennis, daarvan sta ik keer op keer weer versteld. Je was voor mij een vraagbaak en ik heb erg veel steun aan je gehad. We hebben samen veel lol gehad, en er zijn heel wat kilo's salmiakballen doorheen gegaan. Een betere buurman had ik me niet kunnen wensen: A je to!

I want to thank all the colleagues of the Laboratory of Biochemistry, who made it a true joy for me to work there. Jan Willem, met het enthousiasme waarmee je AMBR gaf (en geeft) wekte

je mijn interesse voor fluorescentie spectroscopie. Je bent een geweldige collega en hebt me regelmatig een hart onder de riem gestoken. Sanne, zonder jou was het begin van mijn promotie vast en zeker veel minder plezierig en een stuk moeilijker geweest (en zonder Bouwe Frank hadden we nu geen Saab gereden!). Special thanks go out to Willem's women in the lab: Stefania, Astrid, Teunie, and Agatha. I enjoyed sharing the lab with you, and the fun we had during the lunch breaks. Christoph, you're a great colleague and a friend, and I am honored to have you as my paranymph. Willy, je hebt me maar wat vaak geholpen met kolommen en zuiveringen. Arie van Hoek, je stond altijd weer klaar als ik van de laser-opstelling gebruik wilde maken, alles perfect in orde! I want to thank my students Nanda, Wlodek, Kaiyi and Marre for their interest in my work. Supervising you was an interesting and fun learning experience. Laura, zonder jouw hulp was ik allang verdwaald geraakt in het bureaucratische labyrint van de universiteit!

An important part of my thesis research has been carried out in collaboration with the group of Prof.dr. Gilad Haran at the Weizmann Institute of Science in Rehovot, Israel. The whole group made me feel very welcome, and made my stay in Israel truely enjoyable. In particular I want to thank Gilad for his hospitality and insightful comments, and Menahem for helping me out in the lab and with data-analysis. I hope that we will publish chapter 5 of this thesis to our mutual satisfaction.

Promoveren combineren met een leven buiten het lab is niet altijd makkelijk. Gelukkig staan mijn vrienden en familie altijd voor me klaar. Joran & Chantal, Marijn, Paulus & Carola, René, vrienden sinds de middelbare school, we zijn allemaal een andere kant op gegaan maar als we weer eens bij elkaar zijn is het als vanouds gezellig! Adriaan, Jan, Erwin, Paul, vergeleken met onze HBO-tijd zijn de wilde haren er wel een beetje af (maar de fratsen zijn er niet minder om). Het jaarlijkse weekendje MTB'en (met Patrick erbij) is altijd weer geweldig, of ik nou val of niet. Erwin, het is geweldig om jou nu als mijn paramymf te hebben. Ed & Vesna, Johannes & Sarah, Jeroen & Femke, Bregje & Frank, jullie vriendschap is mij erg waardevol!

Schoonfamilie kies je niet, die krijg je erbij. Gelukkig wel, want een fijnere schoonfamilie dan Peter & Truus, Erwin & Marlies en de oma's & opa's had ik me niet kunnen wensen!

Peter & Teuntje, Saskia & Wiebe en Michiel, het is voor ons niet makkelijk geweest de afgelopen jaren, en we hebben moeilijke tijden voor de boeg. We hebben elkaar hard nodig, en daarom vind ik het fijn dat we straks weer samen in Nederland zijn. Papa & Mama, bedankt dat jullie mij hebben leren kijken naar de wereld om me heen.

Corinne, ik ben blij dat ik jou naast me heb. Jouw onvoorwaardelijke steun heeft me door de afgelopen jaren geholpen.

List of publications

S. Lindhoud*, W.A.M. van den Berg*, R.H.H. van den Heuvel, A.J.R. Heck, C.P.M. van Mierlo, and W.J.H. van Berkel, "Cofactor Binding Protects Flavodoxin against Oxidative Stress," *PLoS ONE*, Vol 7, no. 7, e41363, 2012, doi: 10.1371/journal.pone.0041363 (* authors contributed equally)

Y.J.M. Bollen, A.H. Westphal, S. Lindhoud, W.J.H. van Berkel, and C.P.M. van Mierlo, "Distant residues mediate picomolar-binding affinity of a protein cofactor," *Nature Communications*, 2012, doi: 10.1038/ncomms2010

S.M. Nabuurs, A.H. Westphal, M. aan den Toorn, S. Lindhoud, and C.P.M. van Mierlo, "Topological Switching between an α-β Parallel Protein and a Remarkably Helical Molten Globule," *Journal of the American Chemical Society*, Vol. 131, no, 23, pp. 8290–8295, 2009, doi: 10.1021/ja9014309

R. Engel, A. H. Westphal, D.H.E.W. Huberts, S.M. Nabuurs, S. Lindhoud, A.J.W.G. Visser, and C.P.M. van Mierlo, "Macromolecular crowding compacts unfolded apoflavodoxin and causes severe aggregation of the off-pathway intermediate during apoflavodoxin folding," *The Journal of Biological Chemistry*, Vol. 283, no. 41, pp. 27383–27394, 2008, doi: 10.1074/jbc.M802393200

S. Lindhoud, A.H. Westphal, A.J.W.G. Visser, JW. Borst, and C.P.M. van Mierlo, "Fluorescence of Alexa Fluor dye tracks protein folding," (submitted).

S. Lindhoud, A.H. Westphal, JW. Borst, and C.P.M. van Mierlo, "Illuminating the off-pathway nature of the molten globule folding intermediate of an α-β parallel protein" (submitted).

S. Lindhoud, M. Pirchi, A.H. Westphal, G. Haran, and C.P.M. van Mierlo, "Single-molecule FRET reveals non-cooperative folding of a molten globule," (manuscript in preparation).

Overview of completed training activities

Discipline specific activities

Conferences and meetings

Protein folding Liege, BE	2007, 2008
NWO-CW Protein study group, NL	2007 - 2010
CHAINS, Chemistry as innovating science, NL	2011
Annual Dutch meeting on Molecular and Cellular Biophysics, NL	2007 - 2011
Dutch Chaperone Meeting, NL	2008 - 2012
+ Lecture (2011)	
FASEB Summer Research Conference, Protein Folding in the Cell, Saxtons River, VT, USA	2010

Courses

FEBS advanced course, Microspectroscopy: Monitoring Molecular Interactions in Living Cells	2008
Single Molecule FRET Training, Weizmann Institute of Science, Rehovot, IL	2011

General courses

VLAG PhD Week	2008
Scientific Writing	2010
EMBO Practical Course, Scientific Programming and Data Visualisation for Structural Biology	2010

Optional activities

Biochemistry seminars	2007-2011
Biochemistry PhD retreat, Barcelona, ES	2009

The research described in this thesis was financially supported by the Netherlands Organisation for Scientific Research (NWO; ECHO-700.56.002).

Financial support from Wageningen University for printing this thesis is gratefully acknowledged.

Printed by Wöhrmann Print Service B.V. Zutphen, the Netherlands.